AN EXPERIMENTAL STUDY OF THE HYDRODYNAMIC SUSPENSION OF SPHERES AND SPHERE TRAINS IN A VERTICAL PIPE USING WATER AND POLYMER SOLUTION

AN EXPERIMENTAL STUDY OF THE HYDRODYNAMIC SUSPENSION OF SPHERES AND SPHERE TRAINS IN A VERTICAL PIPE USING WATER AND POLYMER SOLUTION

By

R. A. Anzenavs, B.Eng.

A Thesis

Submitted to the Faculty of Graduate Studies

In Partial Fulfilment of the Requirements

for the Degree

Master of Engineering

McMaster University

September 1972

MASTER OF ENGINEERING (1972)
Mechanical Engineering

McMASTER UNIVERSITY
Hamilton, Ontario

TITLE: An Experimental Study of the Hydrodynamic Suspension of Spheres and Sphere Trains in a Vertical Pipe Using Water and Polymer Solution.

SUPERVISORS: Dr. B. Latto and Dr. G. F. Round

NUMBER OF PAGES: 184

SCOPE AND CONTENTS:

This thesis describes an experimental study of hydrodynamically suspended spheres and sphere trains in a vertical pipe, using water and polymer solution as the suspending medium.

The experiments involved hydrodynamically suspending single spheres in a pipe for the sphere to pipe diameter ratios of 0.105 to 0.956. Drag coefficients were found from a force balance which involved measuring the average velocity of flow approaching the spheres while the pressure drops were found by direct measurement. The experiments on single steel and plastic spheres were carried out in both water and dilute aqueous polymer solution, while the tests on trains of spheres were carried out in water only on train lengths of up to twelve spheres.

From the correlations for drag coefficients and pressure drops of this data, comparison with other authors, especially with data obtained by McNown and Newlin[2], Round and Kruyer[21], and Tawo[28] were made.

ACKNOWLEDGEMENTS

The author wishes to thank Dr. B. Latto and Dr. G. F. Round under whose guidance and encouragement this research was carried out.

Thanks are also due to the engineering machine shop for assistance in building parts of the apparatus, and many friends without whom this project could not have been completed.

The polymer samples, supplied free of charge as well as information and assistance from Hercules Incorporated are gratefully acknowledged.

This research was supported by the Defense Research Board, and the National Research Council of Canada to whom grateful acknowledgement is made.

TABLE OF CONTENTS

NOMENCLATURE

A	Cross sectional area of the sphere
B_l	Similarity law constant for polymer, see Granville[19]
C	Characteristic polymer concentrations, see Granville[19]
C_d^*	Drag coefficient in a bounded medium
C_d	Drag coefficient in an unbounded medium
C_f	Darcy-Weisbach friction factor
D	Diameter of pipe
GPM	Flowrate in Imperial Gallons per Minute
F_i	A force, such as gravity, buoyancy, or drag
$L = \ell_1, \ell_2 + nd$	Distance between pressure taps
L_c	Length of capsule
P	Polymer characteristic, dependant upon species and concentration, see Granville[19]
P_i	An upstream or downstream pressure
PR1, PR2	A pressure ratio term, see Tawo[28]
ΔP	A pressure drop
ΔP_m	Actual pressure drop between pressure taps
ΔP_L	Pressure drop between taps due to liquid alone

$\Delta P_L'$	A pressure drop which when added to ΔP_L gives the pressure drop due to the liquid flowing at V_{AV} whose flow pattern is changed by the presence of the spheres
ΔP_S	The pressure drop associated with the support of the spheres but not including the end effects
ΔP_T	The pressure drop associated with the support of the sphere, but including the end effects
ΔP_E	A total "end effect" pressure term
ΔP_{Ei}	The end effect pressure drop terms for the leading and trailing ends of the trains
$(\frac{dP}{dZ})_T$	Pressure gradient along the sphere train
$(\frac{dP}{dZ})_L$	Pressure gradient due to liquid, with no sphere present
$(\frac{dP}{dZ})_L'$	Pressure gradient which when added to $(dP/dZ)_L$ gives the gradient due to the liquid moving at V_{AV} whose flow pattern has been modified by the presence of the spheres
R_e	Reynolds number
R_{eN}	Apparent Reynolds number, flat platepolymer flows, see White[25]
R_{eX}	Flat plate Reynolds number for Newtonian fluid
T	Temperature
U	Free stream or centerline velocity

V_c	Velocity of capsule
V_{AV}	Average fluid velocity
$\forall$	Volume of sphere
V	Velocity
Wppm	Weight parts per million, a polymer concentration
$Z_i, \Delta Z$	An elevation
c	Capsule to pipe friction
d	Diameter of capsule or sphere
f	Fanning friction factor
g	Local acceleration due to gravity
g_c	Gravitational constant
h_m	Apparent manometer reading (cm. of manometer fluid)
h_{ACT}	Manometer reading, excluding thermal density effects (cm. of manometer fluid)
$h_0 = h_m - h_{ACT}$	Thermal density effects (cm. of manometer fluid)
$(hm)_0$	Manometer reading at no flow
h_f	Head loss
k_c	Surface roughness of capsule
k_p	Surface roughness of pipe

k	Prandtl's mixing length constant
l_i	Characteristic polymer length, see Granville[19]
m_i	Characteristic polymer mass, see Granville[19]
t_i	Characteristic polymer time, see Granville[19]
$\ell^* = \frac{u_* \rho}{\upsilon}$	Characteristic polymer length, see Granville[19]
m	Total mass, water or polymer
$\dot{m}_p$	Mass flowrate of the polymer, not including water
n	Number of spheres in train
$u+ = \frac{u}{u_{*0}}$	Law of the wall variable
u	Velocity at y in a positive x direction
$u_* = \sqrt{\frac{\tau}{\rho}}$	Friction velocity
$u_{*0} = \sqrt{\frac{\tau_0}{\rho}}$	Friction velocity at the wall
u'_{*0}	Threshold friction velocity, see White[25]
x	Distance
$y+ = \frac{y\ u_{*0}}{\upsilon}$	Law of the wall variable
y	Distance normal to the wall
τ	Shearing stress
ρ	Density; not subscripted for solvent
σ	Density of spheres

δ	Boundary layer thickness
β	Law of the wall constant
υ	Kinematic viscosity
μ	Dynamic viscosity
α	Property of the polymer, see White[25]
Θ	Angle of inclination
γ	Specific gravity

SUBSCRIPTS:

p	Polymer
W	Water
T	Total value
0	Value at the wall
AV	Average value
i	Discrete values, 1, 2, 3, etc.

I INTRODUCTION

The behaviour of a sphere moving through a viscous fluid has been the subject of research since 1851, when Stokes first considered a sphere settling in air at a very low Reynolds number. Following Stokes, there have been a succession of authors advancing and refining the theory of settling for both single and agglomerations of spheres.

Recently the need to transport material that cannot be contaminated by the transporting fluid of the pipeline has become apparent. These transportation systems enclose the material to be transported within a spherical or cylindrical capsule whose diameter approaches that of the pipe. The information presently available on the dynamics of dense fields of particles has permitted slurry pipelines to be designed, however this data is not sufficient for the design of capsule pipelines and research had to be carried out to determine what effect the constraining walls had on the motion of the capsules.

The earliest work carried out on this subject was an experimental study performed by McNown and Newlin[2] in 1951 in which they measured the drag coefficient of a sphere rigidly fixed in a uniform flow field constrained within a tube. This work was further extended in 1967 by Round and Kruyer[21] by an experimental study which determined the effect of specific gravity ratio and diameter ratio on spheres suspended in fully developed turbulent flow in inclined tubes. Other authors have studied related topics, such as the movement of capsules through pipelines and the pressure drop along sphere trains rigidly fixed to the pipe wall. Much remains to be done on these studies but an aspect that cannot be neglected is the effect of drag reducing compounds.

The behaviour of a sphere settling in an unbounded drag reducing fluid was studied by A. White[15], [24] in 1966 and 1967, and by Chenard[19] in 1967. The results of these experiments were consistent, and indicated that with a laminar boundary layer the drag on a sphere is reduced, but that with a turbulent boundary layer the drag was increased. This is approximately the reverse of what happens when a drag reducing solution flows through a pipe. In laminar pipe flow, polymer increases the drag while with turbulent flow the drag is reduced. The result of combining these two systems, that is a sphere suspended in a polymer solution within a cylindrical boundary, was studied by Stow and Elliot [32] in 1970, however, their results did not differ from water, and are questionable because of the experimental method used. More will be said regarding these experiments by Stow and Elliot later in chapter II.

The dilute aqueous polymer solution experiments were therefore conceived to determine what effect a drag reducing solution would have on a suspended sphere within cylindrical boundaries. The behaviour of single spheres fixed to the wall of a pipe, and also capsules moving through pipelines have been studied by other authors. To unify these experiments the behaviour of suspended trains of spheres in pure water was included in this study, although time did not permit the experiments to be extended to polymer solutions. In order to make comparison with others the apparatus and procedure had certain similarities to that of other workers.

II LITERATURE SURVEY

The initial part of this study was to obtain data on the flow of water past spheres and sphere trains in a vertical pipe. The earliest work that is related to this subject was that of McNown and Newlin[2] who studied the drag coefficient variation of a sphere rigidly mounted in a tube, as a function of the sphere to tube diameter ratio. Their tests were carried out in air at a fixed Reynolds number and with a uniform velocity distribution across the test section upstream of the sphere, in order to relate their work to the extensive data available on the settling of spheres in an unbounded medium.

As a result of their work they developed the equation for C_d^* in the form;

$$C_d^* = \left[\frac{d/D}{1 - (d/D)^2}\right]^2 \qquad (2.1)$$

which neglects the effects of viscosity but still correlates the data for $d/D > .82$ very well.

Closely related to the topic of spheres and sphere trains suspended in pipes is the subject of the transport of capsules through pipelines. An extensive study, ref. (3) to (10), and (20) on the subject of capsule pipelines was published between the years 1963 and 1967. This series began with a consideration of the concept of capsule pipelining and proceeded to develop and test analytical equations for the velocity and pressure gradient of capsules moving through pipelines.

This analysis brought out the importance of several parameters or

groups of parameters in pipeline flow that are similar or closely related to those found in the support of spheres in pipes. For capsule pipelines a dimensional analysis indicates that;

$$V_c/V_{AV} = [R_e, \frac{\sigma - \rho}{\rho}, \frac{d}{D}, \frac{L}{D}, \text{end shape}, C, \frac{k_c}{d}, \frac{k_n}{D}]$$

where

k_c = capsule surface roughness

k_p = pipe surface roughness

C = capsule to pipe friction

These are much the same groups that would be expected to influence the support velocity of a suspended sphere or sphere train. In addition to the above groups, the pipe Froude number $\frac{V_{AV}^2}{Dg}$, which is the ratio of the inertia forces to the gravity forces, could also be considered. While references (3) to (10) and (20) extensively investigated the above parameters it is difficult to relate their work directly to the present study in that they deal chieflywith capsules moving at a velocity in excess of the average fluid velocity, whereas for a suspended sphere the situation is the exact opposite.

The next work to be considered is that which was done by Round and Kruyer[21], who studied the variation of the drag coefficient and the pressure drop across a sphere as a function of diameter ratio and specific gravity ratio in an inclined tube. It was found that when the quantity

$$\ell n(\Delta P_m - \Delta P_L)/[D \sin \Theta \, (\frac{\sigma - \rho}{\rho})]$$

was plotted as a function of $\ell n(d/D)$ a straight line resulted.

Furthermore, the drag coefficients obtained by Round and Kruyer[21] agreed with those of McNown and Newlin despite the differences in the experimental methods. Contrary to what might be expected, a sphere free to move in a fully developed turbulent flow does not exhibit very large drag coefficient differences to that of a rigidly mounted sphere in a uniform flow field. This subject will be further discussed in chapter VII.

References (3) to (10) and (20) and (21) have dealt with the pipeline flow of capsules and the flow around single spheres. The first consideration of flow around trains of spheres not moving with the liquid was done by Tawo[28], in his study of the pressure drops across a train of spheres fixed rigidly to the inside of a pipe. Pressure drop measurements were made as a function of diameter ratio and Reynolds number. Tawo also developed two pressure ratio terms by which the sphere train pressure drops can be related to those of the pipe free of the sphere train. These expressions were defined as;

$$PR1 = (\Delta P_S)/L \;/\; (\Delta P_L)/L$$

which does not include the end effects, and PR2 defined as;

$$PR2 = (\Delta P_S + \Delta P_E)/L \;/\; (\Delta P_S/L)$$

which does take into account the end effects.

The phenomenon of drag reduction through the addition of trace amounts of long chain polymer molecules to turbulent flow past solid boundaries has been well established for twenty years or more. It has been found that amounts as small as 0.001% by weight or less, can in certain

cases reduce the drag by as much as 70%.

In 1948, B. A. Toms[1] discovered that a solution of polymethyl methacrylate in monochlorobenzene gave drag reductions of up to 50% in turbulent flows through a 0.202 cm. diameter tube. In the ensuing interval the number of papers published on this phenomenon have become too numerous to allow individual mention, however, in general the experimental data fall within the range shown in figure 1. (See also reference (42)).

While experimental data are numerous, a complete explanation of the physical process causing the phenomenon is lacking. It is known that concentrated solutions of polymer are distinctly non-Newtonian, and for certain types of polymers, even dilute solutions exhibit non-Newtonian behaviour, but in general, weak solutions , such as 0.001% by weight, from a viscosity point of view are effectively Newtonian. Experiments by Gadd[13], [14], and White[15], [24] have shown the polymer solutions have unequal normal stresses, in other words in a simple shear flow pressure does not act equally in all directions. Other experiments have shown that the effect of adding polymer is primarily concentrated in the buffer region, the region extending fron $y^+ \cong 11.6$ to $y^+ \cong 70$. It has been observed by Corino and Brodkey[26] that the dissipation of energy takes place through the formation of small scale eddies in the region $11.6 < y^+ < 70$ and it has further been observed that the injection of polymer in the region $y^+ > 70$ produces negligible drag reduction until the polymer diffuses to the wall region. The addition of polymer appears to suppress these eddies resulting in a decrease in friction compared to that for a pure solvent.

Partial differential equations describing the momentum transfer of flow through a boundary layer have been developed, but cannot be solved because of their complexity. Existing mathematical solutions generally make use of a similarity variable which reduces the non linear partial differential

FIGURE 1

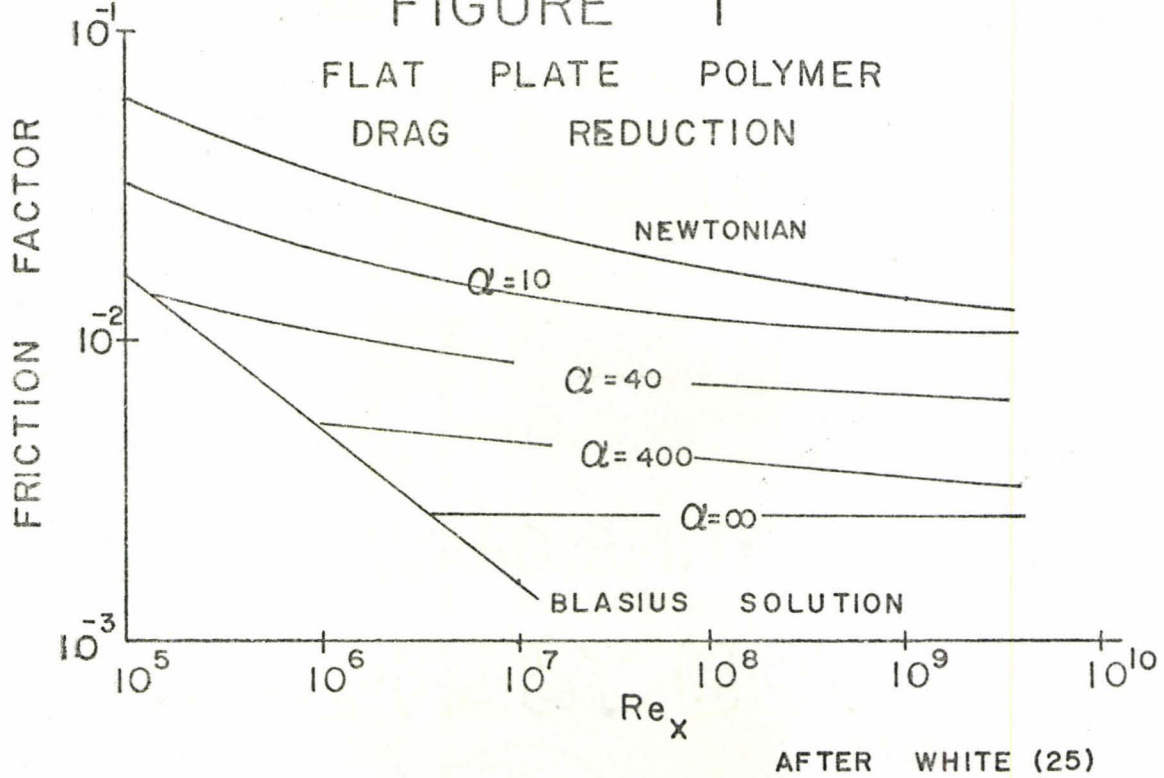
FLAT PLATE POLYMER
DRAG REDUCTION
FRICTION FACTOR
10^{-1}
10^{-2}
10^{-3}
NEWTONIAN
$\alpha = 10$
$\alpha = 40$
$\alpha = 400$
$\alpha = \infty$
BLASIUS SOLUTION
10^5
10^6
10^7
10^8
10^9
10^{10}
Re_x
AFTER WHITE (25)

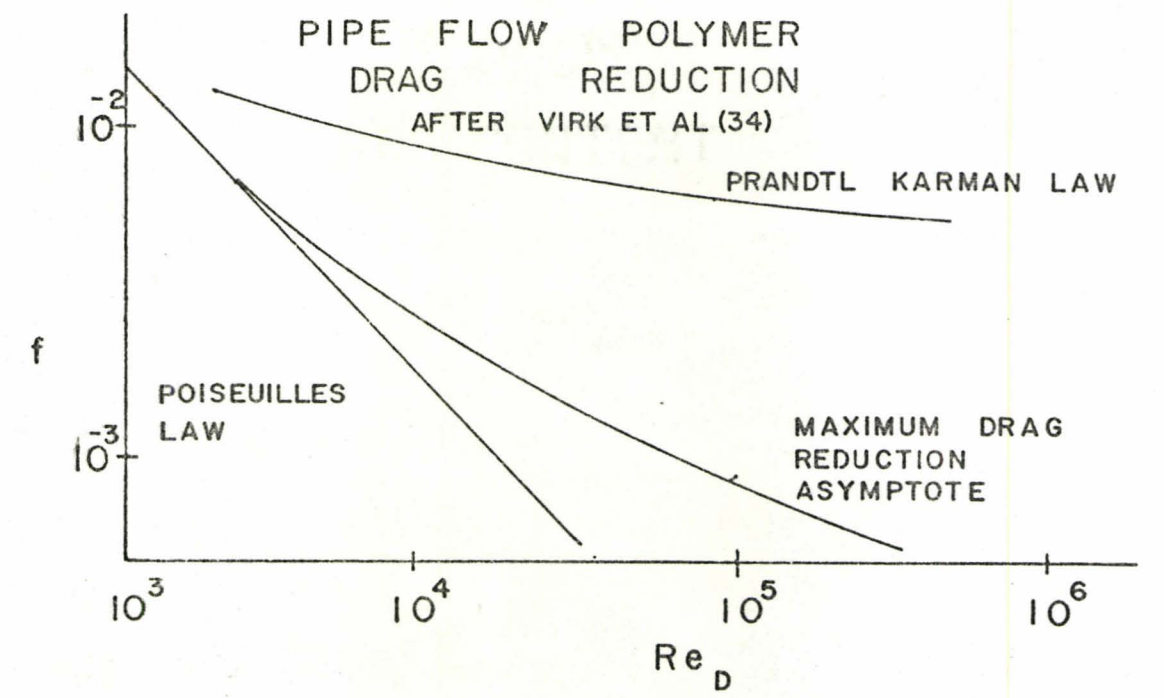
PIPE FLOW POLYMER
DRAG REDUCTION
AFTER VIRK ET AL (34)
10^{-2}
10^{-3}
f
PRANDTL KARMAN LAW
POISEUILLES LAW
MAXIMUM DRAG REDUCTION ASYMPTOTE
10^3
10^4
10^5
10^6
Re_D

equations to ordinary ones. For velocity this new variable depends only on a single position parameter which characterises both distance from the wall and the distance in the direction of the flow. In this way the dimensionless velocity u + now depends only on the dimensionless distance y +.

Prandtl and von Karman were the first to develop such equations. For the turbulent flow of pure solvent Prandtl has determined a universal velocity defect law;

$$\frac{U - u}{u_{*0}} = \frac{1}{k} \ell n \frac{\delta}{y} \tag{2.2}$$

and similarly the universal velocity distribution law;

$$u + = \frac{u}{u_{*0}} = \frac{1}{k} \ell n \left(\frac{y\ u_{*0}}{\upsilon}\right) - \frac{1}{k} \ell n\ \beta \tag{2.3}$$

for $y + = \dfrac{y\ u_{*0}}{\upsilon} > 11.6$

for $y + < 11.6 \quad \dfrac{u}{u_{*0}} = \dfrac{y\ u_{*0}}{\upsilon}$ (2.4)

Equation 2.3 can be converted to a form containing the friction factor by letting;

$$C_f = \frac{8\tau_0}{\rho U^2} = 8 \left(\frac{u_{*0}}{U}\right)^2$$

therefore

$$\frac{1}{\sqrt{C_f}} = 0.868 \ell n \left(Re \sqrt{C_f}\right) - 0.8 \tag{2.5}$$

The work of many authors has been directed towards obtaining an equation similar to equation 2.5, that is applicable to drag reducing solutions. It can be expected that equation 2.5 for a solvent must form the lower asymptote of drag reduction. Virk et. al.[34], have deduced the upper asymptote of drag reduction as;

$$\frac{1}{\sqrt{C_f}} = 4.125 \ln (Re \sqrt{C_f}) - 16.2 \qquad (2.6)$$

Relationships such as the above must be used with caution, because for polymer flows the extent of drag reduction depends upon the thickness of the shear layer. If the shear layer is too thin, as in a pipe of very small diameter, the viscous sublayer and the interactive, or buffer layer remain, but the turbulent portion of the shear layer is either greatly reduced or non existent, and hence the flow becomes that for maximum drag reduction very easily. The result is that greater drag reduction is apparent at lower Reynolds numbers and lower concentrations of polymers than would normally occur where the shear layer is sufficiently thick.

Granville[19], [35] has investigated the limitations of similarity law type solutions applied to polymer flows, and bearing these in mind, several such solutions will be discussed briefly. F. M. White[25] combined the law of the wall developed by Meyer for polymer flows;

$$u^+ = \frac{1}{k} \ln y^+ + 5.5 + \alpha \ln\left(\frac{u^+}{u'^+_{*0}}\right) \qquad (2.7)$$

where α is a property of the polymer and its concentration and u'_{*0} is a threshold friction velocity below which the flow behaves as a pure solvent would, with the two dimensional bounary layer equations to derive an

effective Reynolds number relationship for external flows;

$$R_{eN} \cong R_{eX} \left(\frac{u_*}{u'_{*0}}\right)^{k\alpha} \tag{2.8}$$

The Reynolds number of the Newtonian fluid is calculated as before but it is then modified according to equation 2.8. Using this effective Reynolds number the friction factor can then be calculated from some Newtonian correlation such as;

$$C_f \text{ (NEWTONIAN)} = [2 \log (R_{eN}) - 0.65]^{-2.3}$$

Since the free stream velocity for a flat plate remains constant, the shear stress must decrease as the Reynolds number increases. Therefore, the term $u_* = \sqrt{\frac{\tau}{\rho}}$ must also decrease as the Reynolds number increases. The result is that for a flat plate, polymer addition reduces friction, starting at the threshold Reynolds number but proceeding with decreasing effectiveness as the Reynolds number increases.

Apart from Meyer, there have been many authors who have studied the similarity laws applicable to polymer flows, both theoretically, and experimentally. Granville[19], [35] has published an interesting derivation of these similarity laws, along with a summary of their limitations.

Granville begins his analysis with a statement of the inner velocity law;

$$u = [\tau_0, \rho, \mu_0, y, \rho_p, \ell, \ell_1, \ell_2 \ldots,$$

$$m, m_1, m_2, \ldots, t, t_1, t_2, \ldots]$$

with the boundary conditions;

$$u = 0 \text{ at } y = 0$$

The variables are then grouped by a dimensional analysis and by considering the region of overlap between the outer velocity law and the inner velocity law, a functional form of the inner velocity law has been derived;

$$\frac{u}{u_*} = A \ln y^+ + B_1[\ell^*, C, P] \tag{2.9}$$

where

$$\ell^* = \frac{u_* \ell}{\upsilon_0}$$

is a non dimensional characteristic polymer length, and;

$$C = \left[\frac{\rho_p/\rho}{1 + \rho_p/\rho}\right]$$

ρ_p = polymer concentration (density units)

ρ = density of solvent

is a form of polymer concentration, where;

$$P = \frac{\ell}{\ell_1}, \frac{\ell_1}{\ell_2}, \ldots, \frac{m}{\rho_0 \ell^3}, \frac{m}{m_1}, \frac{m_1}{m_2}, \ldots$$

$$\frac{t\upsilon_0}{\ell^2}, \frac{t}{t_1}, \frac{t_1}{t_2}, \ldots,$$

These relationships indicate what the similarity laws for polymer must be like, unfortunately the exact form can only be determined by experiment.

While considerable data exists on the unhindered settling of spheres in air or water, the subject of unhindered settling in polymer has only recently been studied. In 1967, White[24] showed that the addition of polymer to the flow past a sphere in an unbounded medium caused the drag coefficient to decrease when the boundary layer was laminar and increase when it was turbulent.

This observation is somewhat unexpected because for internal flows in the laminar region the addition of polymer slightly increases the drag while in the turbulent region it produces a marked decrease in drag. White has attributed this occurence in external flows to the delayed separation of the laminar boundary layer and a subsequent decrease in wake diameter. He postulated that the delay in separation is caused by the inequality of normal stresses in the shear flow, resulting in a higher pressure normal to the direction of shear than would be found in a flow of the pure solvent. This would then cause the boundary layer to adhere to the sphere longer than usual. The inequality of normal stresses was first suggested by Gadd[13], [14] and demonstrated by him by the impact of a free jet on an inclined plane.

In 1967, Chenard[16] published a thesis reporting essentially the same results as White[24], however, when these results are compared with those of McNown and Newlin[2] and others who did work on the flow around spheres in tubes, it can be seen that Chenard's drag coefficients should differ by as much as +10 to +15% when compared to those in a truly unbounded medium.

The final paper of immediate interest is one by Stow and Elliot[32] reporting their work on the measurement of drag forces and hence drag

coefficients on a tethered sphere in a polymer solution. The results they obtained indicates that the drag coefficient is not altered by the addition of polymer to the solvent. This disagrees with the results of the present study which indicates that the drag coefficient increases.

An examination of their experimental method suggests a possible explanation. The polymer used was Polyox WSR 301, a polymer that is highly susceptible to shear degradation, and rather than using an open circuit system they used a closed circuit in which the polymer was continually recirculated using a centrifugal pump. To obtain results at different concentrations this original polymer was then diluted. Because of the sensitivity of Polyox to shear degradation it is probable that over the period of the experiment the actual concentration was not accurately known and the polymer was totally degraded.

III THEORY

Referring to figure 2, when the sphere(s) are in stable equilibrium their weight is balanced by their buoyancy and the drag force exerted on them by the fluid. Assuming fully developed turbulent flow upstream of the spheres and neglecting the exact location or motion of the spheres, a drag coefficient can be postulated that encompasses all the effects encountered, and can be distinguished from the drag coefficient occuring in an unhindered configuration.

For the spheres at equilibrium we may write the force balance as, (referring to figure 2).

$$F_3 = F_1 + F_2$$

or

$$W = C_d^* \frac{A_S \rho V_{AV}^2}{2g_c} + n \forall_S \rho \frac{g}{g_c}$$

therefore

$$\frac{n \pi d^3}{6} \sigma \frac{g}{g_c} = C_d^* \frac{\pi d^2}{4} \frac{\rho V_{AV}^2}{2g_c} + \frac{n \pi d^3}{6} \rho \frac{g}{g_c}$$

collecting terms and transposing we have,

$$\frac{C_d^*}{n} = \frac{4}{3} \left(\frac{\sigma - \rho}{\rho}\right) \frac{gd}{V_{AV}^2} \qquad (3.1)$$

FIGURE 2

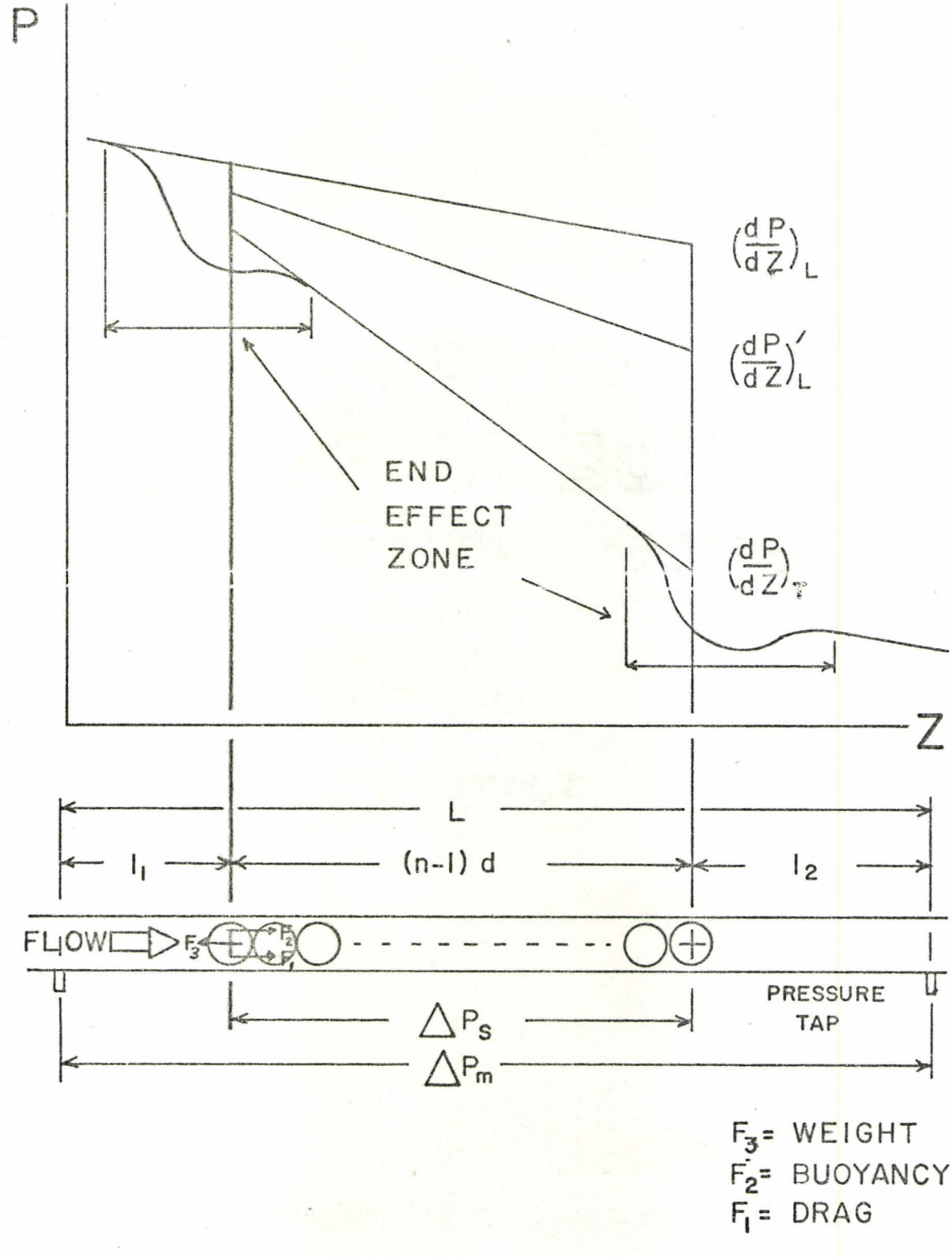
P
$\left(\frac{dP}{dZ}\right)_L$
$\left(\frac{dP}{dZ}\right)'_L$
END
EFFECT
ZONE
$\left(\frac{dP}{dZ}\right)_T$
Z
L
l_1
(n-1) d
l_2
FLOW
F_3
F_2
F_1
PRESSURE
TAP
ΔP_s
ΔP_m
F_3 = WEIGHT
F_2 = BUOYANCY
F_1 = DRAG

Hence for a given fluid and sphere material

$$\frac{C_d^*}{n} \alpha \frac{gd}{V_{AV}^2} \tag{3.2}$$

In order to understand better the phenomenon and how the variables relate to each other, a dimensional analysis, using Buckingham's π theorem has been performed for the system.

It may be assumed that the variables involved may be written:

$$\Delta P = f(d, D, \rho, \sigma, \upsilon, V_{AV}, g_c) \tag{3.3}$$

The units are;

$$\Delta P = FL^{-2}$$

$$d = L$$

$$D = L$$

$$\rho = ML^{-3}$$

$$\sigma = ML^{-3}$$

$$\upsilon = L^2T^{-1}$$

$$V_{AV} = L^2T^{-1}$$

$$g_c = MLF^{-1}T^{-2}$$

Arranging these into four dimensionless groups;

$$\pi_1 = V_{AV}{}^a D^b \rho^c g_c{}^d \Delta P$$

$$\pi_2 = V_{AV}{}^a D^b \rho^c g_c{}^d d$$

$$\pi_3 = V_{AV}{}^a D^b \rho^c g_c{}^d \sigma$$

$$\pi_4 = V_{AV}{}^a D^b \rho^c g_c{}^d \upsilon$$

By satisfying the requirement of dimensional homogeneity for each π group we can solve for a, b, c and d. Hence;

$$\pi_1 = \frac{\Delta P \, g_c}{V_{AV}{}^2 \rho} \tag{3.4}$$

which can be rearranged without altering the requirement of dimensional homogeneity into a friction factor type of term;

$$\pi_1 = \frac{\Delta P}{(\frac{L}{D})\frac{\rho V^2}{2g_c}} = C_f \tag{3.5}$$

and $$\pi_2 = d/D \tag{3.6}$$

$$\pi_3 = \frac{\sigma}{\rho} \text{ or } \frac{\sigma - \rho}{\rho} \tag{3.7}$$

and $$\pi_4 = \frac{\upsilon}{V_{AV} D} \text{ or } \pi_4 = \frac{V_{AV} D}{\upsilon} = R_e \tag{3.8}$$

We can then write that;

$$f(C_f, d/D, \frac{\sigma - \rho}{\rho}, R_e) = 0 \qquad (3.9)$$

Referring back to the derivation of the drag coefficient C_d^* the RHS of equation 3.2 is a form of the Froude number, that is, the ratio of the gravity forces to inertia forces. Two other quantities not considered in the dimensional analysis but which should be included are the number of spheres in the train, and their location in the pipe. Considering the geometry of the test section in cylindrical polar co-ordinates centered on the centerline of the pipe, and letting the eccentricity be represented by the radius vector stretching from the origin to the center of the sphere, it is apparent that for an oscillating sphere or sphere train the time average of the eccentricity will be some finite value.

The resulting effect is a buffeting of the spheres, which is caused by the turbulence inherent in the flow, and the shedding of vortices from the spheres. Above certain limiting diameter ratios, $d/D > 0.75$ the manner in which the wake vortices are produced is altered, causing the sphere to spin or roll rapidly about the inside of the test section. The combination of these effects then renders the concept of a stable symmetrically located sphere invalid. However, since the theory is not dependant upon the spheres being centered but is sufficiently general to encompass these effects the numerical values should be generally valid for all systems where spheres are hydrodynamically supported within a vertical pipe.

Returning to the system of figure 2, the pressure drop across the sphere or spheres will in general consist of four quantities.

(1) The pressure drop ΔP_T associated with the support of the sphere or sphere train, and caused by a combination of form drag and skin friction acting on the spheres only.

(2) The pressure drop ΔP_L caused by the friction between the pipe and fluid, flowing at the velocity required to suspend the spheres.

(3) A pressure drop $\Delta P_L'$ due to the additional shear imposed on the flow by the presence of the sphere, over and above ΔP_L due to the friction between the walls and the fluid in the absence of the sphere.

(4) Leading and trailing end effects of the sphere(s) ΔP_{E1}, and ΔP_{E2}; $\Delta P_E = \Delta P_{E1} + \Delta P_{E2}$.

The pressure ΔP_m is measured at the positions along the tube where the end effects caused by the spheres are negligible, and consists of;

$$\Delta P_m = \Delta P_L + \Delta P_T + \Delta P_L' + \Delta P_E \tag{3.10}$$

The term ΔP_E in the above equation represents the end effect pressure drops of the leading and trailing ends of the sphere train. These quantities can only be obtained empirically becuase of the complex nature of the flow. The flow being turbulent results in a continual buffeting of the spheres, furthermore, vortices are being shed from the trailing end of the sphere train.

An expression ΔP_S can be defined if the constant pressure gradient terms of the total gradient along the section (n - 1)d of the sphere train (see figure 2), are considered. The total pressure gradient is not constant along this entire section, however the deviation from constancy at the beginning and end of the sphere train is included in the end effects. ΔP_S then is,

$$\Delta P_S = \left[\left(\frac{dP}{dZ}\right)_T + \left(\frac{dP}{dZ}\right)_L + \left(\frac{dP}{dZ}\right)_L'\right] (n - 1)d \tag{3.11}$$

$(n - 1)d$ is used rather than nd for the train length because this provides a more realistic approach to the problem of allowing for end effects.

The measured pressure can then be written as;

$$\Delta P_m = \Delta P_S + (\Delta P_{E1} + \Delta P_{E2}) + \left(\frac{dP}{dZ}\right)_L (\ell_1 + \ell_2) \tag{3.12}$$

where

$$L = (n - 1)d + \ell_1 + \ell_2$$

Substituting for ΔP_S;

$$\Delta P_m = \left[\left(\frac{dP}{dZ}\right)_T + \left(\frac{dP}{dZ}\right)_L + \left(\frac{dP}{dZ}\right)_L'\right] (n - 1)d + (\Delta P_{E1} + \Delta P_{E2})$$

$$+ \left(\frac{dP}{dZ}\right)_L (\ell_1 + \ell_2)$$

and grouping the terms we have;

$$\Delta P_m = \left[\left(\frac{dP}{dZ}\right)_T (n - 1)d + \left(\frac{dP}{dZ}\right)_L' (n - 1)d\right]$$

$$+ \left(\frac{dP}{dZ}\right)_L [(n - 1)d + \ell_1 + \ell_2] + \Delta P_{E1} + \Delta P_{E2} \tag{3.13}$$

The quantity $(dP/dZ)_L'$ cannot be measured independantly of the term $(dP/dZ)_T$, therefore they have been combined into the single term $(\Delta P_S/L)$. Therefore,

$$\Delta P_m = \left(\frac{\Delta P_S}{L}\right) (n - 1)d + \left(\frac{\Delta P_L}{L}\right) (L) + \Delta P_E \tag{3.14}$$

and transposing we have;

$$\Delta P_m - \Delta P_L = \left(\frac{\Delta P_S}{L}\right) (n - 1)d + \Delta P_E \qquad (3.15)$$

Once a section of developed flow has been achieved along the sphere train, it shall be assumed that regardless of the length of the train, the end effects remain constant. It is then a simple matter to determine $(\Delta P_S/L)$ from a graph of $\Delta P_m - \Delta P_L$ against n, and from these to determine ΔP_E.

Tawo[28] in his thesis on fluid flow in pipes containing sphere trains, has developed a pressure ratio PR1, which compared the pressure gradient in a tube containing a sphere train to that of a free tube. Such a ratio could be used to predict the pressure gradient in a pipe containing a sphere train if the pressure gradient of the free tube is known. The pressure ratio PR1, is defined as;

$$PR1 = (P_{1n} - P_{2n})/L \Big/ (dP/dZ)_L$$

where $(P_{1n} - P_{2n})/L$ is the pressure gradient along the train, excluding end effects.

For the purpose of comparison, an expression similar to PR1 will be developed in the present work. From equation (3.12);

$$\Delta P_S = \Delta P_m - \Delta P_E - \left(\frac{dP}{dZ}\right)_L [L - (n - 1)d] \qquad (3.16)$$

the gradient then is;

$$\frac{\Delta P_S}{(n - 1)d} = \frac{\Delta P_m}{(n - 1)d} - \frac{\Delta P_E}{(n - 1)d} - \left(\frac{dP}{dZ}\right)_L \left[\frac{L - (n - 1)d}{(n - 1)d}\right] \qquad (3.17)$$

defining;

$$PR1 = \left[\frac{\Delta P_S}{(n - 1)d}\right] / \left(\frac{dP}{dZ}\right)_L \tag{3.18}$$

and substituting, we have;

$$PR1 = \frac{\Delta P_m}{(n - 1)d} - \frac{\Delta P_E}{(n - 1)d} - \left(\frac{\Delta P_L}{L}\right)\left[\frac{L - (n - 1)d}{(n - 1)d}\right]$$

On collecting the terms together we have;

$$PR1 = 1 + \frac{L}{(n - 1)d}\left[\frac{\Delta P_m}{\Delta P_L} - \frac{\Delta P_E}{\Delta P_L} - 1\right] \tag{3.19}$$

Once a graph of $\Delta P_m - \Delta P_L$ has been plotted and ΔP_E is known, equation (3.19) can be used to calculate PR1, however, should ΔP_E not be known, a close approximation to PR1 can be made if ΔP_E is included in ΔP_m, this would then make,

$$PR1 = 1 + \frac{L}{nd}\left[\frac{\Delta P_m}{\Delta P_L} - 1\right] \tag{3.20}$$

where $(n - 1)d$ has been changed to nd to facilitate calculation.

A major portion of the experiments presented in this work deal with the effects of polymer on single spheresdynamically suspended in a vertical pipe. For these situations a developed $(dP/dZ)_T$ cannot exist, since a single sphere does not provide sufficient length in the direction of flow. Furthermore, the pressure drop across the single sphere is not equivalent to the end effects observed for the sphere trains, since these effects may extend for several diameters along the sphere train.

When dealing with polymer it is assumed that low solution concentrations (< 100 Wppm) produce solutions that are equivalent to Newtonian fluids, except that they produce less drag.

For unbounded external flows, such as flows around a sphere White[15], [24] and Chenard[16] have observed that the addition of polymer causes the drag coefficient in the laminar region to decrease, and in the turbulent region to increase; however for confined flows, that is where a sphere is suspended within a tube, the effect on the drag coefficient cannot be predicted. For these reasons the results of the polymer experiments were not compared with theory, but rather simply with the results of the water experiments.

IV EXPERIMENTAL APPARATUS

IV-1 The Flow System

The experimental apparatus consists of a vertical loop of 2" ID pipe approximately eighty feet in length, assembled as shown in figure 3. The fluid is circulated using a Worthington model 2CN-32 single stage centrifugal pump powered by a General Electric three horsepower 3600 RPM induction motor.

(Since the system can be, but is generally not intended to be used as a recirculating system, two sources of water have been used; the city mains for open circuit flow, and an eighty gallon reservoir for recirculating flow.)

Upon being discharged from the pump the water travels past a 904 cubic inch variable volume surge chamber, which dampens pressure fluctuations. Immediately after the surge tank are located two "Brooks" rotameter type flowmeters. The rotameters are installed in such a manner that the flow can be directed through either one, independent of the other. During the course of the experiments it was found that the original two rotameters did not adequately cover the entire flow range, and for this reason one of the existing rotameters was replaced by a third low flow rate rotameter.

After leaving the rotameters the flow passed along the pipework down to the level of the first floor, then back through a vertical section twenty feet long, to the second floor. The last ten feet of this vertical section is a glass tube which was used as a test section. A fine honeycomb filter is located at the entrance to the test section to homogenize and reduce the turbulence. Two ports for inserting the spheres were located

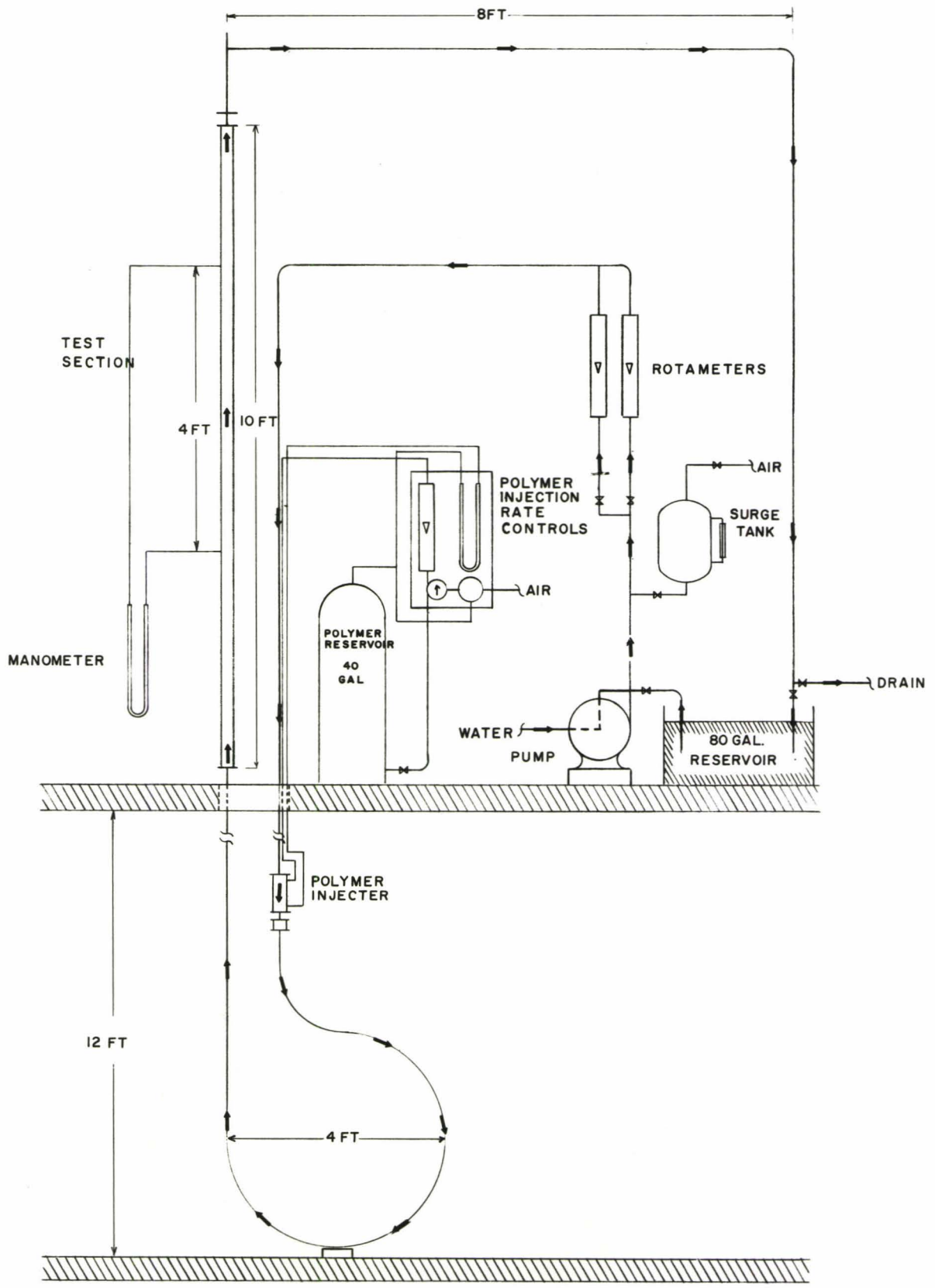

Apparatus Schematic

immediately above the test section.

A number of pressure taps are located along the entire length of the metal pipe below the test section, while the initial test section had pressure taps located twelve inches apart along its entire length. Two later versions of the test section, on which the majority of the tests were performed had pressure taps on the midsection, located four feet (five feet for the second one) apart.

Because the glass test section was extremely fragile, and subject to considerable mechanical and thermally induced stresses it was necessary to brace it at 2.5 foot intervals using rubber lined clamps. It was also necessary to isolate the tube at the bottom flange by a thick rubber gasket and at the top by a flexible tygon bellows piece to prevent the tube from breaking.

After leaving the test section the water passed along pipework into either the reservoir or the drains, depending upon the requirement. In order to recover the single spheres a gate valve was located in the vertical section above the reservoir, which when opened allowed the water and the sphere to be pumped into the reservoir. The trains of spheres were retrieved by hooking a metal eye located at the end of the train.

IV-2 The Polymer System

The circulation system used throughout these experiments was an open circuit system. This was done because in a recirculating system polymer rapidly becomes mechanically degraded.

The polymer injection apparatus consisted of a 40 gallon reservoir which held the concentrated aqueous polymer solution (2000 Wppm). The polymer from this reservoir was injected into the main stream using compressed air, controlled by a precision air line regulator, while the

injection rate was monitored using a "Brooks" flowmeter.

The polymer was injected into the flow of the main stream through a chamber located approximately thirty feet upstream of the test section. Immediately following this injection chamber was a turbulence promoter in the form of a centrally located sphere, occupying approximately 50% of the area of the pipe. It was expected that this sphere combined with the existing turbulence in the interval between the turbulence promoter and the test section would provide sufficient agitation to uniformly distribute the polymer throughout the flow. Visual inspection of poorly mixed polymer batches passing through the test section confirmed this.

During the course of the experiments it was found to be difficult to maintain a steady flow of polymer because of fluctuating main line pressures. Consequently, the system was modified to incorporate a differential manometer which measured the pressure difference between the air space above the polymer in the reservoir and the pressure in the injection chamber. This permitted continuous monitoring of the "driving" pressure and thus better control over the injection rate.

Preparation of the stock solution of polymer took place in plastic lined bins, using a "Hercules Standard Eductor" (manufactured by Hercules Inc.). The solution was later transferred to the reservoir using a hand operated positive displacement pump, which reduced polymer degradation in transfer, and permitted inspection of the batches to check for evidence of poor mixing.

IV-3 The Pressure Measuring System

Two manometer arrangements were used to measure the pressures during these experiments. The first method used a bank of inclined manometers to check the pressure gradient along the glass section of the pipe and

enabled the selection of the actual test section. The second arrangement used a single inclined manometer which was used to measure the pressure drops across the test section with and without the spheres.

Because of the short test section (four to five feet) and the relatively low velocities encountered in the experiments a very accurate device was required to measure the pressure. The manometer eventually used was a water jacketed carbon tetrachloride-in-glass inclined U tube manometer.(see figure 26 and plate 4). The manometer could be inclined from 6° to 30° from the horizontal, and was provided with a level to measure the angle of inclination. It was found that because of the temperature difference between the test section and the manometer that an apparent manometer reading was created when there was no flow through the test section. To minimize this reading the entire thirty inches of each manometer leg, as well as the connecting tubes were enclosed in a water jacket.

IV-4 The Spheres

The steel and plastic spheres used in this study had specific gravities of approximately 8.1, and 1.1 respectively.*

During the tests they were hydrodynamically suspended in four configurations eg.

(i) single spheres,

(ii) unattached sphere trains,

(iii) flexibly attached sphere trains, and

(iv) rigidly attached sphere trains.

For cases (iii) and (iv), the spheres were drilled and connecting hooks fitted into the cavities. The change in specific gravity caused by the installation of these devices was negligible.

---

* For exact value see Appendix VII - Data Tables.

V EXPERIMENTAL PROCEDURE

V-1 Tests Using Water Only

Experiments using water as the working fluid were carried out using all the sphere configurations, eg. single spheres, non attached sphere trains, flexibly attached trains, and rigidly attached trains. The resulting data had two fold value in that it provided data that could be compared to that of other experimenters as well as providing original data, as in the case of the sphere trains.

The procedure for single spheres and trains of spheres was similar. The flow of water would be started at least several hours prior to the actual testing to allow the temperature of the water and that of the apparatus in general to stabilize. When the apparatus was at thermal equilibrium the flow was stopped and the manometer no flow reading, as well as the water and room temperature recorded. The flow was then restarted and adjusted to stabilize the spheres in the center of the test section. When it was evident that the spheres were stable the flowrate and pressure drop, in addition to the mode of oscillation of the spheres, was recorded and the flow shut off and again the no flow manometer reading noted. This procedure was repeated for all the different diameters of steel and plastic spheres available. The diameter and weight of the spheres was also measured and recorded.

For the case of the steel sphere trains only one diameter ratio was comprehensively investigated because of the violent motion of the steel spheres. The rotating steel spheres had sufficient momentum to cause the test section to vibrate very violently which sometimes resulted in the spheres striking the inside entrance to a pressure tap. On one occasion the steel spheres actually broke

the test section, and after this the testing of steel sphere trains was discontinued.

V-2 Polymer Tests

The polymer experiments were carried out in much the same manner as those involving water, however, they were performed on single steel spheres only. Again the water flow was started and the water and apparatus allowed to come to thermal equilibrium. The flow of water was then stopped and the manometer zero reading as well as the water and room temperature recorded, and a sphere then inserted into the tube. The water flow was then restarted to raise the sphere to the center of the test section. When the system had stabilized the polymer injection was commenced and the appropriate concentration established in the test section. During the experiments requiring polymer additions it was required that the flowrates be carefully manipulated to maintain both the sphere in the center of the test section, and the required polymer concentration. When it was apparent that the sphere was stationary in the direction of the flow, the flowrates and pressure drops were noted. The foregoing procedure was repeated for concentrations of 25 Wppm and 50 Wppm. After the 50 Wppm tests the spheres were removed, and the system flushed for several minutes.

As a check, all the readings were repeated at least twice.

Plate #1 Overall view of apparatus, second floor

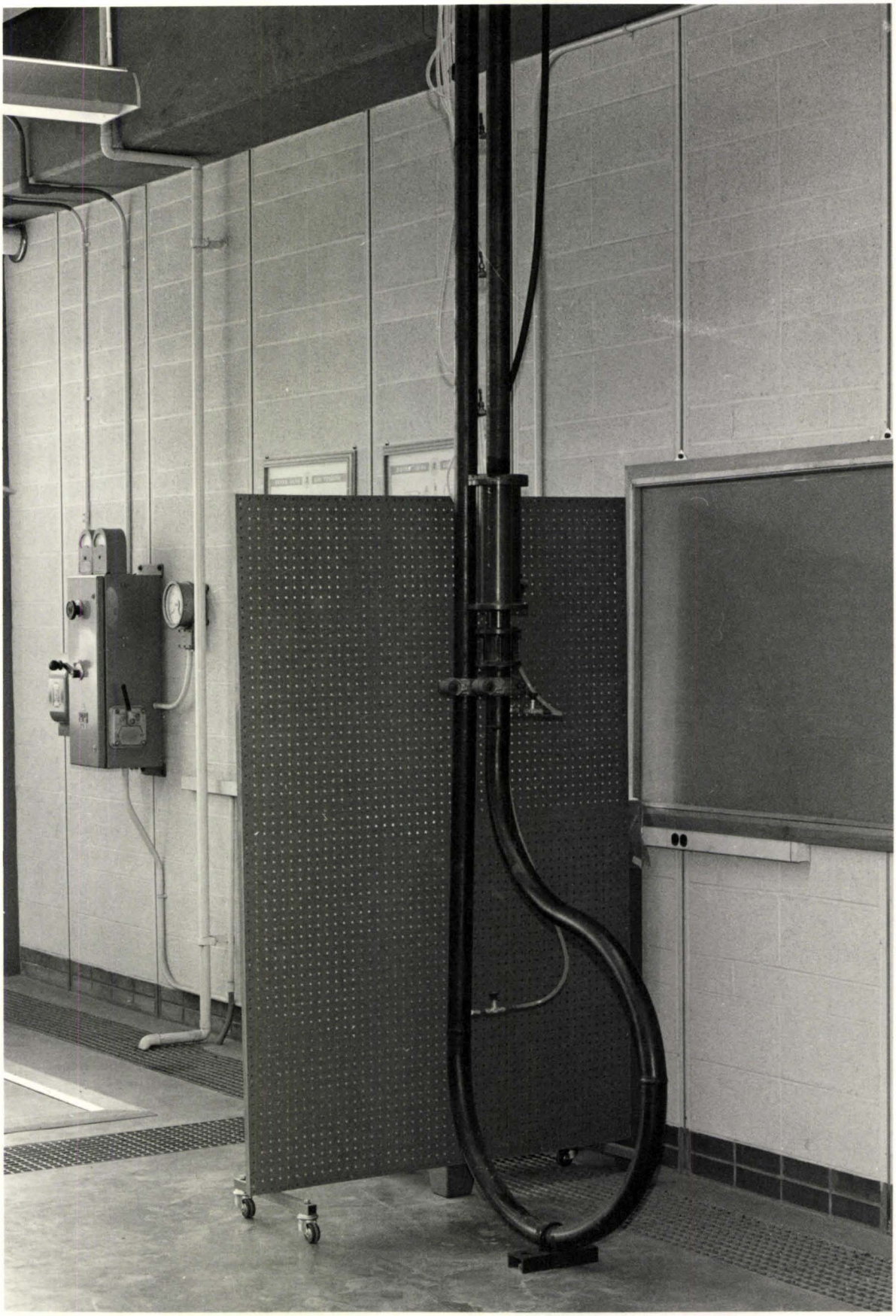

Plate #2 Apparatus on first floor, showing injection chamber and turbulence promoter

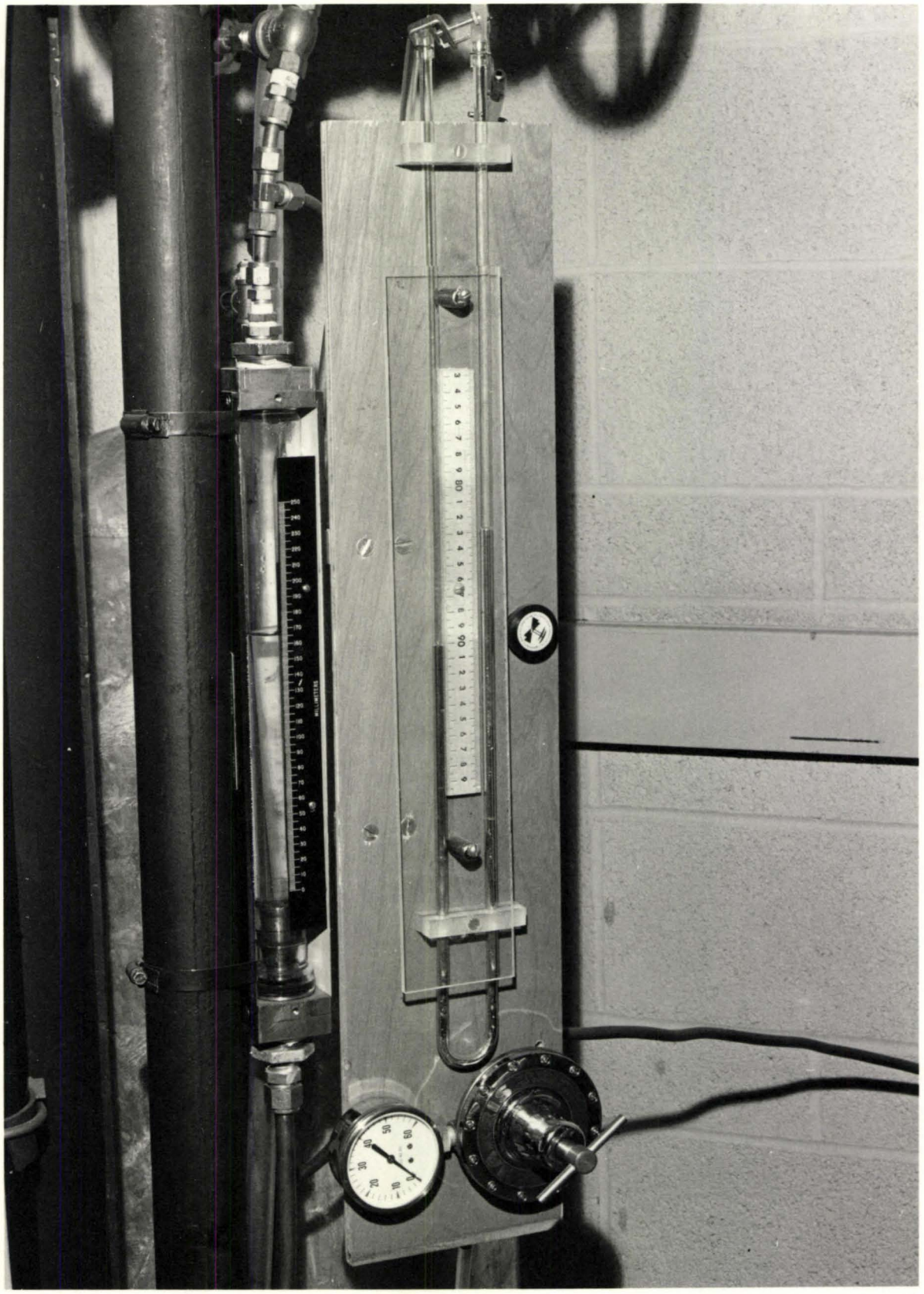

Plate #3 Polymer injector controls and flowmeter

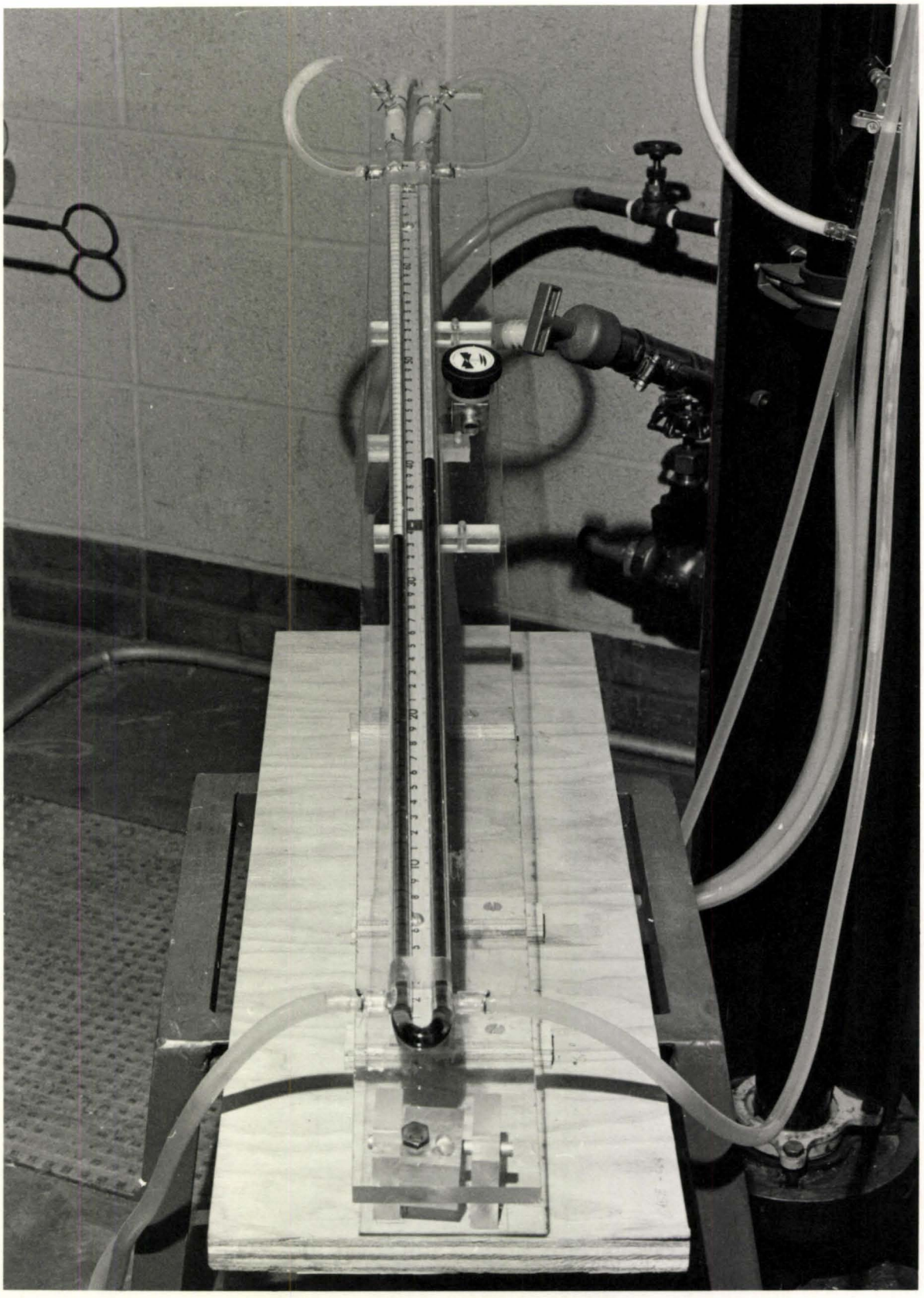

Plate #4 Water jacketed carbon tetrachloride in glass manometer, used for most measurements

SECTION VI

RESULTS

The graphs displayed in this section are based upon the measured data presented in tabular form in Appendix VII.

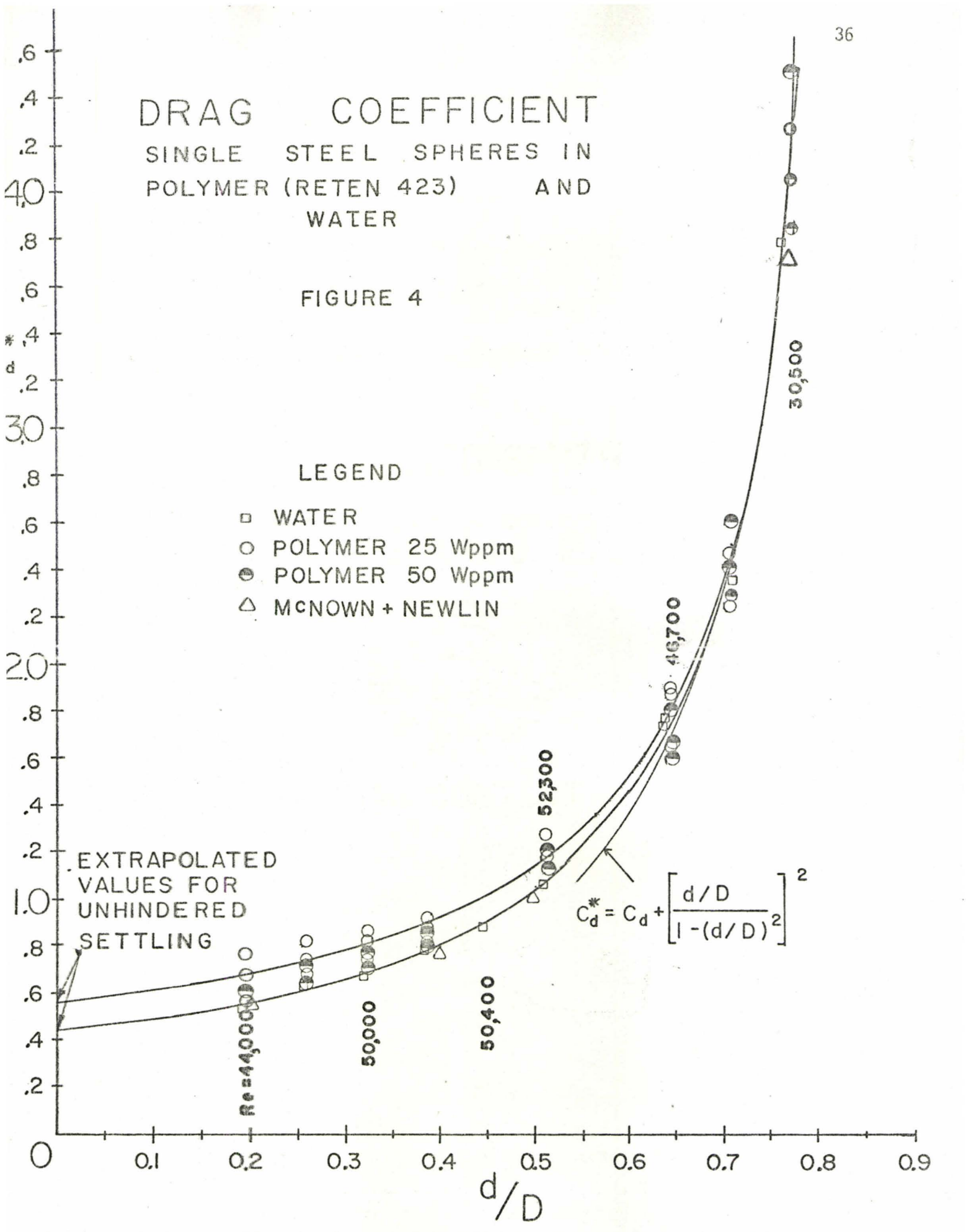
DRAG COEFFICIENT
SINGLE STEEL SPHERES IN POLYMER (RETEN 423) AND WATER
FIGURE 4
LEGEND
WATER
POLYMER 25 Wppm
POLYMER 50 Wppm
McNOWN + NEWLIN
EXTRAPOLATED VALUES FOR UNHINDERED SETTLING
$C_d^* = C_d + \left[\frac{d/D}{1-(d/D)^2}\right]^2$
Re=44,000
50,000
50,400
52,300
46,700
30,500
C_d^*
d/D
0
0.1
0.2
0.3
0.4
0.5
0.6
0.7
0.8
0.9
1.0
2.0
3.0
4.0

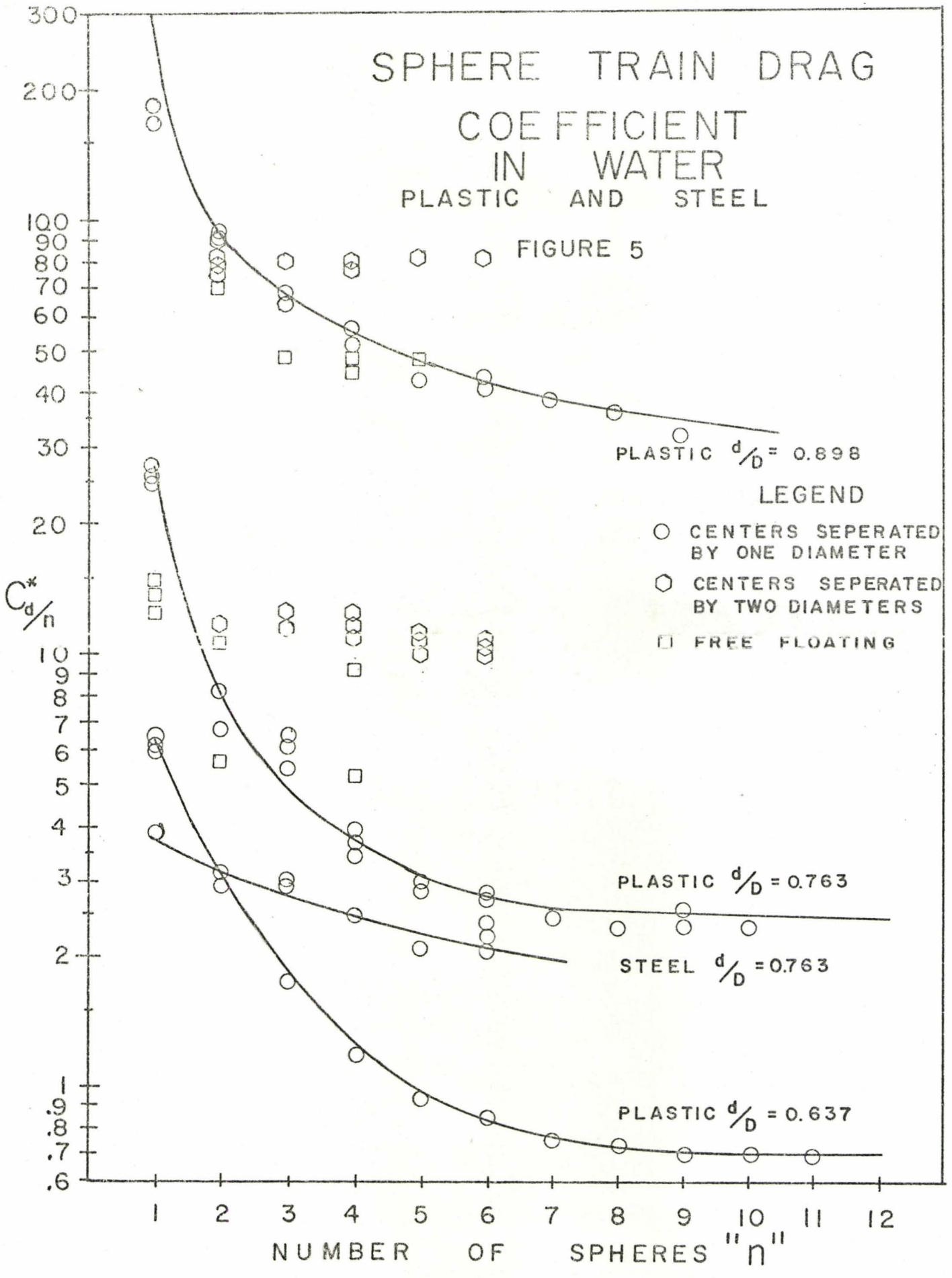
SPHERE TRAIN DRAG
COEFFICIENT
IN WATER
PLASTIC AND STEEL
FIGURE 5
PLASTIC d/D = 0.898
LEGEND
CENTERS SEPERATED BY ONE DIAMETER
CENTERS SEPERATED BY TWO DIAMETERS
FREE FLOATING
PLASTIC d/D = 0.763
STEEL d/D = 0.763
PLASTIC d/D = 0.637
C*d/n
NUMBER OF SPHERES "n"
300
200
100
90
80
70
60
50
40
30
20
10
9
8
7
6
5
4
3
2
1
.9
.8
.7
.6
1
2
3
4
5
6
7
8
9
10
11
12

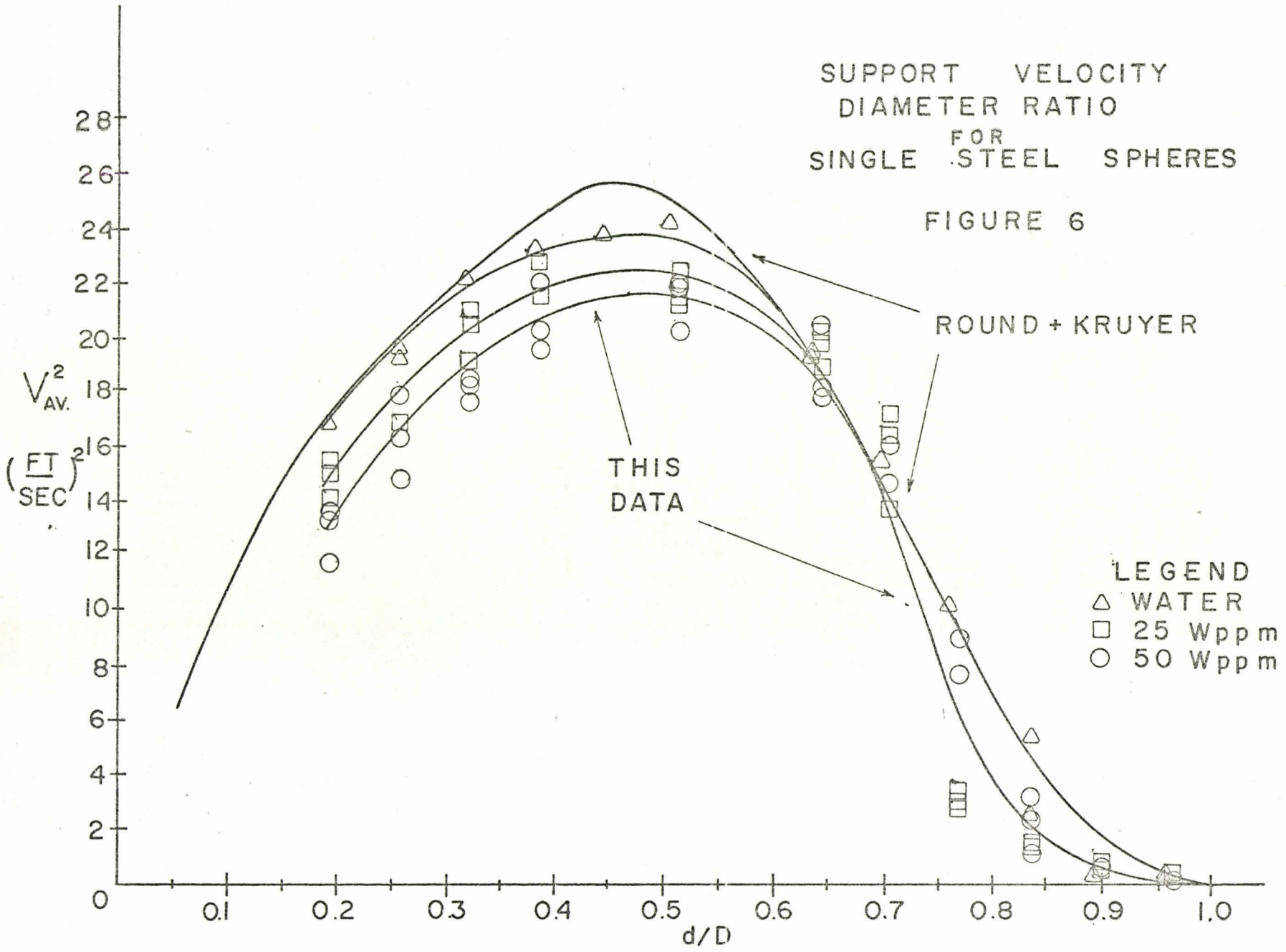
SUPPORT VELOCITY
DIAMETER RATIO
FOR
SINGLE STEEL SPHERES
FIGURE 6
ROUND + KRUYER
THIS DATA
LEGEND
WATER
25 Wppm
50 Wppm
$V^2_{AV.}$
$(\frac{FT}{SEC})^2$
d/D
0
2
4
6
8
10
12
14
16
18
20
22
24
26
28
0.1
0.2
0.3
0.4
0.5
0.6
0.7
0.8
0.9
1.0

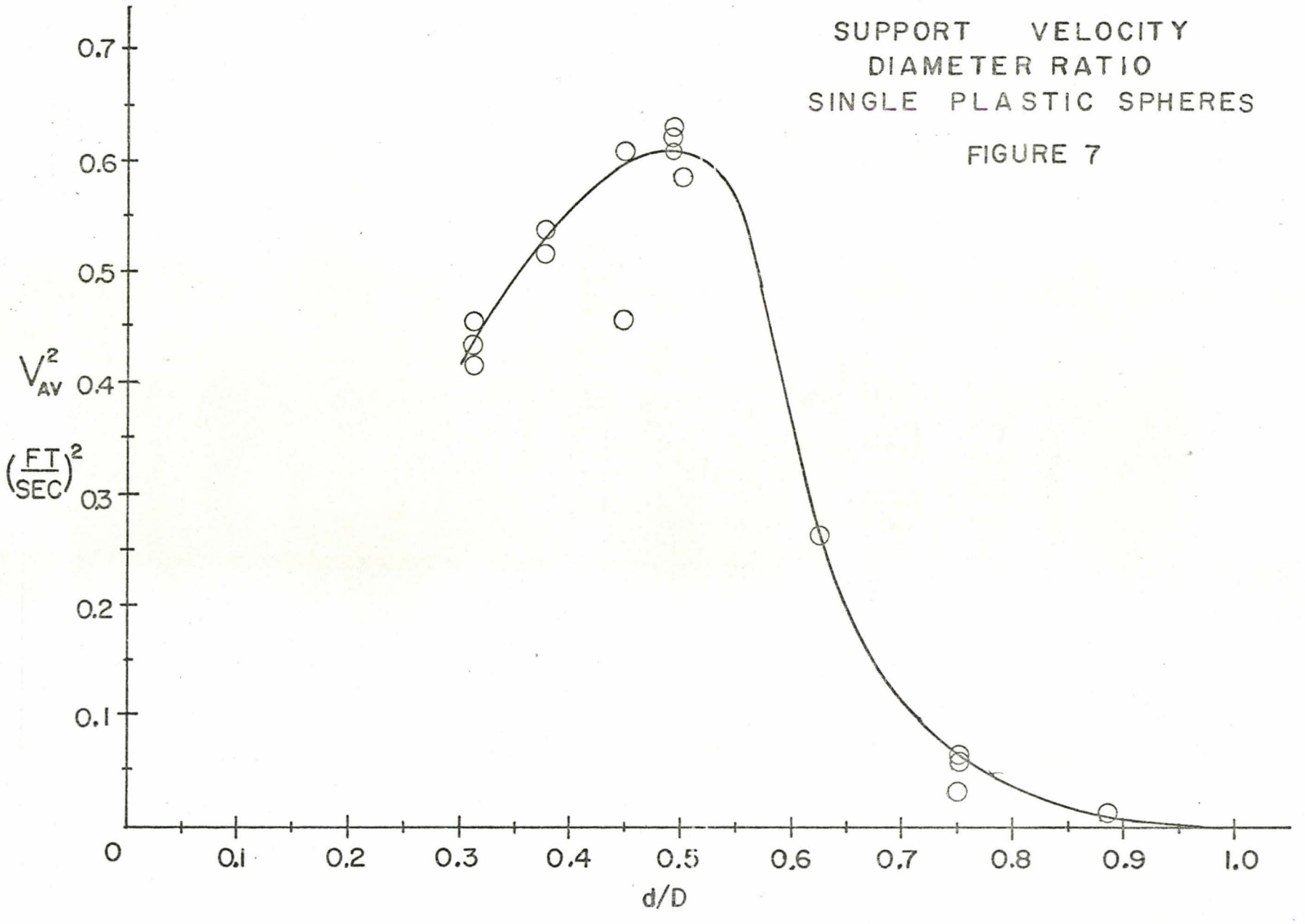
SUPPORT VELOCITY
DIAMETER RATIO
SINGLE PLASTIC SPHERES
FIGURE 7
V_{AV}^2
$\left(\frac{FT}{SEC}\right)^2$
0.7
0.6
0.5
0.4
0.3
0.2
0.1
0
0.1
0.2
0.3
0.4
0.5
0.6
0.7
0.8
0.9
1.0
d/D

SUPPORT VELOCITY

SINGLE SPHERES IN WATER
AND POLYMER
RETEN 423

FIGURE 8

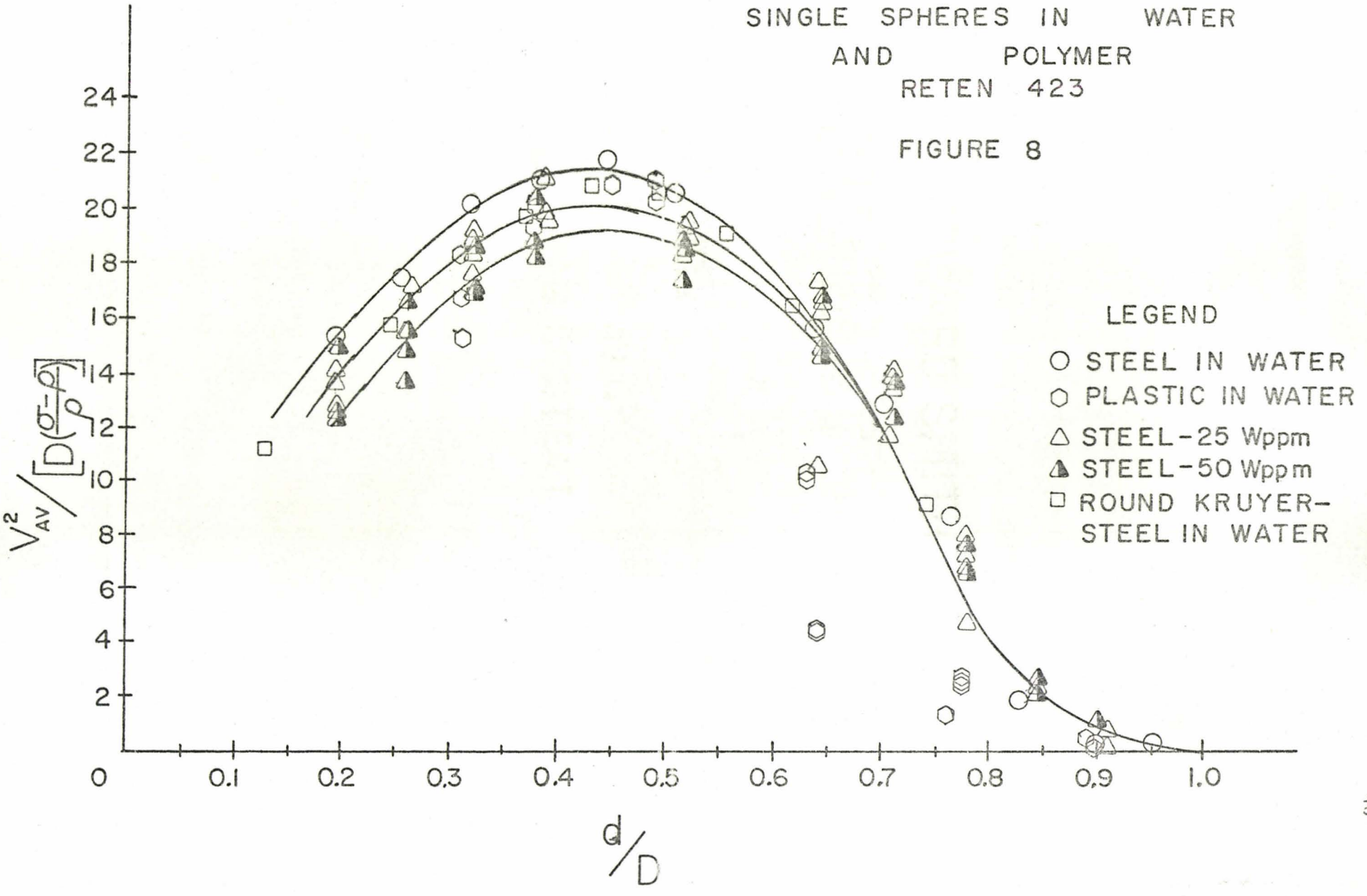

SPHERE TRAIN SUPPORT VELOCITIES

SEPERATION - d WATER ONLY

FIGURE 9

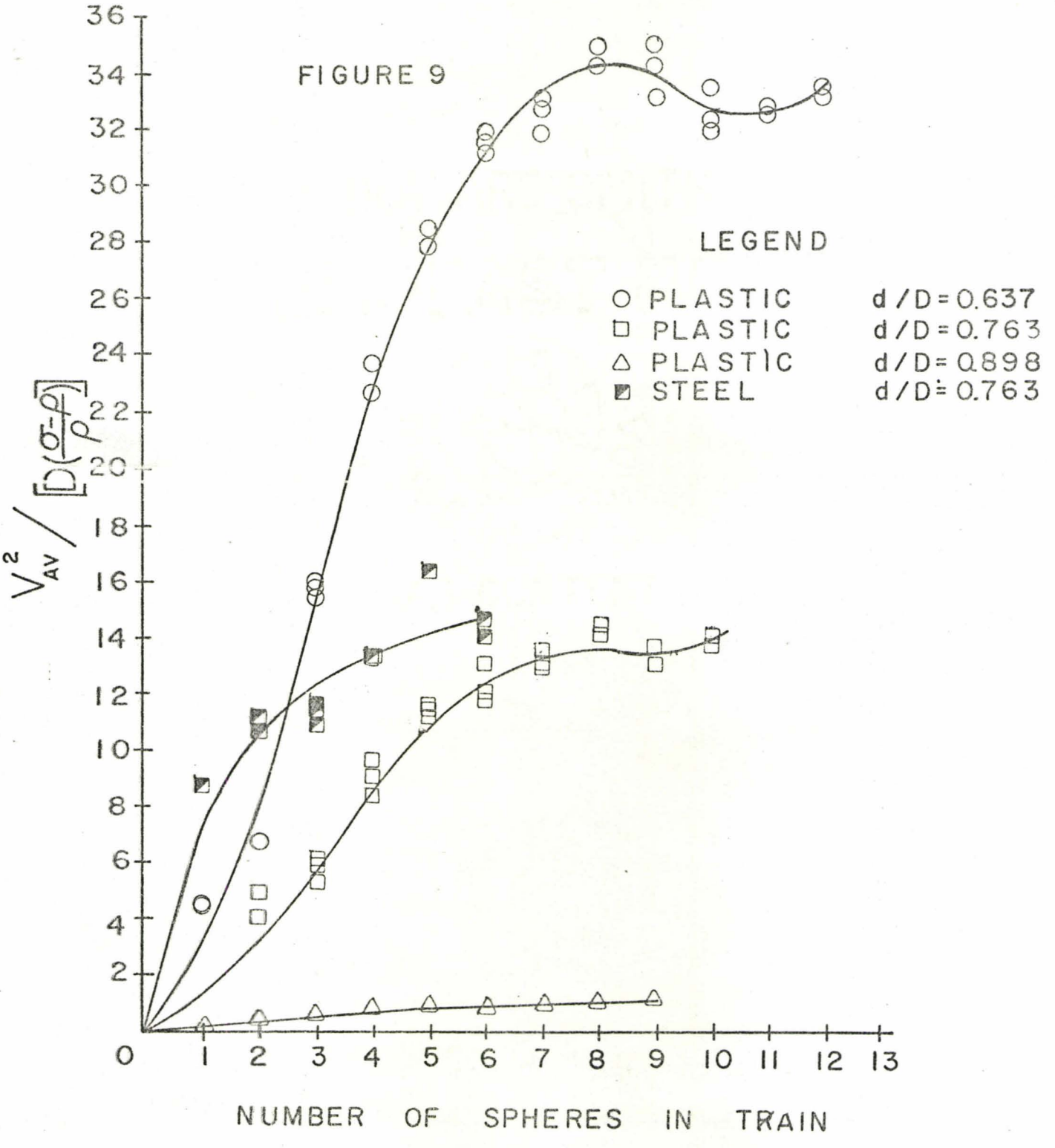

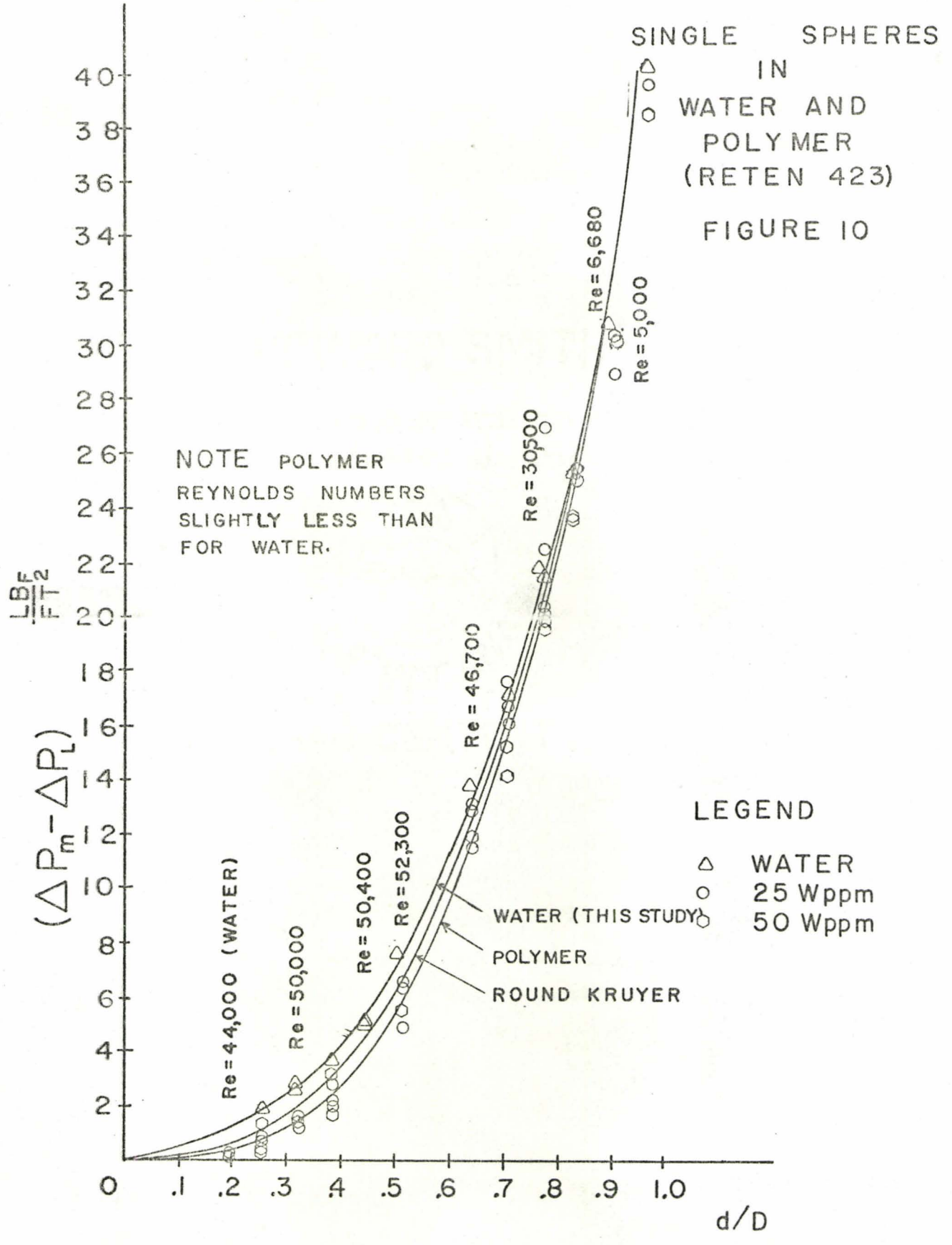
SINGLE SPHERES IN WATER AND POLYMER (RETEN 423)
FIGURE 10
NOTE POLYMER REYNOLDS NUMBERS SLIGHTLY LESS THAN FOR WATER.
$(\Delta P_m - \Delta P_L)$ $\frac{LB_F}{FT^2}$
d/D
Re = 44,000 (WATER)
Re = 50,000
Re = 50,400
Re = 52,300
Re = 46,700
Re = 30,500
Re = 6,680
Re = 5,000
WATER (THIS STUDY)
POLYMER
ROUND KRUYER
LEGEND
WATER
25 Wppm
50 Wppm

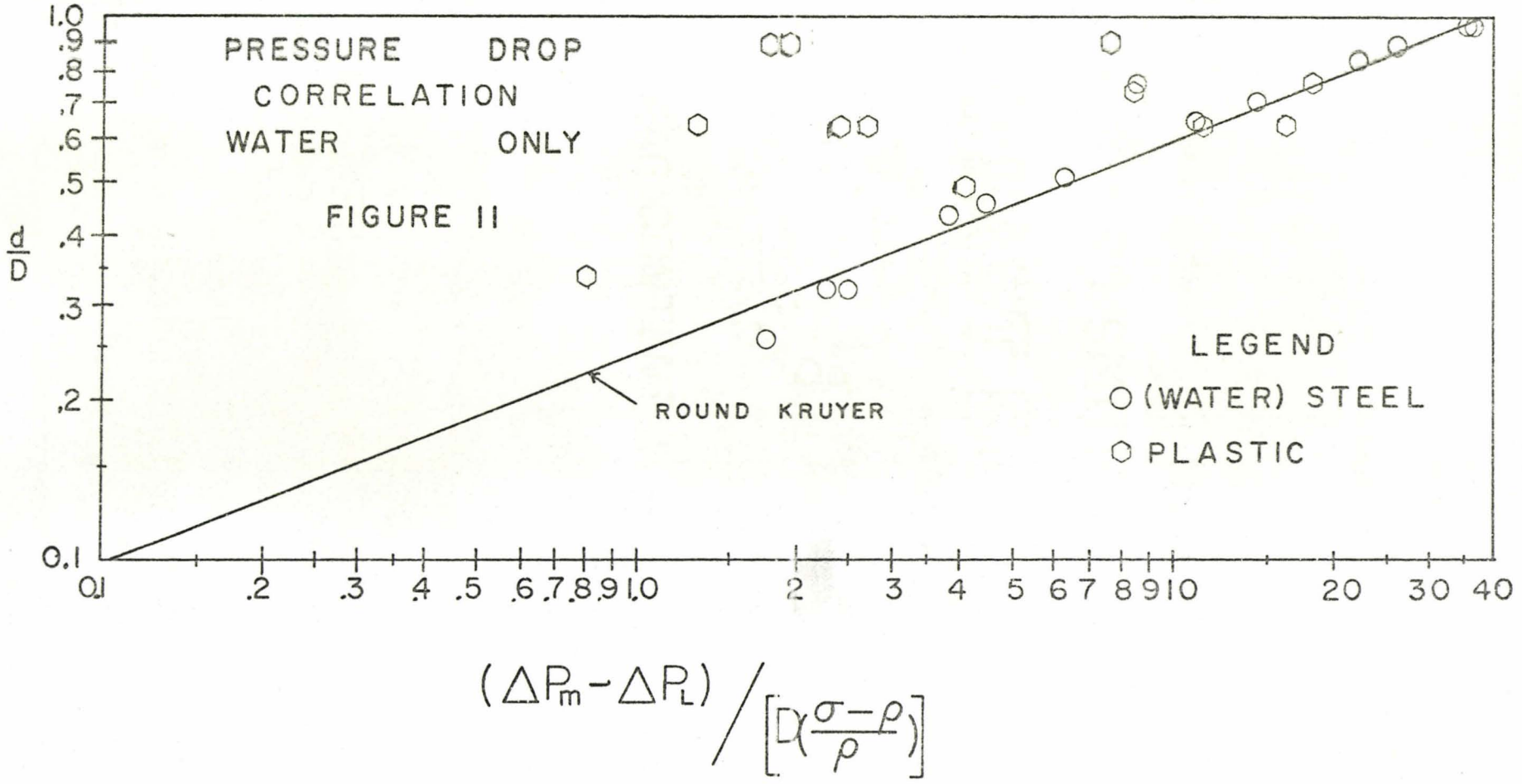
PRESSURE DROP
CORRELATION
WATER ONLY
FIGURE II
ROUND KRUYER
LEGEND
(WATER) STEEL
PLASTIC
d/D
1.0
.9
.8
.7
.6
.5
.4
.3
.2
0.1
0.1
.2
.3
.4
.5
.6
.7
.8
.9
1.0
2
3
4
5
6
7
8
9
10
20
30
40
$(\Delta P_m - \Delta P_L) \Big/ \left[D\left(\frac{\sigma-\rho}{\rho}\right)\right]$

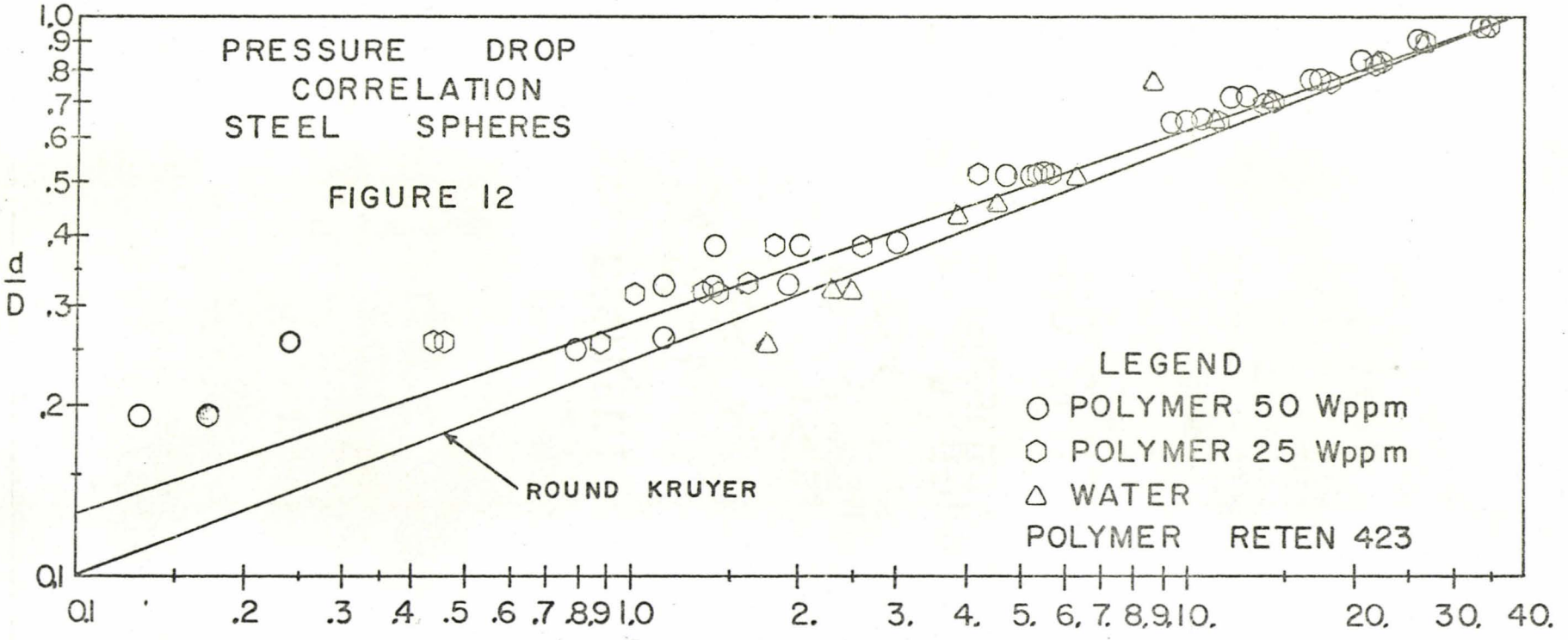

$$(\Delta P_m - \Delta P_L) \Big/ \left[D\left(\frac{\sigma - \rho}{\rho}\right) \right]$$

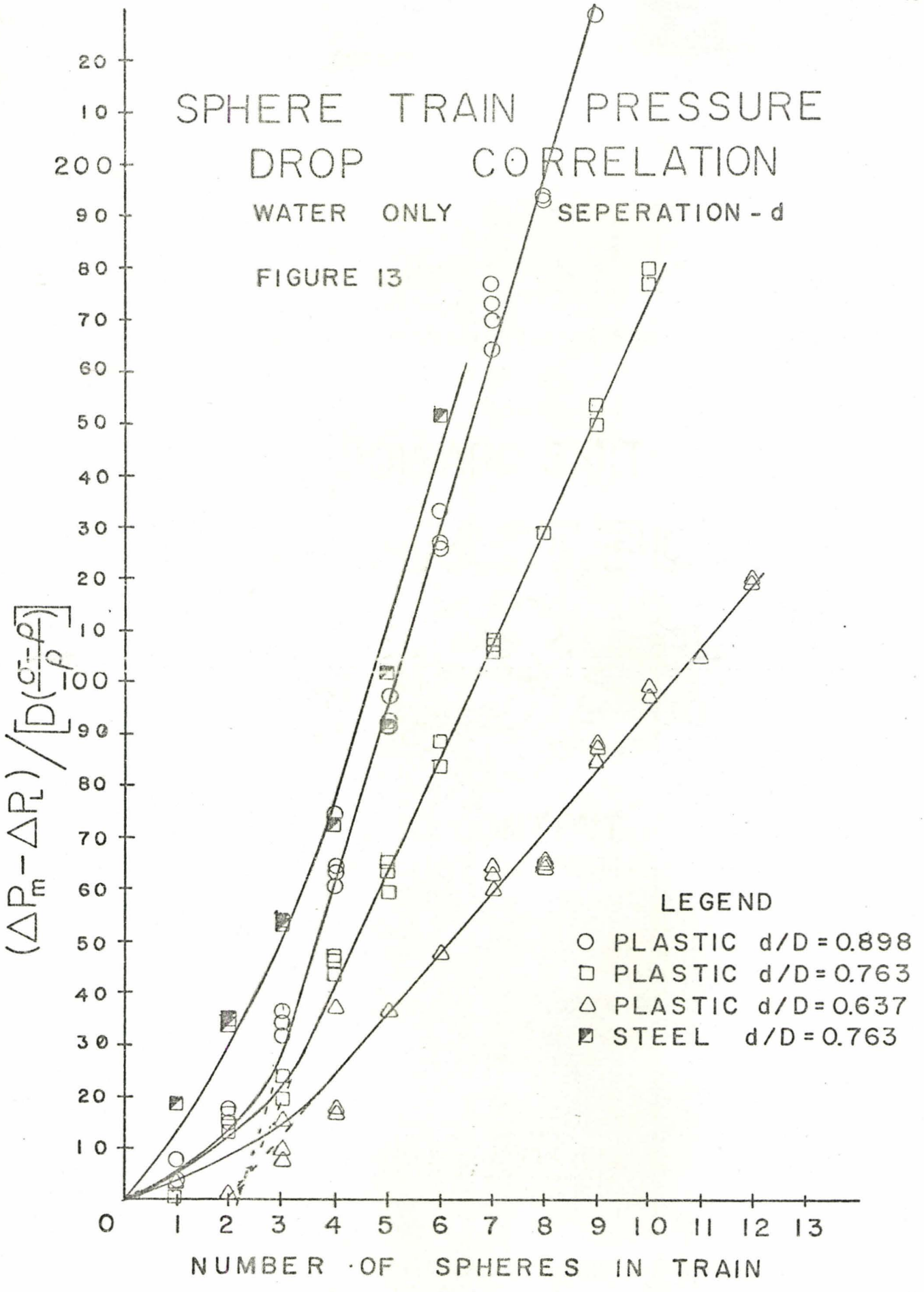
SPHERE TRAIN PRESSURE DROP CORRELATION
WATER ONLY
SEPERATION - d
FIGURE 13
$(\Delta P_m - \Delta P_L) / \left[D\left(\frac{\sigma - \rho}{\rho}\right)\right]$
NUMBER OF SPHERES IN TRAIN
LEGEND
PLASTIC d/D = 0.898
PLASTIC d/D = 0.763
PLASTIC d/D = 0.637
STEEL d/D = 0.763

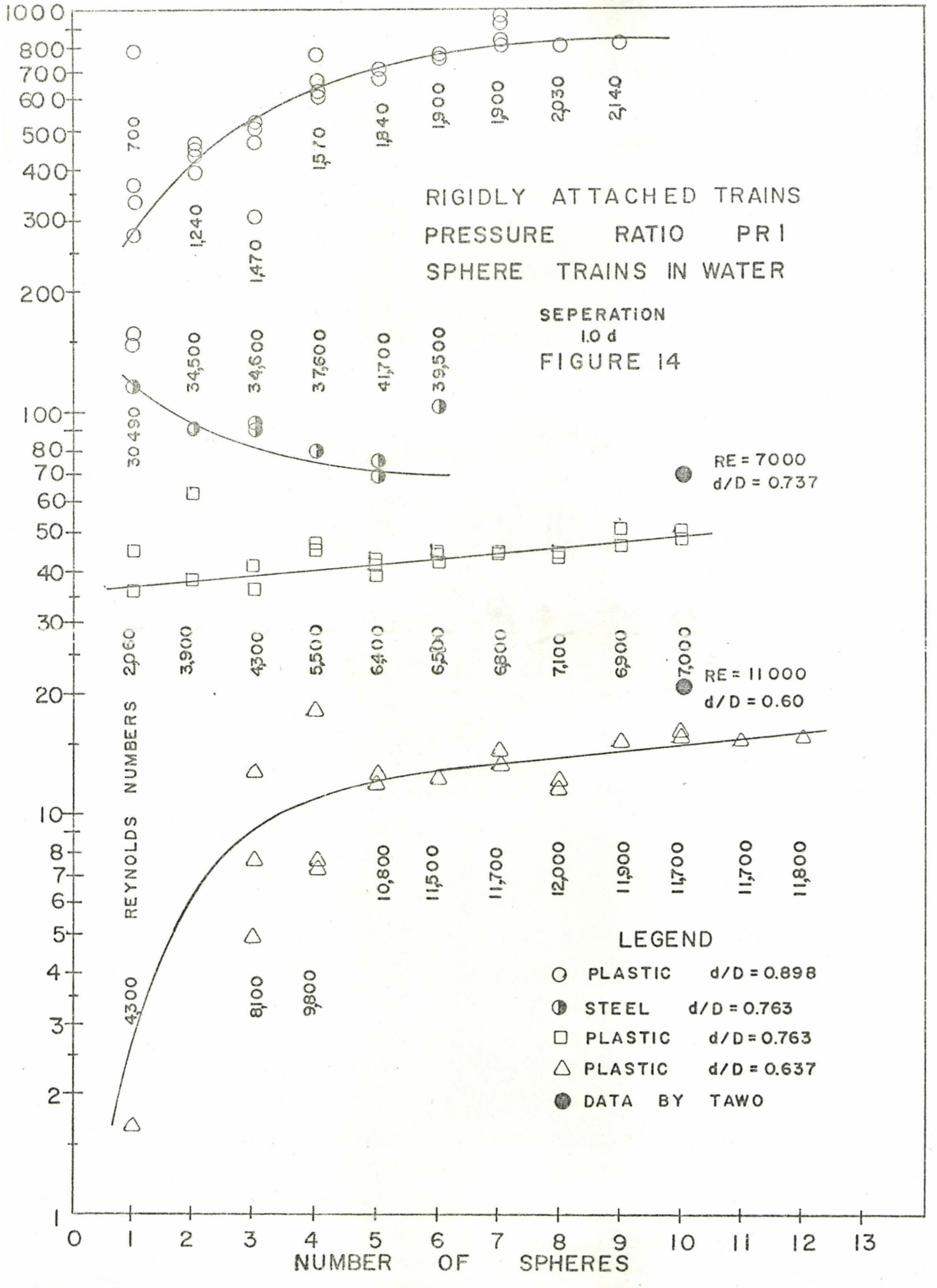
RIGIDLY ATTACHED TRAINS
PRESSURE RATIO PR1
SPHERE TRAINS IN WATER
SEPERATION
1.0 d
FIGURE 14
RE = 7000
d/D = 0.737
RE = 11000
d/D = 0.60
REYNOLDS NUMBERS
NUMBER OF SPHERES
LEGEND
PLASTIC d/D = 0.898
STEEL d/D = 0.763
PLASTIC d/D = 0.763
PLASTIC d/D = 0.637
DATA BY TAWO
700
1,240
1,470
1,570
1,840
1,900
1,900
2,030
2,140
30 490
34,500
34,600
37,600
41,700
39,500
2,060
3,900
4,300
5,500
6,400
6,500
6,800
7,100
6,900
7,000
4,300
8,100
9,800
10,800
11,500
11,700
12,000
11,900
11,700
11,700
11,800

VII DISCUSSION

One important portion of these experiments dealt with the study of the hydrodynamic suspension of single spheres in water and polymer solution. Referring to figure 4, a graph of the drag coefficient as a function of the diameter ratio for single steel spheres in water and polymer, it can be seen that the anticipated trend is followed. That is, at d/D = 0 for both water and polymer the curve extrapolates to an unbounded settling value of $C_{d_{WATER}}$ = 0.44 or $C_{d_{POLY.}}$ = 0.56 while asymptotically approaching $C_d^* = \infty$ as d/D approaches unity. The region between these limits is described by equation (3.1), chapter III where

$$C_d^* = \frac{4}{3} \left(\frac{\sigma - \rho}{\rho}\right) \frac{dg}{V_{AV}^2} \qquad (7.1)$$

This equation emphasises the dependence of the drag coefficient on the Froude number.

For water the data presented in figure 4 compares favourably to that of McNown and Newlin[2] and Round and Kruyer[21] although the tests by McNown and Newlin were performed at a constant Reynolds number with the sphere rigidly fixed in the center of the pipe, whereas the results of Round and Kruyer were determined using a freely suspended sphere in an inclined tube. When tests are performed using freely suspended spheres, which can absorb energy by movement in addition to the usual manner through skin friction and pressure change, an increase in the drag coefficient can be expected, as shown by the results of Round and Kruyer when compared to those of McNown and Newlin. The results of this study generally follow the same trend as those

of Round and Kruyer, but have more scatter because of the less accurate support velocity measurements.

There is, of course, a great discrepancy between the equation;

$$C_d^* = \left[\frac{d/D}{1 - (d/D)^2}\right]^2 \qquad (7.2)$$

and experimental results below d/D = 0.82; since this equation does not consider the effects of viscosity which are apparently predominant at the lower diameter ratios. At the higher diameter ratios the results of this study and those of references (2) and (21) agree. Figure 4 does not show results beyond a diameter ratio of 0.775 although tests were performed for diameter ratios up to 0.956. This is becuase the results in that range are adequately represented by equation (7.2).

When spheres are suspended in a dilute aqueous polymer solution the drag coefficients are similar to those obtained in water, as figure 4 shows, however, below a d/D ratio of 0.72 they are slightly greater than those for water. Equation (7.1) indicates that for C_d^* to increase in value, the supporting velocity V_{AV} must decrease, since for a given diameter ratio, all other factors remain constant.

It has been generally observed by other authors that the addition of polymer to turbulent pipe and flat plate flow decreases the skin friction. It is reasonable then to assume that along with the usual decrease in pressure drop accompanying a decrease in velocity, the polymer would further decrease the pressure drop due to skin friction along the wall of the pipe, as well as along the surface of the sphere. However, the weight of the sphere remains unchanged, therefore, the sum of the skin friction, and form drag components as well as buoyancy must still equal the weight of the sphere. This means that the form drag component must increase if the sphere skin friction decreases.

From figure 13, which shows the measured pressure drop across the sphere less the tube skin friction pressure drop, it can be seen that the pressure drop for polymer is less than that for water. Since it appears that the form pressure drop component is increased by the presence of polymer, then the pipe skin friction loss caused by the disturbance of flow around the sphere, and the skin friction component along the sphere, must have been greatly decreased to account for the net decrease.

For the case of a sphere settling in a unbounded polymer solution, White[15] explained the increased drag, when the boundary layer was turbulent, as being due to an increased wake diameter. For this case, of confined flow past a sphere, it would appear that the same situation exists, provided the diameter ratio is less than 0.72.

It is interesting to note that polymer effects become noticeable as viscous effects become predominant in the system; since it is apparently because of viscous effects that equation (7.2) becomes invalid at approximately the same diameter ratio as polymer effects become apparent.

A question that has been raised is, what effects can the addition of drag reducing polymer have on the dynamics of the transport of capsules through pipelines? Since the precise physical characteristics, such as the ratio of the capsule specific gravity to fluid specific gravity, and the capsule shape and dimensions, play a very important part (references (3) to (10) and (20)) in determining the flow characteristics of a sphere through a pipeline, a rigorous answer cannot be made on the basis of this study. However, it can be postulated from the data presented in figure 4 and figure 12 that at high diameter ratios (where most capsule pipelines operate) the addition of polymer would reduce the drag of the transporting fluid passing through the pipework, thereby speeding the transfer of capsules in addition to lowering the energy

requirements. Furthermore, if the pipelines were to be operated at lower diameter ratios, where the addition of polymer has increased the drag coefficient, it might be expected that a further increase in the speed of capsule transfer would ocuur.

Since the drag coefficient is calculated from the support velocity it is to be expected that graphs of V_{AV} show the same trend as those of C_d*. This is evident in figures 6 and 8, where the use of polymer produces a reduced supporting velocity; the velocity decreasing with increasing polymer concentration up to 50 Wppm at which point the maximum effect is observed.

In figures 6 and 8 the data of this study is also compared to that obtained by Round and Kruyer under similar circumstances. It can be seen that the support velocities obtained by Round and Kruyer[21] are above those of this study. The reason for this is that spheres freely suspended in an inclined tube do not have the same degree of freedom that spheres suspended in a vertical tube have. In an inclined tube the spheres would rest on the wall, partly restricting their motion and ability to absorb energy through modes other than skin friction and pressure change. This would result in a decreased drag coefficient and increased support velocity, compared to that observed for a sphere suspended in a vertical tube. This type of effect was observed earlier, when the results of Round and Kruyer were compared to those of McNown and Newlin. The latter's results were for a sphere rigidly fixed in a tube, and showed a drag coefficient that was slightly less than that observed by Round and Kruyer for their freely suspended spheres.

In figure 8 an attempt has been made to correlate all available data to a single set of curves by taking into account the specific gravity ratio and the diameter of the test section. The resulting grouping of variables then is $V_{AV}^2/[D(\sigma - \rho)/\rho]$. The justification for this particular

grouping is that the drag coefficient analysis (see chapter III) indicated that the drag coefficient was a function of the Froude Number, and the above group is a form of the Froude Number. The diameter of the pipe has been used, rather than that of the sphere to allow data from different diameter test sections to be compared.

A similar type of correlation has been attempted with the pressure drops, as was done with the support velocities. The term $(\Delta P_m - \Delta P_L)$ was divided by $[D(\sigma - \rho/\rho)]$ and plotted against d/D, logarithmically. By doing this it appears that the data can be correlated using straight lines, as shown in figures 11 and 12. The resulting equations are, for water;

$$\ell n(d/D) = 0.395\ \ell n\left\{(\Delta P_m - \Delta P_L)/[D(\frac{\sigma - \rho}{\rho})]\right\} - 1.408 \qquad (7.3)$$

and for polymer;

$$\ell n(d/D) = 0.331\ \ell n\left\{(\Delta P_m - \Delta P_L)/[D(\frac{\sigma - \rho}{\rho})]\right\} - 1.271 \qquad (7.4)$$

The values for steel spheres in water agree very well with equation (7.3), and the results of Round and Kruyer[21]. The polymer results display a greater scatter than do those for water, but this can be expected because of the difficulties encountered in maintaining sphere stability while at the same time maintaining the appropriate polymer concentration. It is possible that this scatter conceals two separate lines, one for 25 and one for 50 Wppm polymer as was the case for the support velocity (V_{AV}^2 vs d/D). However, the graph of $(\Delta P_m - \Delta P_L)$ as a function of d/D for single spheres supported in a polymer solution, also had only a single line for both polymer concentrations. It is therefore possible that the effects on the pressure drop

of increasing the polymer concentration beyond 25 Wppm are so slight as to be negligible.

The results for plastic spheres in water however show considerable scatter. From the Error Analysis, Appendix I, the estimated error in this range of measurement was about $\pm$ 200%. The reason for this is that the manometer no flow reading is considerably larger than the actual pressure drop reading.

From a consideration of single spheres we now turn to the consideration of trains of spheres. Figure 5 shows the variation of "drag coefficient per sphere", as a function of the number of spheres in the train, for both rigidly and flexibly attached trains of plastic and steel spheres. It can be seen that C_d^*/n becomes virtually independent of the number spheres in the train, once the length is beyond approximately eight or nine spheres. This trend is also evident in figure 13, a graph of sphere train pressure drop $(\Delta P_m - \Delta P_L)/D[\frac{\sigma - \rho}{\rho}]$ as a function of n, the number of spheres in the train.

From figure 5 it can be seen that the drag coefficients for unattached and flexibly attached sphere trains are greater than those for rigidly attached trains. The reason for this is that being less restricted the flexible sphere trains were able to absorb energy by movement, in addition to the usual manner, through skin friction and pressure change.

The single spheres had extremely complex modes of oscillation, which were partly carried over to the sphere trains. The very small single spheres alternated between clinging to the wall of the test section and bouncing back and forth on the wall. As the diameter ratio increased the excursion distance from the wall increased, until at a diameter ratio of approximately 0.5 the spheres were centalized in the flow, and rocked gently back and forth. As the diameter ratio approached 0.7 the rocking decreased,

and occasionally changed to violent spinning about the inside wall of the test section. This spinning action restricted the degrees of freedom of the spheres and consequently decreased the drag coefficient. The above described modes of oscillation of single spheres were also evident in the trains of both flexible and rigidly attached spheres. The motion of the unattached spheres was in every respect identical to that of the single spheres, while the motions of the flexibly attached trains were slightly restricted by the connections. The flexibly attached spheres tended to rotate in the free stream, or roll about the inside wall of the test section. For both these motions the centers of the individual spheres were approximately 120 to 180 degrees out of phase with those of the adjacent ones (ie., a spiralling motion). The rigidly attached trains were centered in the free stream, and moved with a pitching or rocking motion, or rolled or transgressed about the inside wall of the pipe.

A graph of $V_{AV}^2/[D(\frac{\sigma - \rho}{\rho})]$ similar to that for the single spheres, has been plotted for the trains of spheres and is shown in figure 9. As expected the same trend that was evident in figure 5 and 13 is evident in this graph; that is, the support velocity increases with increasing numbers of spheres until the train is seven or eight spheres long. At this point however the behaviour deviates from the expected. Rather than the support velocity becoming constant it decreases, then starts to increase again, when four or five more spheres have been added. Apparently this effect is related to the end effects, and the length of developed flow achieved along the spheres, although the precise mechanism cannot be postulated.

It was stated in the chapter on theory (chapter III) that the sphere train end effects could be determined from a graph of $\Delta P_m - \Delta P_L$ against n. Figure 13 is such a graph, showing $(\Delta P_m - \Delta P_L)/[D(\frac{\sigma - \rho}{\rho})$ as a function of n.

It was shown in chapter III, that the end effects, pressure drops, and the number of spheres could be related by the following equation;

$$(\Delta P_m - \Delta P_L) = (\frac{\Delta P_S}{L})\ (n - 1)d + \Delta P_E \qquad (3.15)$$

By obtaining the value of $\Delta P_m - \Delta P_L$ from figure 13 for two different values of n, it is possible using equiption (3.15) to compute values for $\Delta P_S/L$ and ΔP_E. Substituting for the sphere train having d/D = 0.898, for n = 4, and n = 5, (plastic);

$$60 \times 0.043 = (\frac{\Delta P_S}{L})(3)(\frac{1.74}{12}) + \Delta P_E$$

and

$$195 \times 0.043 = (\frac{\Delta P_S}{L})(7)(\frac{1.74}{12}) + \Delta P_E$$

solving;

$$\frac{\Delta P_S}{L} = 10.05\ lb_F/ft^2/ft$$

$$\Delta P_E = -1.78\ lb_F/ft^2$$

The negative sign in ΔP_E indicating that it is a pressure decrease. For a sphere train having d/D = 0.763, for n = 4, and n = 8, (plastic);

$$41 \times 0.0394 = (\frac{\Delta P_S}{L})(3)(\frac{1.478}{12}) + \Delta P_E$$

and

$$129 \times 0.0394 = \left(\frac{\Delta P_S}{L}\right)(7)\left(\frac{1.478}{12}\right) + \Delta P_E$$

therefore

$$\frac{\Delta P_S}{L} = 7.0 \text{ lb}_F/\text{ft}^2/\text{ft}$$

$$\Delta P_E = -0.96 \text{ lb}_F/\text{ft}^2$$

For a sphere train having d/D = 0.763, for n = 4, and n = 6, (steel);

$$79. \times 1.169 = \left(\frac{\Delta P_S}{L}\right)(3)\left(\frac{1.497}{12}\right) + \Delta P_E$$

$$144 \times 1.169 = \left(\frac{\Delta P_S}{L}\right)(7)\left(\frac{1.497}{12}\right) + \Delta P_E$$

therefore

$$\frac{\Delta P_S}{L} = 305 \text{ lb}_F/\text{ft}^2/\text{ft}$$

$$\Delta P_E = -21.7 \text{ lb}_F/\text{ft}^2$$

For a sphere train having d/D = 0.637, for n =4, and n = 8, (plastic);

$$85.0 \times 0.0465 = \left(\frac{\Delta P_S}{L}\right)(3)\left(\frac{1.235}{12}\right) + \Delta P_E$$

$$70. \times 0.0465 = \left(\frac{\Delta P_S}{L}\right)(7)\left(\frac{1.235}{12}\right) + \Delta P_E$$

therefore

$$\left(\frac{\Delta P_S}{L}\right) = 5.1 \text{ lb}_F/\text{ft}^2/\text{ft}$$

$$\Delta P_E = -0.415 \text{ lb}_F/\text{ft}^2$$

It is evident that as the diameter ratio decreases the pressure gradient $\Delta P_S/L$ and the end effects also decrease.

The final quantity of interest is the pressure ratio PR1 which is shown in figure 14 plotted as a function of n, the number of spheres. The quantity PR1 is a ratio of the pressure gradient in the free tube, to that in the tube occuplied by the sphere train and is a function of the diameter ratio and Reynolds number also. Knowing this ratio, and the pressure gradient in the free tube, would, if PR1 is sufficiently general, allow the pressure gradient in a tube containing a stationary sphere train to be predicted. To determine how general this ratio is, a comparison of PR1 obtained under two slightly different conditions has been made. The data obtained by Tawo[28] for a train rigidly fixed to the tube wall was compared to the data of this present study wherein the train was freely suspended in a vertical tube.

The data of this study, presented in figure 14 can be described by equation (3.20) (chapter III), however, to compare it to that obtained by Tawo requires that the end effects be eliminated as in equation (3.19) (chapter III).

$$PR1 = 1 + \frac{L}{(n-1)d}\left[\frac{\Delta P_m}{\Delta P_L} - \frac{\Delta P_E}{\Delta P_L} - 1\right] \qquad (3.19)$$

Substituting into equation (3.19), for the plastic spheres having d/D = 0.763 at the point where n = 10, which is the point at which this data can best be compared to that of Tawo.

$$PR1 = 1 + \frac{5.0}{9 \times 1.978}\left[\frac{7.37}{.560} + \frac{.96}{.560} - 1\right]$$

therefore

$$PR1 = 63.5$$

which compares favourably with the result PR1 = 68 achieved by Tawo.

VIII CONCLUSIONS

On the basis of analysis and experimental results presented earlier, the following conclusions can be made;

(1) For steel spheres dynamically suspended in a dilute aqueous polymer solution within a cylindrical boundary, the drag coefficient in the range $0 < d/D < 0.7$ is increased over that observed in water. Apparently this increase in drag coefficient is accompanied by a decrease in skin friction pressure drop along the pipe wall and along the sphere surface, and an increase in form pressure drop across the sphere.

(2) For single spheres hydrodynamically suspended in water the pressure drop can be expressed by the implicit equation;

$$\ell n(d/D) = 0.395\ \ell n\left\{ (\Delta P_m - \Delta P_L)/[D(\frac{\sigma - \rho}{\rho})]\right\} - 1.408$$

(3) For a single sphere suspended in dilute aqueous polymer solutions the pressure drop can be expressed by the implicit equation;

$$\ell n(d/D) = 0.331\ell n\left\{ (\Delta P_m - \Delta P_L)/[D(\frac{\sigma - \rho}{\rho})]\right\} - 1.271$$

(4) For sphere trains dynamically suspended in water, within a cylnindrical boundary, the drag coefficient per sphere is a function of the diameter ratio, the specific gravity ratio, and the method of connecting the spheres. For rigidly connected spheres the drag

coefficient per sphere is less than for flexibly attached ones. The drag coefficient per sphere in the rigidly attached trains decreased to an approximately constant value as the number of spheres approached nine.

(5) For trains of rigidly attached spheres dynamically suspended in water, the pressure drop $(\Delta P_m - \Delta P_L)/[D(\frac{\sigma}{\rho} - \rho)]$ is a linear function of the number of spheres in the train, and a function of the diameter ratio and specific gravity ratio of the spheres, provided the number of spheres in the train is greater than five.

(6) For trains of spheres the ratio of the pressure gradient along the sphere train to the pressure gradient in the free pipe, becomes a constant value once the number of spheres in the train is greater than nine. This final value of PRl is a function of the diameter ratio and specific gravity ratio of the suspended spheres as well as the pipe Reynolds number. The values for PRl obtained in this study are in agreement with those obtained by Tawo.

IX REFERENCES

1. Toms, B. A. "Some Observations on the Flow of Linear Polymer Solutions Through Straight Tubes at Large Reynolds Numbers." Proc. Int. Rheological Congress II, pages 135-141. Schreveninger Netherlands, 1948.
2. McNown, J. S. and Newlin, J. T. "Drag of Spheres Within Cylindrical Boundaries." Proc. Ist.U.S. Natl. Congr. Appl. Mech. Chicago, 1951, pages 801-806.
3. Hodgson, G. N. and Charles, M. E. "The Pipeline Flow of Capsules; part 1; The Concept of Capsule Pipelining." Can. J. Chem. Eng. V. 41 (2), 1963, pages 46-51.
4. Charles, M. E. "The Pipeline Flow of Capsules; part 2; Theoretical Analysis of the Concentric Flow of Cylindrical Forms." Can. J. Chem. Eng. V. 41 (2), 1963, pages 46-51.
5. Ellis, H. S. "The Pipeline Flow of Capsules; part 3; An Experimental Investigation of the Transport by Water of Single Cylindrical and Spherical Capsules With Density Equal to That of the Water." Can. J. Chem. Eng. V 42 (1), 1964, pages 1-8.
6. Ellis, H. S. "The Pipeline Flow of Capsules; part 4; An Experimental Investigation of the Transport in Water of Single Cylindirical Capsules With Density Greater Than That of Water." Can. J. Chem. Eng. V 42 (2), 1964, pages 69-76.
7. Ellis, H. S. "The Pipeline Flow of Capsules; part 5; An Experimental Investigation of the Transport by Water of Single Spherical Capsules With Density Greater Than That of the Water." Can. J. Chem. Eng. V. 42 (5), 1964, pages 201-210.

8. Newton, R., Redberger, P. J. and Round G. F. "The Pipeline Flow of Capsules; part 6; Numerical Analysis of Some Variables Determining Free Flow." Can. J. Chem. Eng. V. 42 (4), 1964, pages 168-173.

9. Ellis, H. S. and Bolt, L. H. "The Pipeline Flow of Capsules; part 7; An Experimental Investigation of the Transport by Two Oils of Single Cylindrical and Spherical Capsules With Density Equal to That of the Oil." Can. J. Chem. Eng. V. 42 (5), 1964, pages 201-210.

10. Round, G. F. and Bolt, L. H. "The Pipeline Flow of Capsules; part 8; An Experimental Investigation of the Transport in Oil of Single Denser than Oil Spherical and Cylindrical Capsules." Can. J. Chem. Eng. V. 43 (4), 1965, pages 197-205.

11. Olsen, R. M. Essentials of Engineering Fluid Mechanics International Textbook Co., 1965.

12. Elata, C. and Tirosh, J. "Frictional Drag Reduction." Isreal J. Techn. V. 3 N1, 1965, pages 1-6.

13. Gadd, G. E. "Turbulence Damping and Drag Reduction Produced by Certain Additives in Water." Nature V. 206, May 1, 1965, pages 463-467.

14. Gadd, G. E. "Reduction of Turbulent Friction in Liquids by Dissolved Additives." Nature V. 212, November 26, 1966, pages 874-877.

15. White, A. "Turbulent Drag Reduction with Polymer Additives." J. Mech. Eng. Scie. V. 8 N4, 1966, pages 452-455.

16. Chenard, J. H. "Drag of Spheres in Dilute Aqueous Solutions of Poly (Ethyline Oxide) Within the Region of the Critical Reynolds Number." Master's thesis. United States Naval Postgraduate School, Monterey, Calif., AD 828254, (1967).

17. Ernst, W. D. "Turbulent Flow of an Elasticoviscous Non-Newtonian Fluid." AIAA Journal, V. 5 N5, May 1967, pages 906-909.

18. Goren, Y. and Norbury, J. F. "Turbulent Flow of Dilute Aqueous Polymer Solutions." Fluids Engineering Division Winter Annual Meeting, Pittsberg, Pa., Nov. 1967, ASME paper N67-WA/FE-3.

19. Granville, P. S. "The Frictional Resistance and Velocity Similarity Laws of Drag Reducing Polymer Solutions." NSRDC Report 2502 (Sept. 1967) also J. Ship Research V. 12 N3, September 1968.

20. Jan Kruyer, and Redberger, "The Pipeline Flow of Capsules; part 9." Journal of Fluid Mechanics V. 30 (3), 1967, pages 513-531.

21. Round, G. F. and Kruyer, J. "Experiments on the Suspension of Spheres in Inclined Tubes. I-Suspension by Water in Turbulent Flow". Chem. Eng. Scie. 1967, V. 22, pages 1133-1145.

22. Virk, P. S., Merrill, E. W., Mickley, H. S., Smith, K. A., Mollo-Christensen, E. L. "The Toms Phenomenon; Turbulent Pipe Flow of Dilute Polymer Solutions." J. Fluid Mech., 1967, V. 30 part 2, pages 305-328.

23. Wells, C. S. and Spangler, J. S. "Injection of a Drag Reducing Fluid into Turbulent Pipe Flow of a Newtonian Fluid." The Physics of Fluids, V. 10 N9, Sept. 1967, pages 1890-1894.

24. White, A. "Drag of Spheres in Dilute High Polymer Solutions." Nature V. 216, Dec. 9, 1967, pages 994-995.

25. White, F. M. "An Analysis of Flat Plate Drag With Polymer Additives." J. Hydronautics V. 2 N4, Oct. 1968, pages 181-186.

26. Corino, E. R. and Brodkey, R. S. "A Visual Investigation of the Wall Region in Turbulent Flow." J. Fluid Mech. (1969) V. 37, pages 1-30.

27. Seyer, F. A. and Metzner, A. B. "Turbulence Phenomenon in Drag Reducing Systems." AIChE J., May 1969, pages 426-434.

28. Tawo, E. N. "An Experimental Study of Incompressible Turbulent Flow in Pipes Containing Sphere Trains." Master's thesis, McMaster University,

November 1969.

29. Gordon, R. J. "On the Explanation and Correlation of Turbulent Drag Reduction in Dilute Macromolecular Solutions." J. Appl. Polymer Scie. V. 11, 1970, pages 2097-2105.

30. Gordon, R. J. "Mechanism for Turbulent Drag Reduction in Dilute Polymer Solutions." Nature V. 227, August 8, 1970, pages 699-700.

31. Seyer, F. A. "Friction Reduction in Turbulent Flow of Polymer Solutions." J. Fluid Mech. 1970, V. 40 part 4, pages 807-819.

32. Stow Jr., F. S. and Elliott, J. H. "Drag on A Tethered Ball in a Solution of Drag Reducing Polymers." Polymer Letters V. 8, 1970, pages 611-615.

33. Verma, S. K. "Turbulent Drag Reductions in Tubes with Polymer Solutions." McMaster University, Master's thesis (1970).

34. Virk, P. S., Mickley, H. S., and Smith, K. A. "The Ultimate Asymptote and Mean Flow Structure in Toms Pnenomenon." Trans, ASME J. Appl. Mech., June 1970, pages 488-493.

35. Granville, P. S. "Limiting Conditions to Similarity Law Correlations for Drag Reducing Solutions." NSRDC Report 3635, Aug. 1971.

36. Rubin, A. and Elata, C. "Turbulent Flow of Dilute Aqueous Polymer Solutions." AIChE J. V. 17 N4, July 1971, pages 990-996.

37. Virk, P. S. "An Eslastic Sublayer Model for Drag Reduction by Dilute Solutions of Linear Macro Molecules." J. Fluid Mech. 1971, V. 45 part 3, pages 417-440.

38. Rudd, M. J. "Velocity Measurements made with a Laser Doplometer on the Turbulent Pipe Flow of a Dilute Polymer Solution." J. Fluid Mech. 1972, V. 51 part 4, pages 673-685.

39. Wade, J. H. T. and Kumar, P. "Electron Microscope Studies of Polymer Degradation." J. Hydrodynamics, V. 6 N1, Jan. 1972, pages 40-45.

40. Schlicting H. Boundary Layer Theory, McGraw Hill, Sixth Ed.

41. Czaban, Z. J. G. "Polymer Effects on Centrifugal Pumping." McMaster University, Dept. of Mech. Eng. Publication, March 1972.

42. Hoyt, J. W. "The effect of Additives on Fluid Friction". J. of Basic Eng. June 1972.

APPENDIX I

ERROR ANALYSIS

It is difficult to exactly specify the error in any given measurement or calculation, usually however a range can be specified. It is customary when a large number of readings are taken to specify the measurement as being within a given number of standard deviations from the mean of the readings. Such a measure gives the degree of reproducibility, or precision of a measurement.

The accuracy of a measurement however is a measure of how close the value is to the "true" value; it is obvious that a measurement can have good precision but poor accuracy. In this chapter an attempt will be made to estimate the accuracy of the results.

In table 1 are listed estimates of the accuracy of the primary measurements made in this experiment. They are based on the type of instrument they were recorded with and the experience gained in using them.

I-1 Error in V_{AV} - Without Polymer

The accuracy of the measurement V_{AV} is based on the accuracy of the component measurements using the "most probable" method to estimate the errors. Now,

$$V_{AV} = \frac{GPM}{D^2} \times K$$

where

$$K = \frac{4}{\pi \times 6.229 \times 60}$$

then

TABLE I

ERROR ESTIMATES IN MEASURED QUANTITIES

Description	Symbol	Error
Tube diameter	D	$\pm$ 1.0%
Sphere diameter Steel	d	$\pm$ 0.1%
Plastic		$\pm$ 0.9%
Rotameter reading	GPM	#1 (15-40 GPM) $\pm$ 5 $\rightarrow$ $\pm$ 1%
		#2 (1-14 GPM) $\pm$ 7 $\rightarrow$ $\pm$ 1%
		#3 (0-5 GPM) $\pm$ 5 $\rightarrow$ $\pm$ 1%
Polymer flowmeter	$\dot{m}_p$	$\pm$ 10 $\rightarrow$ $\pm$ 4%
Distance between pressure taps	L	$\pm$ .1%
Error in manometer reading	h_m	$\pm$ 20 $\rightarrow$ $\pm$ 1% (Both legs combined)
Error in manometer inclination (sin Θ)		$\pm$ 0.05%
SG of manometer fluid	γ_m	$\pm$ .08%
Error in weighing spheres Steel		$\pm$ .5%
Plastic		$\pm$ 1.0%
Variation in weight of polymer powder	m_p	$\pm$ 2%
Error in water in polymer mix	m_w	$\pm$ 0.3%
Error in water temperature	T_w	$\pm$ 1°C

$$d(V_{AV}) = \sqrt{\Sigma \left(\frac{\delta V_{AV}}{\delta x} * dx\right)^2}$$

therefore

$$d(V_{AV}) = \left\{ \left[\frac{d(GPM)}{D^2}\right]^2 + [2(GPM)d(D)]^2 \right\}^{1/2}$$

Dividing by V_{AV} we have;

$$\frac{d(V_{AV})}{V_{AV}} = \left\{ \left[\frac{d(GPM)}{GPM}\right]^2 + \left[\frac{2d(D)}{D^2}\right]^2 \right\}^{1/2}$$

I From table 1 using the estimatederror in the rotameters at low flow rates;

Rotameter #1

$$\frac{d(V_{AV})}{V_{AV}} = \left\{ [5]^2 + [2(1)]^2 \right\}^{1/2} = \pm 5.4\%$$

Rotameter #2

$$\frac{d(V_{AV})}{V_{AV}} = \left\{ [7]^2 + [2(1)] \right\}^{1/2} = \pm 7.3\%$$

Rotameter #3

$$\frac{d(V_{AV})}{V_{AV}} = \left\{ [5]^2 + [2(1)] \right\}^{1/2} = \pm 5.9\%$$

II Similarly from table 1 at high flow rates we have;

$$\frac{d(V_{AV})}{V_{AV}} = \left\{[1]^2 + [2(1)]^2\right\}^{1/2} = \pm 2.2\%$$

I-2 Error in V_{AV} with Polymer

With polymer V_{AV} is;

$$V_{AV} = (GPM_{WATER} + GPM_{POLY.}) \frac{K}{D^2}$$

I At low flow rates; (using rotameter #2)

$$\Delta GPM_{WATER} = 0.07 \times 4.2 = 0.294$$

$$\Delta GPM_{POLY.} = 0.10 \times 0.13 = 0.013$$

therefore;

$$\Delta GPM = \frac{(0.294 + 0.013) \times 100}{4.2 + 0.13} = \pm 7.08\%$$

It is apparent that injecting polymer does not appreciably alter the accuracy with which V_{AV} is measured in spite of the relatively large fluctuations in the polymer flowrate.

I-3 Error in Pressure Drop Measurements

The pressure drop is calculated from the equation;

$$\Delta P_m = h_{ACT} (\gamma_m - 1) \sin \Theta K \qquad (1.1)$$

h_m is the manometer reading including density effects, while h_{ACT} is the true manometer reading, corrected for density effects;

$$h_{ACT} = h_m - h_0$$

hence the error in h_{ACT} is;

$$\Delta h_{ACT} = \frac{\Delta h_m + \Delta h_0}{h_m - h_0} \tag{1.2}$$

and at low flow rates as $(h_m - h_0) \to 0$, $\Delta h_{ACT} \to \infty$.

I At low flow rates; ($R_e \cong 2600$)

There is considerable scatter in the C_f vs R_e data obtained in this experiment but it seems to be consistently below the Blasius line, therefore using the experimental results at $R_e = 2600$;

$$V_{AV} = \frac{R_e \upsilon}{D} = 0.28 \text{ ft/sec}$$

and

$$\Delta P_m = C_f \left(\frac{L}{D}\right) \frac{\rho \upsilon^2}{2g_c}$$

therefore

$$\Delta P_m = 0.027 \times \left(\frac{5.0}{0.1615}\right) \times \frac{62.4 \times (.028)^2}{.1615} = 0.0565 \text{ lb}_F/\text{ft}^2$$

A typical value of h_0 at this flow rate is $h_0 = .75$ cm. using equation (1.1);

$$\Delta P_0 = 0.258 \text{ lb}_F/\text{ft}^2$$

Using equation (1.2) the error in the manometer reading is;

$$\Delta h_{ACT} = \frac{[0.2 \times (.258 + .565)] + [.2 \times .258] \times 100}{.056} \cong \pm 200\%$$

Combining this with the error in manometer fluid density, and angle of inclination measurements the error in the pressure measurement is;

$$\Delta P_m = \left\{ [200]^2 + [.08]^2 + [.05]^2 \right\}^{1/2} \cong \pm 200\%$$

The value at first seems very large, however it must be remembered that this is in a region where the pressure drops are very small, and the initial reading caused by the density differences is larger than the actual reading. It is to be expected that the results in this region would be poor. At low flow rates therefore the pressure drops were obtained from the theoretical correlation $C_f = \frac{64}{R_e}$. At higher flow rates, where the no flow manometer reading (which remains relatively constant) is a smaller percentage of the total reading, the error in the pressure measurement becomes less.

II For the high flow rates ($R_e \cong 50{,}000$)

As before,

$$V_{AV} = 5.38 \text{ ft/sec}$$

and

$$\Delta P = 15.2 \text{ lb}_F/\text{ft}^2$$

Again for

$$h_0 = .75 \text{ cm.}, \Delta P_0 = .258 \text{ lb}_F/\text{ft}^2$$

therefore

$$\Delta h_{ACT} = \frac{[0.01 \times (15.2 \times .258)] + [.2 \times .258] \times 100}{15.2} = \pm 1.36\%$$

and similarly

$$\Delta P_m = \left\{(1.36)^2 + (.08)^2 + (.05)^2\right\}^{1/2} \cong \pm 1.36\%$$

I-4 Error in the Friction Factor

The friction factor was calculated from the equation;

$$C_f = \frac{\Delta P_m}{(\frac{L}{D})\frac{\rho V^2}{2g_c}} = \frac{\Delta P_m}{(\frac{L}{D})\frac{(GPM)^2}{D^4} \times K}$$

where the various conversion constants are fluid density (assumed completely accurate compared to the other measurements) have been lumped into K.
then;

$$\Delta C_f = \left\{[\Delta(\Delta P_m)]^2 + [\Delta L]^2 + [2(\Delta GPM)]^2 + [5(\Delta D)]^2\right\}^{1/2}$$

The variation in the accuracy of ΔC_f with Reynolds number must be expected to be highly non linear because of the non-linearity of the component terms, and since the friction factor Reynolds number results are so important,

it was decided to calculate the accuracy of C_f for a complete range of Reynolds numbers. The listing of the computer program to do this is in table 2. Figure 15 shows the variation of the accuracy of the friction factor with the Reynolds number and figure 16 shows the percent deviation of the experimental results from the theoretically expected value of the friction factor.

I-5 Error in Polymer Concentration

The error in the concentration of polymer in the test section consists of two basic components, firstly the error in the concentration of the stock solution, and secondly the error caused by the mixing of the solution with the main flow of water to the test section.

I The Concentration Error in Mixing of the Stock Solution at 2000 Wppm:

$$\text{Concentration} = \frac{m_p}{m_w} = \frac{2 \times 10^3}{10^6}$$

$$\Delta(\text{CONC.}) = (\Delta \text{ POLY.} + \Delta \text{ WATER}) = (2.0 + 0.3) \cong 2\%$$

The polymer powder can be weighed to a much better accuracy than $\pm$ 2%, however in mixing some of it clings to the walls of the eductor.

II Error in the Concentration in the Test Section:

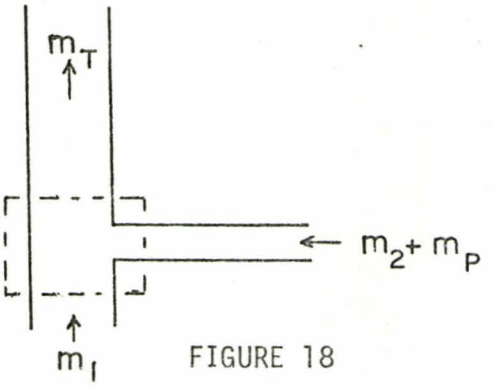

FIGURE 18

TABLE 2

```
                      PROGRAM TST (INPUT,OUTPUT,TAPE5=INPUT,TAPE6=OUTPUT)
00003                 REAL NU
00003                 DIMENSION ID(100),IX(100),IY(100),RRE(5,100),DDPT(5,100),V(30),
                     1 GPM(30),DGPM(30),XE(30),DPA(30),DEL(30),DDP(30),DCF(30),XRE(30)
                     2 ,DP(30)
00003                 COMMON/111/RE(5,100),DPT(5,100),D,NU,RO,N
00003                 COMMON/222/ ISUB(5)
00003                 RO=62.4
00005                 D=0.1615
00006                 NU=1.744E-05
00010                 VF=5.0
00011                 VO=0.05
00013                 GPMF=1.0
00014                 GPMO=5.0
00015                 DPF=0.07
00016                 DPI=0.01
00020                 DDPO=0.258
               C
               CC     READ DIGITIZER DATA
               C
00021                 K=1
00022                 NN=500
00023            340  DO 300 I=1,NN
00025                 IF (NN.EQ.1) GO TO 310
00027                 READ (5,305) ID(I),IX(I),IY(I)
00040            305  FORMAT (3I10)
00040                 IF (IX(I).EQ.0) GO TO 320
00042                 RRE(K,I)=FLOAT(IX(I))/100.0
00046                 DDPT(K,I)=FLOAT(IY(I))/100.0
00053            300  CONTINUE
00055            320  K=K+1
00057                 ISUB(K-1)=I-1
00061                 IF (K.GE.5) GO TO 330
00063                 GO TO 340
00064            330  NN=1
00065                 GO TO 340
00066            310  READ(5,42) XPL,YPL,XACT,YACT
00102             42  FORMAT (4F20.2)
               CC
               CCC    CONVERT DIGITIZER DATA TO ACTUAL VALUES
               C
00102                 SFX1=XPL/(ALOG(XACT)-ALOG(1000.0))
00111                 SFY1=YPL/(ALOG(YACT)-ALOG(0.001))
00117                 DO 43 I=1,4
00120                 WRITE (6,70)
00123             70  FORMAT (60X,*PE*,20X,*CF*//)
00123                 KK=ISUB(I)
00125                 DO 43 J=1,KK
00127                 RE(I,J)=EXP((RRE(I,J)/SFX1)+ALOG(1000.0))
00143                 DPT(I,J)=EXP((DDPT(I,J)/SFY1)+ALOG(0.001))
00156                 WRITE (6,46) RE(I,J),DPT(I,J)
00170             46  FORMAT (45X,2E20.5)
00170             43  CONTINUE
               C
00175                 DO 700 I=1,21
00176                 V(I)=(FLOAT (I-1)*(VF-VO)/20.0)+VO
00205                 GPM(I)=V(I)*D*D*3.14159*6.229*60.0/4.0
```

```
000210            DGPM(I)=(FLOAT (I-1)*(GPMF-GPMO)/20.0)+GPMO
000216            XE(I)=V(I)*D/NU
000221            L=1
000222            CALL INTERP(V(I),L,DP(I),XRE(I))
000225            DPA(I)=((FLOAT(I-1)*(DPF-DPI)/20.0)+DPI)*DP(I)
000234            DEL(I)=DPA(I)+DDPO
000237            DDP(I)=(DEL(I)*100.0)/DP(I)
000242            DCF(I)=SQRT((DDP(I)**2)+1.0+((2.0*DGPM(I))**2)+16.0)
000253        700 CONTINUE
000255            WRITE (6,701)
000260        701 FORMAT (20X,*VEL*,11X,*RE*,13X,*GPM*,12X,*DGPM*,10X,*DP*,10X,
                 1 *DPA*,12X,*DEL*,12X,*DDP*//)
000260            DO 705 I=1,21
000262            WRITE (6,702) V(I),XE(I),GPM(I),DGPM(I),DP(I),DPA(I),DEL(I),DDP
000305        702 FORMAT (10X,8F15.3//)
000305        705 CONTINUE
000307            WRITE(6,746)
000313        746 FORMAT (H1,35X,*ESTIMATED ERROR IN FRICTION FACTOR*//)
000313            WRITE (6,748)
000317        748 FORMAT (46X,*RE*,14X,*CF*//)
000317            DO 747 I=1,21
000321            WRITE (6,703) XE(I),DCF(I)
000330        703 FORMAT (40X,2F15.3)
000330        747 CONTINUE
000332            STOP
000334            END

UNUSED COMPILER SPACE
006700
```

```
                SUBROUTINE INTERP  (V,L,DH,CLR)
      C
000007            REAL NU
000007            COMMON/111/RE(5,100),DPT(5,100),D,NU,RO,N
000007            COMMON/222/ ISUB(5)
      C
000007            IF (L.GE.10) GO TO 200
000011            DL=5.0
000013            D=0.1615
000014         50 CLR=V*D/NU
000017            IF (CLR.LE.2500.0) GO TO 130
000021            IF (CLR.LT.9400.0) K=1
000024            IF (CLR.LT.9400.0) GO TO 230
      C
000026            IF (L-5) 210,210,220
000030        210 K=3
000031            GO TO 230
000032        220 K=4
000033        230 J=ISUB(K)
000035            DO 100 I=1,J
000037            IF (CLR.LE.RE(K,I)) GO TO 110
000043        100 CONTINUE
      C
000045            WRITE (6,120) L
000052        120 FORMAT (10X,*DATA NOT IN RANGE*,5X,*SET NUMBER*,5X,I2//)
000052            DH=0.00
000055            GO TO 500
      C
000056        110 I=I-1
000060            CF=(DPT(K,I)-DPT(K,I+1))*((CLR-RE(K,I))/(RE(K,I+1)-RE(K,I)))+DPT
                 1,I+1)
000074            DH=(CF*DL*RO*V*V)/(D*2.0*32.17)
000102            GO TO 500
000103        130 DH=(32.0*DL*RO*V*V)/(32.17*D*CLR)
000112            GO TO 500
      C
000113        200 WRITE (6,300)
000116        300 FORMAT (2X,*CF DATA EXCEEDED*//)
000116        500 RETURN
000117            END

UNUSED COMPILER SPACE
010100
```

ESTIMATED ERROR IN FRICTION FACTOR

RE	CF
463.016	2487.560
2754.946	407.689
5046.875	124.708
7338.804	54.435
9630.734	36.813
11922.663	32.003
14214.593	27.872
16506.522	24.686
18798.452	22.453
21090.381	20.362
23382.311	19.028
25674.240	17.985
27966.170	17.035
30258.099	16.426
32550.029	15.499
34841.958	14.759
37133.888	14.234
39425.817	14.123
41717.747	13.697
44009.676	13.788
46301.606	13.271

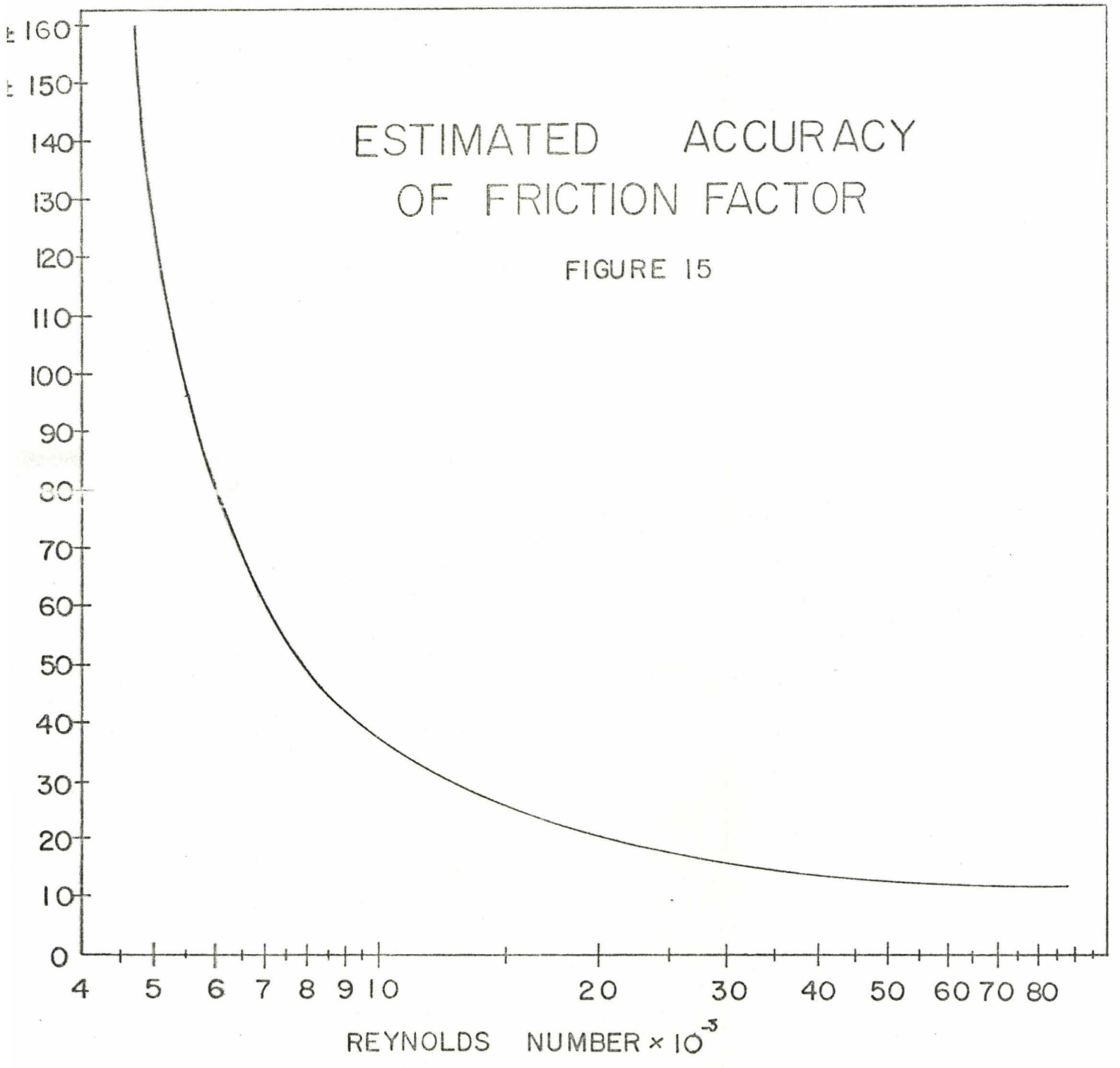
ESTIMATED ACCURACY
OF FRICTION FACTOR
160
150
140
130
120
110
100
90
80
70
60
50
40
30
20
10
0
4
5
6
7
8
9
10
20
30
40
50
60
70
80
REYNOLDS NUMBER × 10⁻³

FIGURE 15

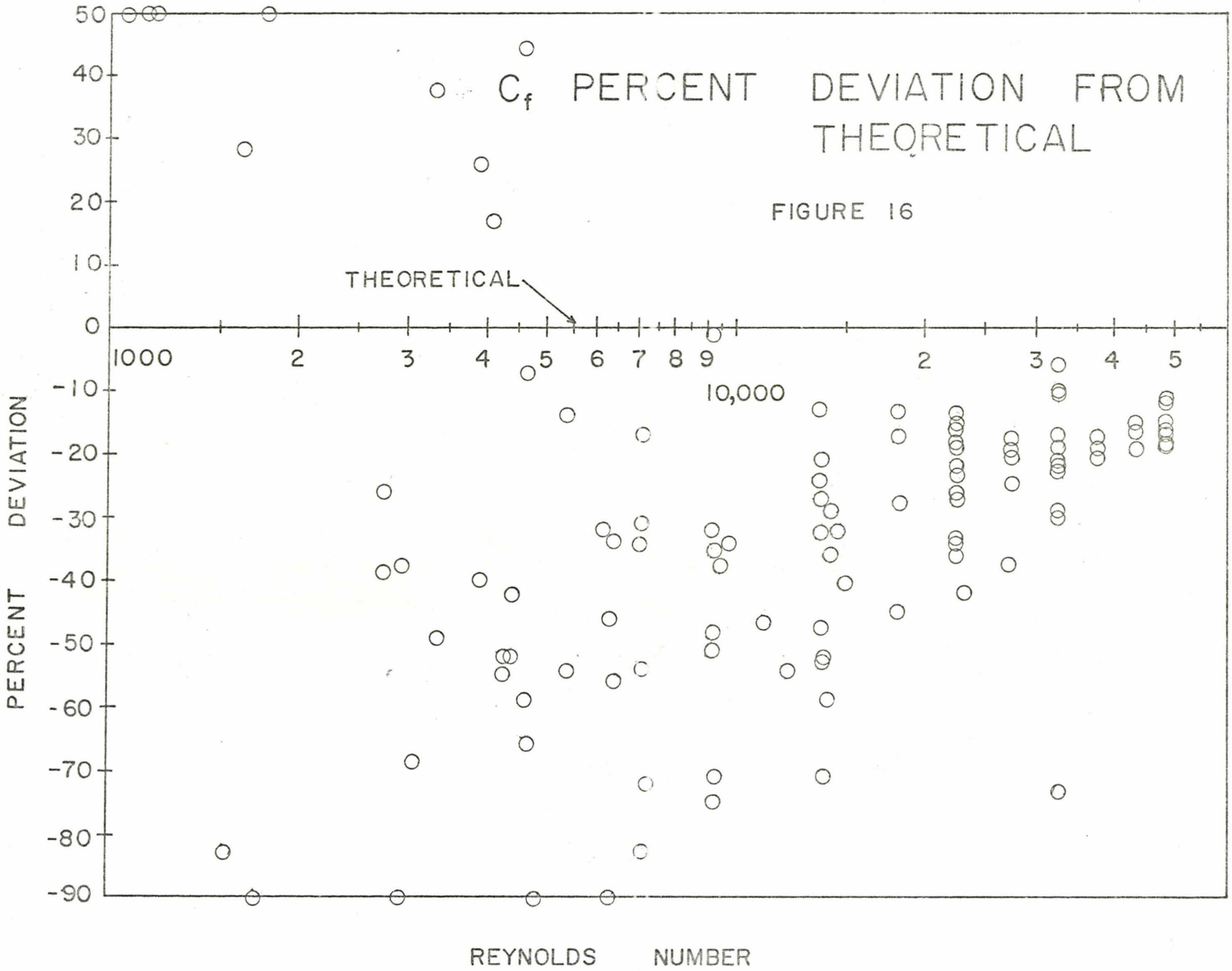
C_f PERCENT DEVIATION FROM THEORETICAL
THEORETICAL
50
40
30
20
10
0
-10
-20
-30
-40
-50
-60
-70
-80
-90
1000
2
3
4
5
6
7
8
9
10,000
2
3
4
5
PERCENT DEVIATION
REYNOLDS NUMBER

FIGURE 16

$$m_2 = m_p + m_w$$

$$m_T = m_1 + m_2 = m_1 + m_p + m_w$$

But $m_p << m_w$

therefore

$$\text{CONC.} \cong \frac{m_p}{m_1 + m_w}$$

(i) at low flow rates;

$$\Delta m_1 = 0.04 \times 8.5 = 0.34$$

$$\Delta m_w = 0.2 \times 0.1 = 0.002$$

therefore

$$\Delta \text{CONC.} = \left\{ (20)^2 + \left[\frac{.34 + .002}{85 + .1} \times 100\right]^2 \right\}^{1/2} = \pm 20.4\%$$

Most of this error is due to the error in measuring the polymer flow rate which was observed at times to fluctuate as much as $\pm$ 20% at very low flow rates.

(ii) at high flow rates;

$$\Delta m_1 = 0.01 \times 38 = .38$$

$$\Delta m_w = 0.04 \times 0.5 = 0.02$$

and $$\text{CONC.} = \left\{ (4)^2 + \left[\frac{.38 + .02}{38 + .5} \times 100\right]^2 \right\}^{1/2} = \pm 4.1\%$$

I-6 Error in Reynolds Number

The Reynolds number is calculated using;

$$R_e = \frac{V_{AV} D}{\upsilon}$$

The value of the kinematic viscosity is a direct function of the temperature of the water, which could be measured to within 1°C. This would cause a variation in υ of;

3°C $\upsilon = 1.7435 \times 10^{-5}$ ft^2/sec

4°C $\upsilon = 1.6885 \times 10^{-5}$ ft^2/sec

5°C $\upsilon = 1.0364 \times 10^{-5}$ ft^2/sec

$$\Delta\upsilon = \left[\frac{(1.7435 - 1.6364) \times 10^{-5}}{1.6885 \times 10^{-5}}\right] \times 100 = \pm 6.32\%$$

I At low flow rates;

$$\Delta R_e = \left\{ (5.4)^2 + (1)^2 + (6.32)^2 \right\}^{1/2} = \pm 8.4\%$$

II At high flow rates;

$$\Delta R_e = \left\{ (3)^2 + (1)^2 + (6.32)^2 \right\}^{1/2} = \pm 7.05\%$$

I-7 Error in Diameter Ratio

For steel spheres (from table 1);

$$\Delta (d/D) = \left\{ (1.0)^2 + (.1)^2 \right\}^{1/2} \cong \pm 1\%$$

For plastic spheres (from table 1);

$$\Delta (d/D) = \left\{ (1.0)^2 + (.5)^2 \right\}^{1/2} \cong \pm 1\%$$

I-8 Error in the Combined Pressure Drop Terms

I For low pressure drop values; for

$$(\Delta P_m - \Delta P_L)/[D(\frac{\sigma - \rho}{\rho})] = 5.0$$

and d/D = 0.763 (Plastic), from figure 6,

$$V_{AV}^2 = .075$$

therefore

$$R_e \cong 2500$$

Since this value is in the laminar region the error in

$$(\Delta P_m - \Delta P_L)/[D(\frac{\sigma - \rho}{\rho})]$$

is essentially that in ΔP_m which was earlier found to be about $\pm$ 200%.

II For the Region Where $\Delta P_m - \Delta P_L$ is larger; from figure 9 for d/D = 0.563, and $(\Delta P_m - \Delta P_L) = 10$, and from figure 6

$$V_{AV}^2 = 22.8$$

therefore

$$R_e \cong 44{,}000$$

From figure 27

$$C_f = 0.0175$$

therefore

$$\Delta P_L = 11.98 \text{ lb}_F/\text{ft}^2$$

therefore

$$\Delta P_m = 10.0 + 11.98 = 21.90 \text{ lb}_F/\text{ft}^2$$

It was calculated in section I-3 that at high flow rates the error in the pressure drop measurement was about $\pm$ 1.5%. Therefore

$$\Delta(\Delta P_m - \Delta P_L) = \frac{(0.015 \times 21.98) + (0.015 \times 11.98) \times 100}{10.0} = \pm 5.1\%$$

I-9 Error in the Specific Gravity of the Spheres

$$SG = \frac{m}{\frac{\pi d^3}{6}}$$

where m is in gm and d is in cm.

For steel (from table 1);

$$\Delta SG = \left\{ (.5)^2 + [3(1)]^2 \right\}^{1/2} \cong \pm .6\%$$

For plastic (from table 1);

$$\Delta SG = \left\{ (1.0)^2 + [3(1)]^2 \right\}^{1/2} \cong \pm 2\%$$

I-10 Error in the Drag Coefficient

In chapter III (Theory),it was shown that,

$$C_d^* = \frac{4}{3} \left(\frac{\sigma - \rho}{\rho}\right) \frac{dg}{V_{AV}^2}$$

It will be assumed that ρ and g are exact compared to the other variables; therefore

$$C_d^* = \left\{ [d(d)]^2 + [2(d\, V_{AV}^2)]^2 + [d(G)]^2 \right\}^{1/2}$$

For steel a typical accuracy is;

$$\Delta C_d^* = \left\{ (.1)^2 + [2(3.0)]^2 + [.6]^2 \right\}^{1/2} \cong 6\%$$

For plastic a typical accuracy is;

$$\Delta C_d^* = \left\{ (.5)^2 + [2(4.0)]^2 + (2)^2 \right\}^{1/2} \cong \pm 8.75\%$$

APPENDIX II

MIXING THE POLYMER

The polymer used throughout this experiment was Reten 423, a polyacrylamide drag reducing polymer manufactured and supplied by Hercules Inc., and having an approximate molecular weight of 10^{10}. All the polymer used in these experiments came from one batch to minimize variation in polymer properties.

Before mixing, it was necessary to determine the moisture content of the polymer powder. This was done by taking three samples of approximately six grams each and heating them in an oven at 140°C for several hours. The results are shown in table 3.

Sample	Initial Wt.	Final Wt.	% moisture
1	7.276 gm	7.0135 gm	3.21%
2	3.035 gm	3.8479 gm	2.74%
3	5.500 gm	5.264 gm	4.29%

TABLE 3

An average moisture content being about 3.75%, or say 4% for convenience.

The polymer used in the experiments was mixed in bins lined with disposable plastic liners. Bins #4, #5, and #6 contained 149.6 lbm, and bin #3 contained 136.4 lbm of water when filled to a predetermined mark.

A stock solution having a concentration of 2000 Wppm of polymer was required; the appropriate water polymer amounts are; (say for bin #4)

$$\frac{m_p}{m_w} = \frac{2 \times 10^3}{10^6}$$

therefore

$$m_p = m_w \times 2 \times 10^{-3}$$

$$= 149.6 \times 2 \times 10^{-3}$$

$$= 0.299 \text{ lbm}$$

allowing for 4% moisture;

$$m_p = 1.04 \times 0.299 = 0.311 \text{ lbm}$$

The polymer was mixed with the water using a Hercules Standard Eductor, and allowed to stand undisturbed for several hours before being gently and very briefly stirred, and again several hours before use. All the polymer batches were allowed to stand at least eighteen hours before use.

When the polymer was required it was transferred from the bins to the reservoir by a hand operated positive displacement pump.

APPENDIX III

CALIBRATION CURVES

The average velocity of the water flowing through the test section was measured using rotameters. Only one of the four incorporated in the apparatus had a calibration curve available that could be used. Two of the remaining three did not have reliable cuves and the third one was used to monitor the polymer injection rate, and so required special recalibration.

The calibration of the water rotameters was carried out by measuring the change in the volume of water in a tank of known dimensions while recording the elapsed time. The tank used, was the reservoir of the main flow system.

The dimensions of the tank are;

$L = 47.75 \pm 0.125$ inches

$W = 24.0 \pm 0.0625$ inches

$h = h_1 - h_2 \pm 0.1$ cm.

The height (or depth of water) is measured in centimeters for convenience. Therefore

$U = 1.628\ h$ imperial gallons.

The maximum possible error in reading the stop watch was $\pm$ 0.1 sec. Some typical results for the large rotameter (#1) are shown in Table 4.

#	$h_1 - h_2$ (cm)	Time (sec)	GPM	Flowmeter
1	20	58.4	33.4	130
2	22	72.0	29.8	120
3	20	77.8	25.1	109
4	20	91.4	21.4	99
5	20	109.4	17.8	90
6	20	139.8	14.0	80
7	20	189.4	10.3	69
8	7	100.0	6.8	59
9	5	131.9	3.7	50
10	1.5	166.5	.88	41

TABLE 4

The error in the flow rate is;

$$\Delta GPM = \left\{ (\Delta L)^2 + (\Delta W)^2 + (\Delta T)^2 \right\}^{1/2}$$

For reading #1;

$$\Delta GPM = \left\{ \left(\frac{.125}{47.75}\right)^2 + \left(\frac{.0625}{24.00}\right)^2 + \left(\frac{.1}{20}\right)^2 + \left(\frac{.1}{58.4}\right)^2 \right\}^{1/2} \pm .64\%$$

For reading #9;

$$\Delta GPM = \left\{ \left(\frac{.125}{47.75}\right)^2 + \left(\frac{.0025}{24.00}\right)^2 + \left(\frac{.1}{5}\right)^2 + \left(\frac{.1}{131.9}\right)^2 \right\}^{1/2} \pm 2.0\%$$

The smallest rotameter was also calibrated using this tank and typical results are summarized in table 5. Since the same tank was used to calibrate both flowmeters the errors can be expected to be similar. For reading #1, in table 5;

$$\Delta GPM = \left\{ \left(\frac{.125}{47.75}\right)^2 + \left(\frac{.0025}{24.00}\right)^2 + \left(\frac{.0625}{2.875}\right)^2 + \left(\frac{.1}{350}\right)^2 \right\}^{1/2} = \pm 2.21\%$$

For reading #10;

$$\Delta GPM = \left\{ \left(\frac{.125}{47.75}\right)^2 + \left(\frac{.0625}{24.00}\right)^2 + \left(\frac{.0625}{0.500}\right)^2 + \left(\frac{.1}{180}\right)^2 \right\}^{1/2} = \pm 12.5\%$$

#	Gallons	Time (Minutes)	GPM	Flowmeter
1	2.065	5.83	.35	1.1
2	4.131	5.82	.71	3.1
3	4.647	4.32	1.07	4.95
4	7.229	4.86	1.48	7.03
5	6.713	3.59	1.87	9.05
6	10.844	4.79	2.26	11.1
7	8.262	3.08	2.68	13.15
8	10.327	3.33	3.10	15.0
9	6.713	2.90	2.31	16.95
10	11.877	2.93	4.05	19.45
11	11.877	2.57	4.62	22.20
12	11.360	2.15	5.27	24.50

TABLE 5

The third rotameter came with a calibration curve supplied by the manufacturer. The calibration curves for all the rotameters are shown in figures 17, 18 and 19.

It was necessary to recalibrate a flowmeter for use with the polymer solution. This was done by preparing a stock solution of 2000 Wppm of the polymer that would be used in experiments under exactly the same conditions as would be found in the experiments. The apparatus was assembled exactly as it would be when the experiments would be performed except that

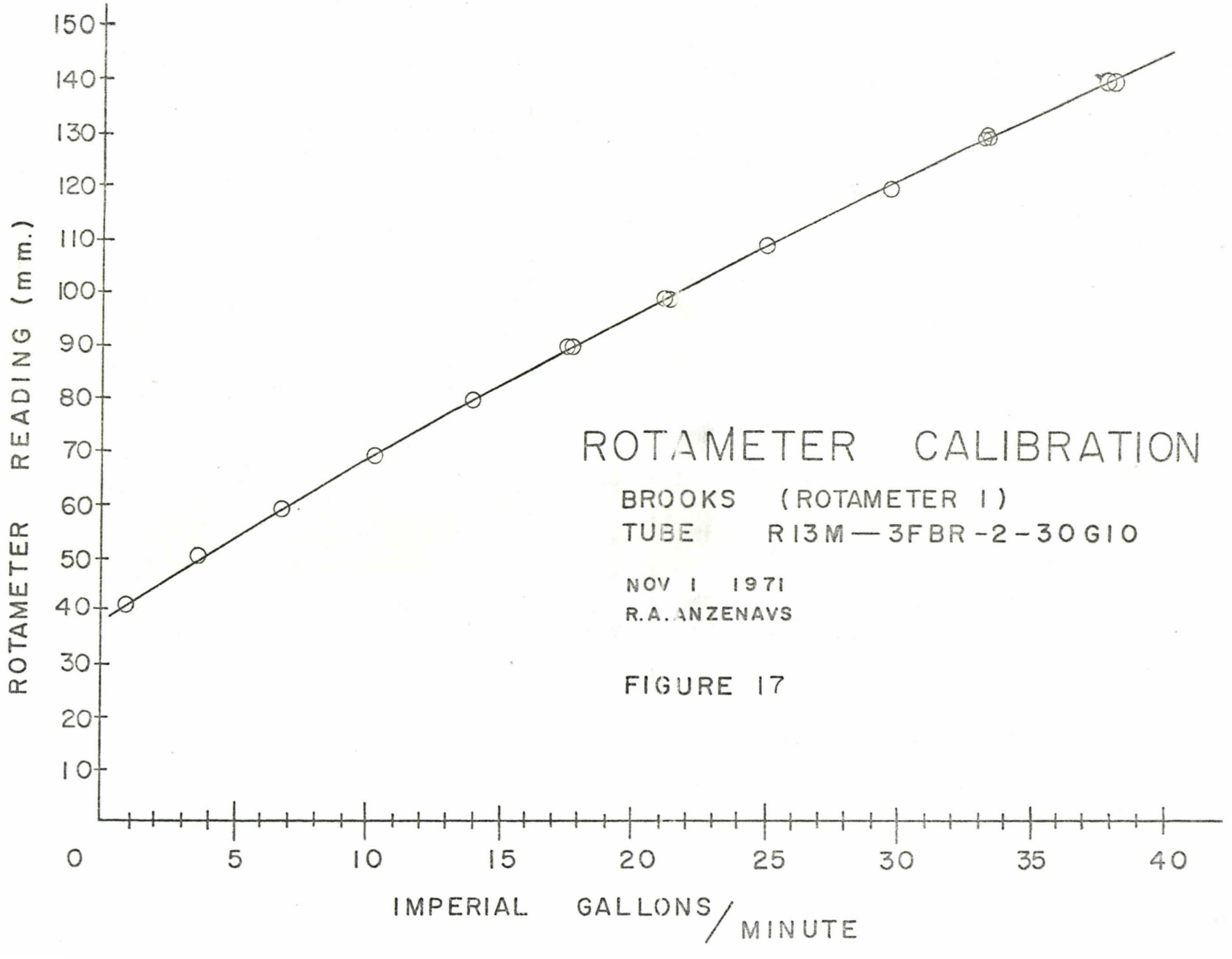
ROTAMETER READING (mm.)
150
140
130
120
110
100
90
80
70
60
50
40
30
20
10
0
5
10
15
20
25
30
35
40
IMPERIAL GALLONS / MINUTE
ROTAMETER CALIBRATION
BROOKS (ROTAMETER 1)
TUBE R13M—3FBR-2-30G10
NOV 1 1971
R.A. ANZENAVS

FIGURE 17

ROTAMETER CALIBRATION

BROOKS (ROTAMETER 2)
TUBE R 12M – 127-3F
FLOAT 12 - RV - 221

CONVERTED FROM ORIGINAL (USGPM)

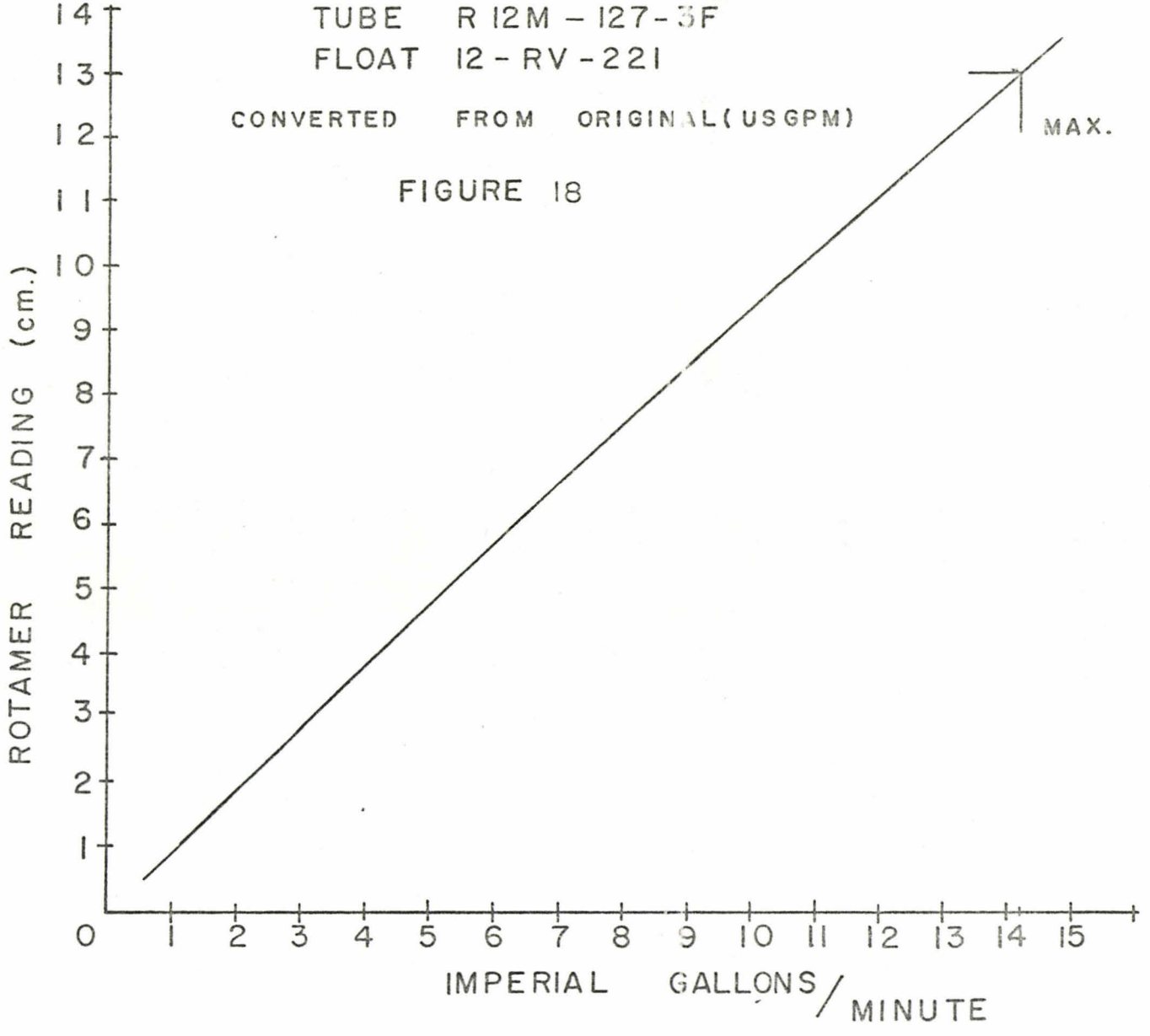

FIGURE 18

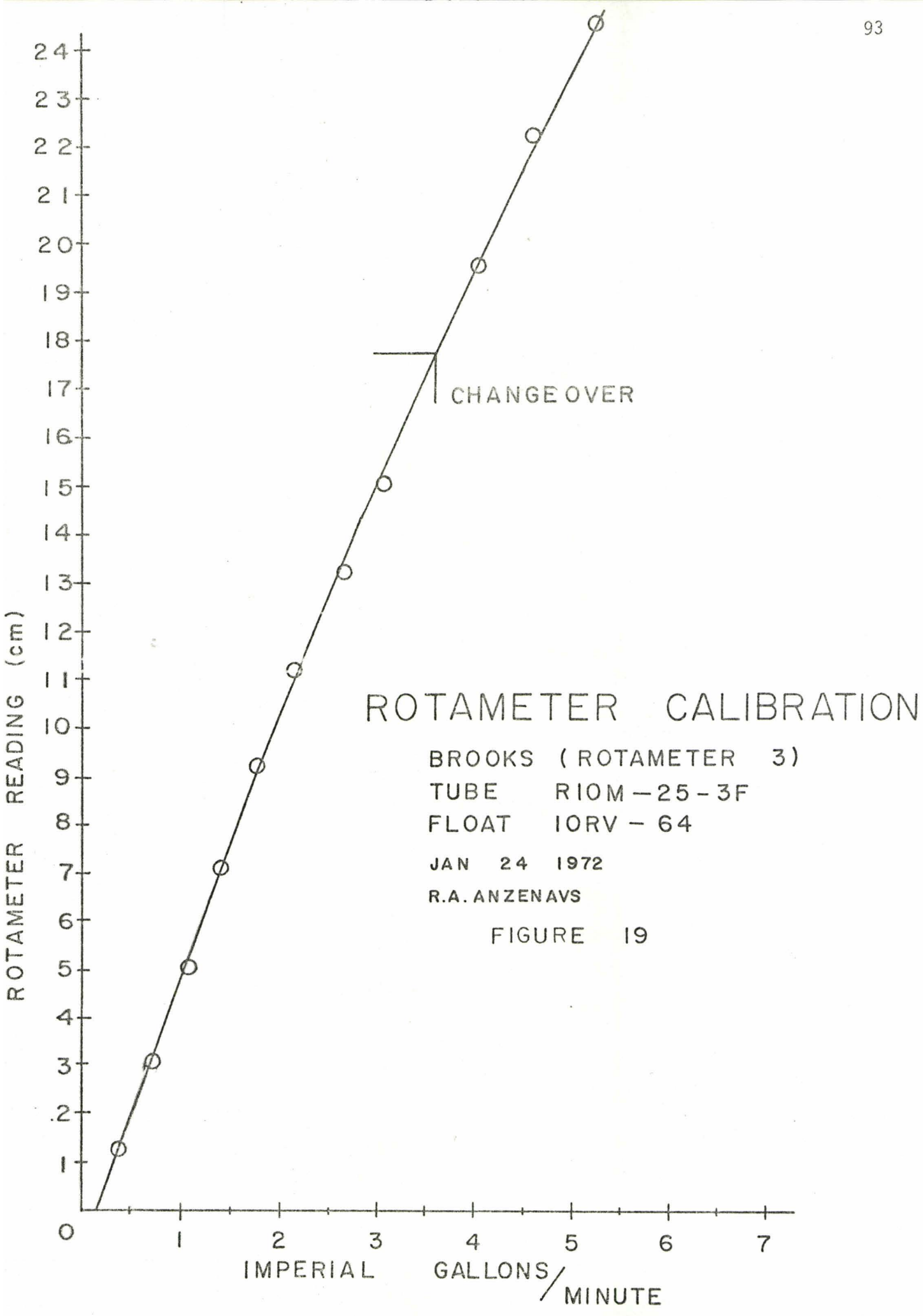

ROTAMETER CALIBRATION

BROOKS (ROTAMETER 3)
TUBE R10M-25-3F
FLOAT 10RV-64

JAN 24 1972

R.A. ANZENAVS

FIGURE 19

POLYMER ROTAMETER CALIBRATION

RETEN 423 CONCENTRATION
2000 Wppm
BROOKS ROTAMETER
TUBE R10M 25 5FBK

NOV 1 1971
R.A. ANZENAVS

FIGURE 20

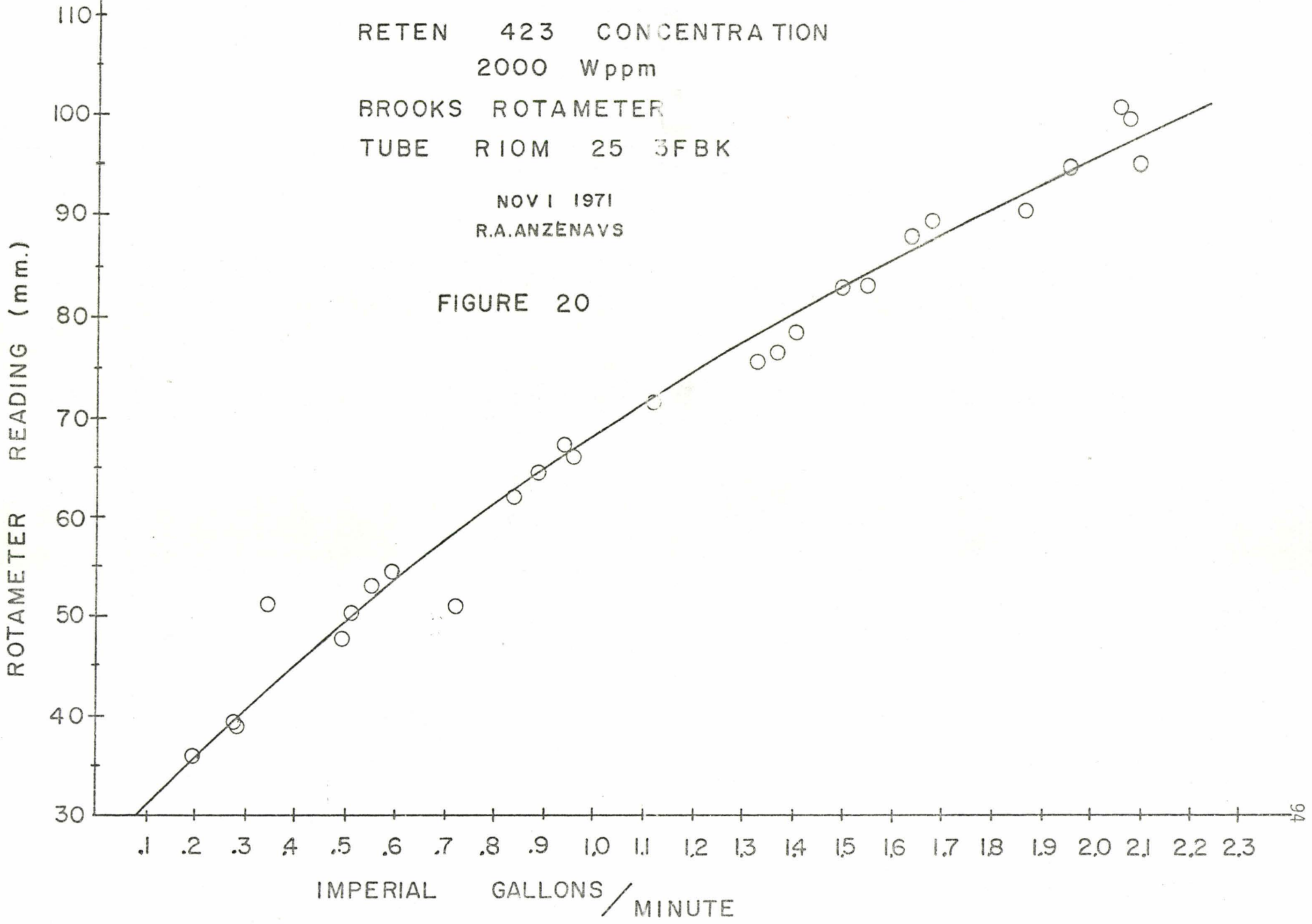

the discharge from the rotameters was hooked into a tank calibrated in imperial gallons. A series of measurements of volume discharged against time were taken as with the other rotameters and the results are shown in figure 20.

During the course of the calibration it was found that both aging and mixing of the polymers had a profound effect on the accuracy of the results, and therefore great care was taken during the calibration procedure to ensure that the results were truly representative of 2000 Wppm polymer used.

An estimate of the error in the calibration of the flowmeter is not presented because the errors caused by reading the stop watch and the tank volume are far less than the error caused by variation in the polymer properties. Hence the error in the rotameter is taken as being represented by the scatter in the points.

Once all the rotameters were calibrated it was necessary to make a cross reference chart that showed the appropriate flow meter settings for a given concentration.

Referring to figure 21; for 10 Wppm in the test section.

$$\frac{m_p}{m_2} = 2 \times 10^{-3} \qquad \text{- stock solution}$$

$$\frac{m_p}{m_1 + m_2} = 10^{-5} \qquad \text{- desired concentration}$$

therefore

$$\frac{m_1 + m_2}{m_2} = \frac{2 \times 10^{-3}}{10^{-5}} = 200$$

therefore

$$m_2 = \frac{m_1}{200} + \frac{m_2}{200}$$

and $$m_2 = m_1 \left[\frac{1}{200 - 1}\right]$$

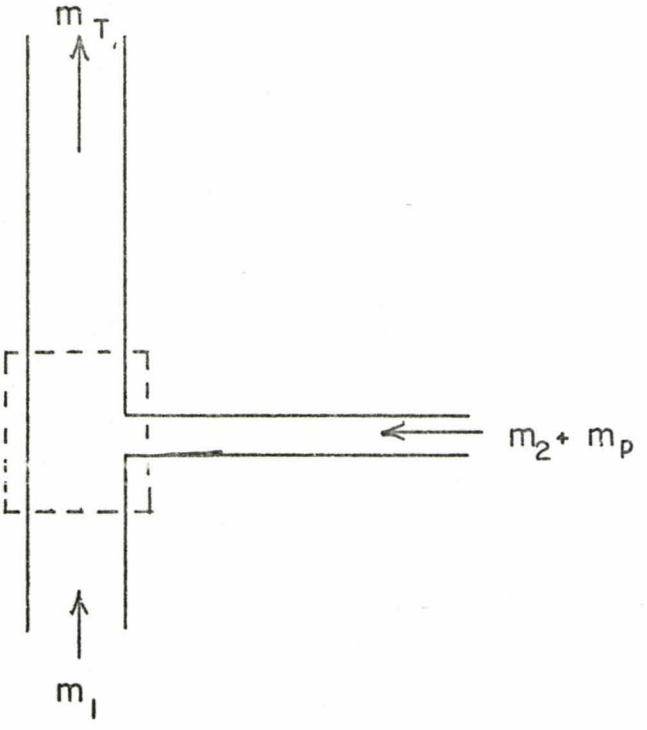

FIGURE 21

For 25 Wppm;

$$\frac{m_1 + m_2}{m_2} = \frac{2 \times 10^{-3}}{2.5 \times 10^{-5}} = 80$$

For the pertinent concentrations;

Conc. (Wppm)	10	25	50	75	100
$m_1 + m_2/m_2$	200	80	40	26.75	20
m_2 in terms of m_1	$\frac{1}{200 - 1}$	$\frac{1}{80 - 1}$	$\frac{1}{40 - 1}$	$\frac{1}{26.75 - 1}$	$\frac{1}{20 - 1}$

TABLE 6

Table 7 summarizes the necessary calculations to obtain a cross reference chart. Figures 22 and 23 show the flow meter setting for the required concentrations as calculated in Table 7.

Main m_1 Flowmeter		10 Wppm		25 Wppm		50 Wppm		75 Wppm		100 Wppm	
Rot.	GPM(m_1)	GPM(m_2)	Rot.	GPM(m_2)	Rot.	GPM(m_2)	Rot.	GPM(m_2)	Rot.	GPM(m_2)	Rot.
140	38.2	.192	33.5	.484	49.2	.98	67.8	1.48	82.4	2.01	95.7
130	33.9	.170	34.5	.429	76.9	.869	64.0	1.315	78.0	1.782	90
120	29.69	.149	33.5	.376	44.8	.760	60.0	1.151	73.0	1.562	84.5
110	25.50	.128	32.5	.323	42.1	.654	56.0	.99	68.0	1.341	78.6
100	21.55			.272	39.5	.551	52.0	.835	63.0	1.131	72.4
90	17.80			.225	37.5	.456	48.1	.69	57.3	.936	66.0
80	14.25			.181	35.0	.365	44.3	.554	52.0	.75	59.6
70	10.75			.136	33.0	.276	39.3	.417	76.2	.569	52.8
60	7.25					.186	35.5	.282	40.0	.382	44.8
50	3.65							.142	33.0	.192	35.6

TABLE 7

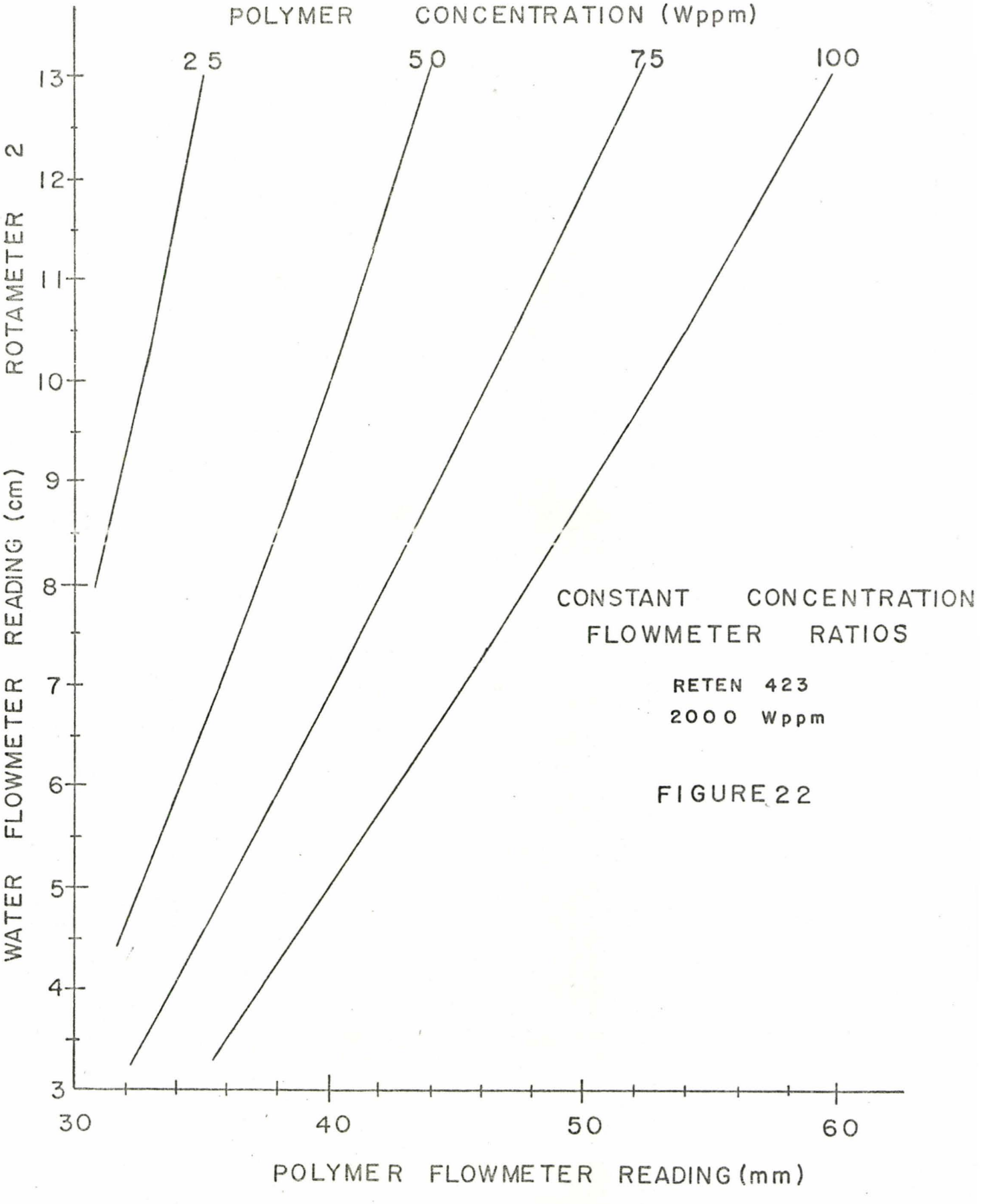

CONSTANT CONCENTRATION
FLOWMETER RATIOS

RETEN 423
2000 Wppm

FIGURE 22

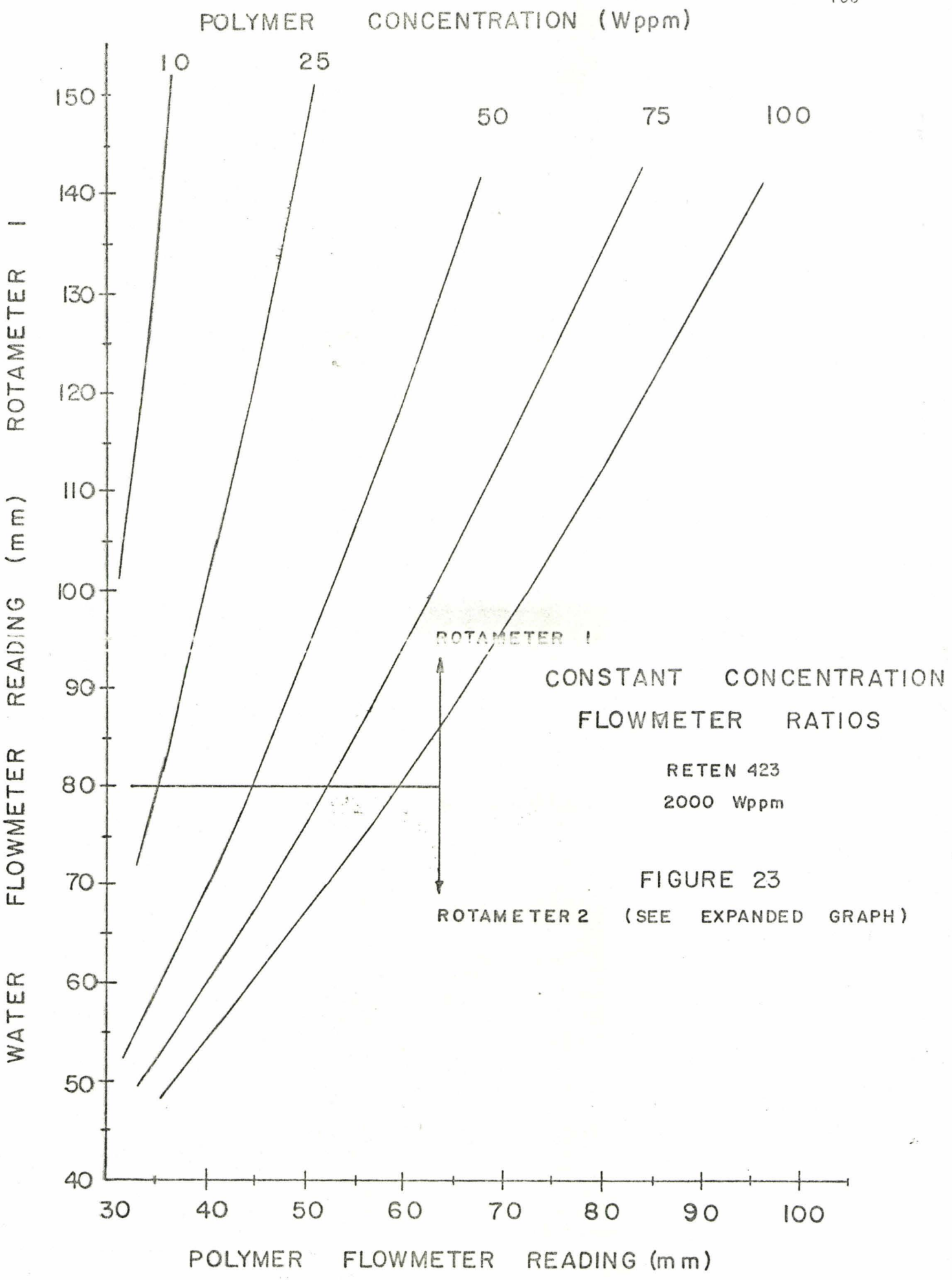

CONSTANT CONCENTRATION
FLOWMETER RATIOS

RETEN 423
2000 Wppm

FIGURE 23

APPENDIX IV

DETERMINATION OF THE INSIDE DIAMETER OF THE TEST SECTION

From the error analysis performed in Appendix I it can be seen that the diameter of the test section enters into the friction factor calculations to the fifth power. It is therefore important that an accurate value for the diameter be known. To determine this, the test section was filled with water to approximately 80% of its length, the length noted, and the volume of water discharged measured using a graduated cylinder. This procedure was repeated twice.

Because of their relatively small size it was obvious that the bell shaped entrances to the pressures taps had negligible effect on the measurements, hence they were neglected. Table 8 summarizes the results.

TABLE 8

$\forall_1$ (litres)	$\forall_2$ (litres)	$\overline{\forall}$ (litres)	L (inches)	D (ft)	
4.452	4.453	4.453	80.94	0.1634	TUBE 1
4.063	4.061	4.062	84.00	0.1615	TUBE 2

APPENDIX V

PRESSURE GRADIENT WITHIN THE TEST SECTION

It was demonstrated in the chapter on theory (chapter III) that the pressure gradient due to the liquid alone is an important part of the calculation of pressure drop across the spheres or sphere trains. Furthermore the measurement itself provides an indication of the kind of accuracy that can be expected from the equipment.

When the polymer is injected it would also be expected that the pressure gradient would change, since the polymer is a friction reducing agent. The ammount of change being an indication of the polymer's effectiveness.

The first phase of this study was to determine if the flow in the test section was developed. This was done by measuring the pressure gradient along the length of pipe. Where the flow is developed that pressure gradient becomes constant. To determine this, the vertical section of the apparatus had pressure taps fitted at frequent intervals, and a bank of inclined manometers were used to measure a continuous pressure gradient between the taps.

Figure 24 shows the manometer used, and figure 25 shows the pressure at each station. From these figures it can be seen that flow in the test section is fully developed, but that the flange and the change in diameter at the entrance to the test section causes a slight disturbance. For subsequent tests the bank of manometers and the series of readings were discarded and only two pressure taps, located four and five feet apart depending on the tube, were used to make the measurements.

MANOMETER SCHEMATIC

FIGURE 24

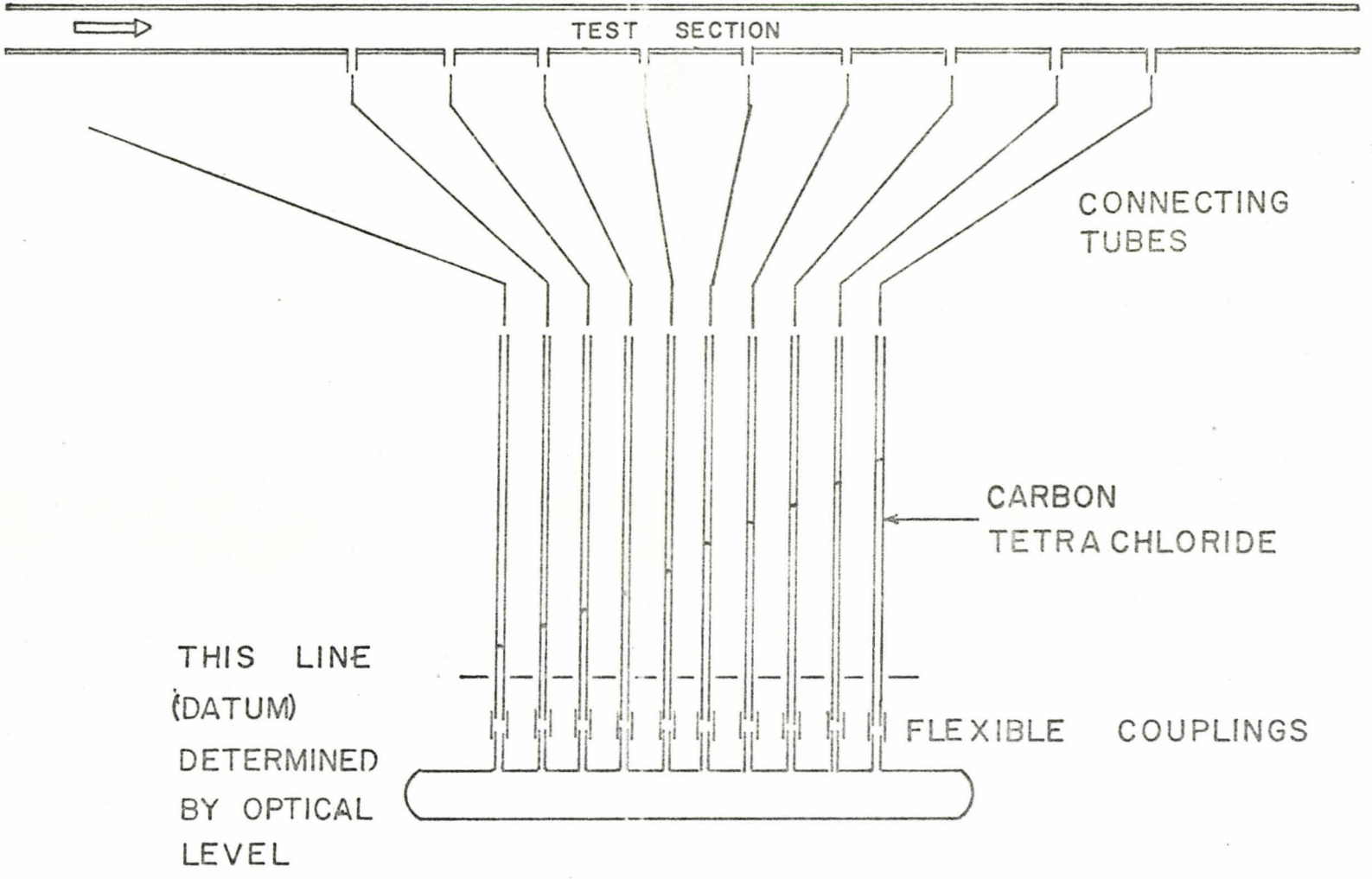

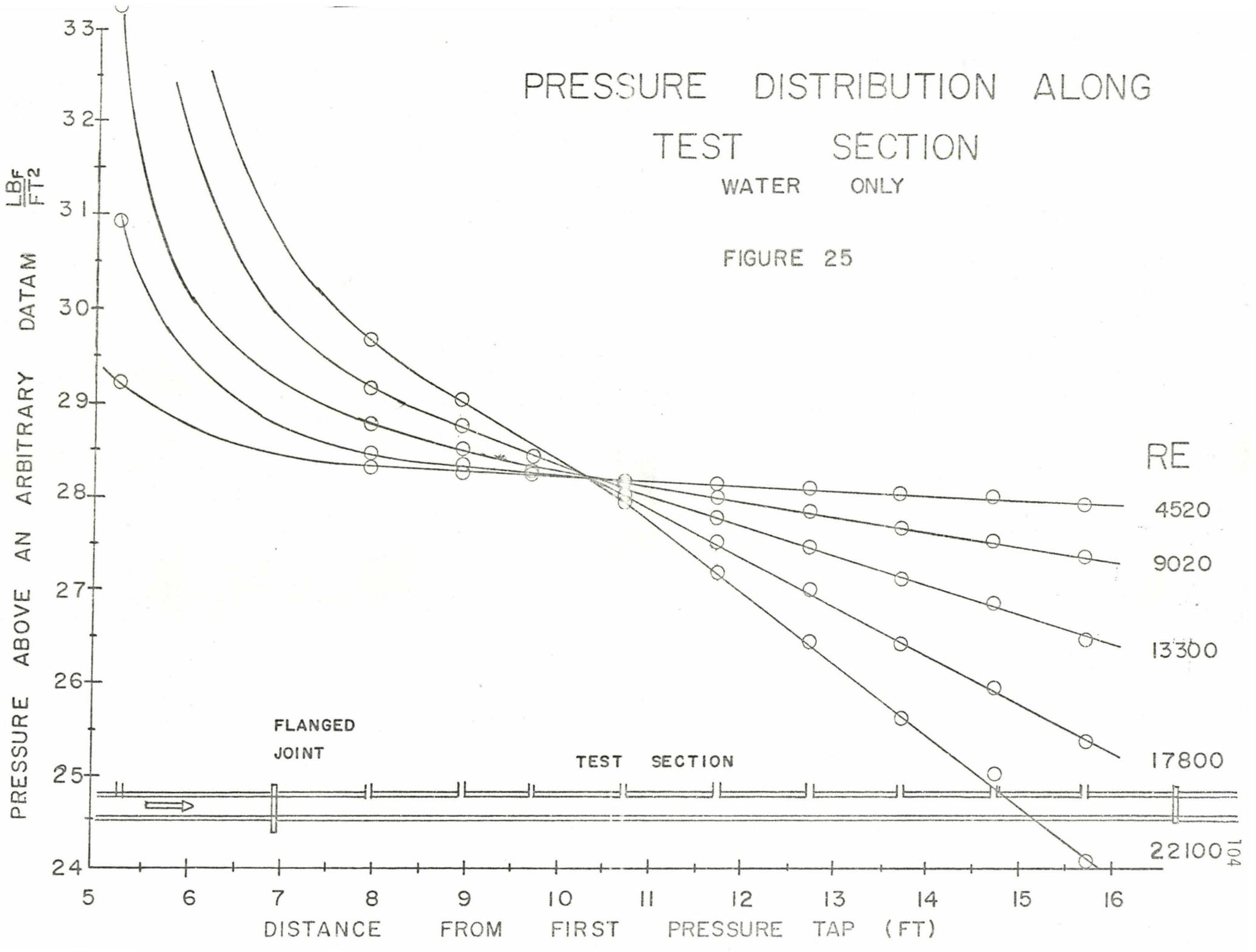
PRESSURE DISTRIBUTION ALONG TEST SECTION
WATER ONLY
FIGURE 25
PRESSURE ABOVE AN ARBITRARY DATAM $\frac{LB_F}{FT^2}$
33
32
31
30
29
28
27
26
25
24
RE
4520
9020
13300
17800
22100
FLANGED JOINT
TEST SECTION
5
6
7
8
9
10
11
12
13
14
15
16
DISTANCE FROM FIRST PRESSURE TAP (FT)

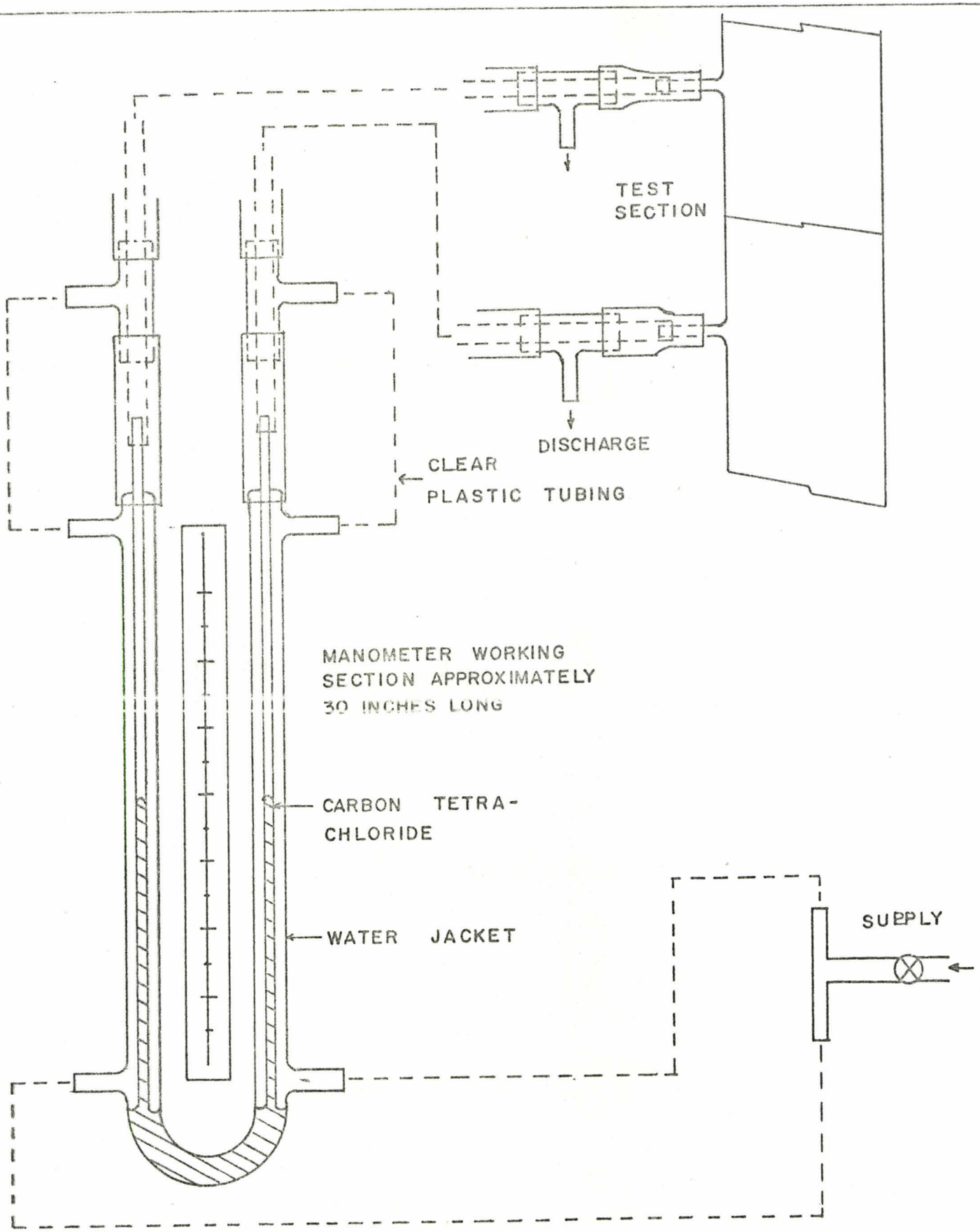

MANOMETER SCHEMATIC

FIGURE 26

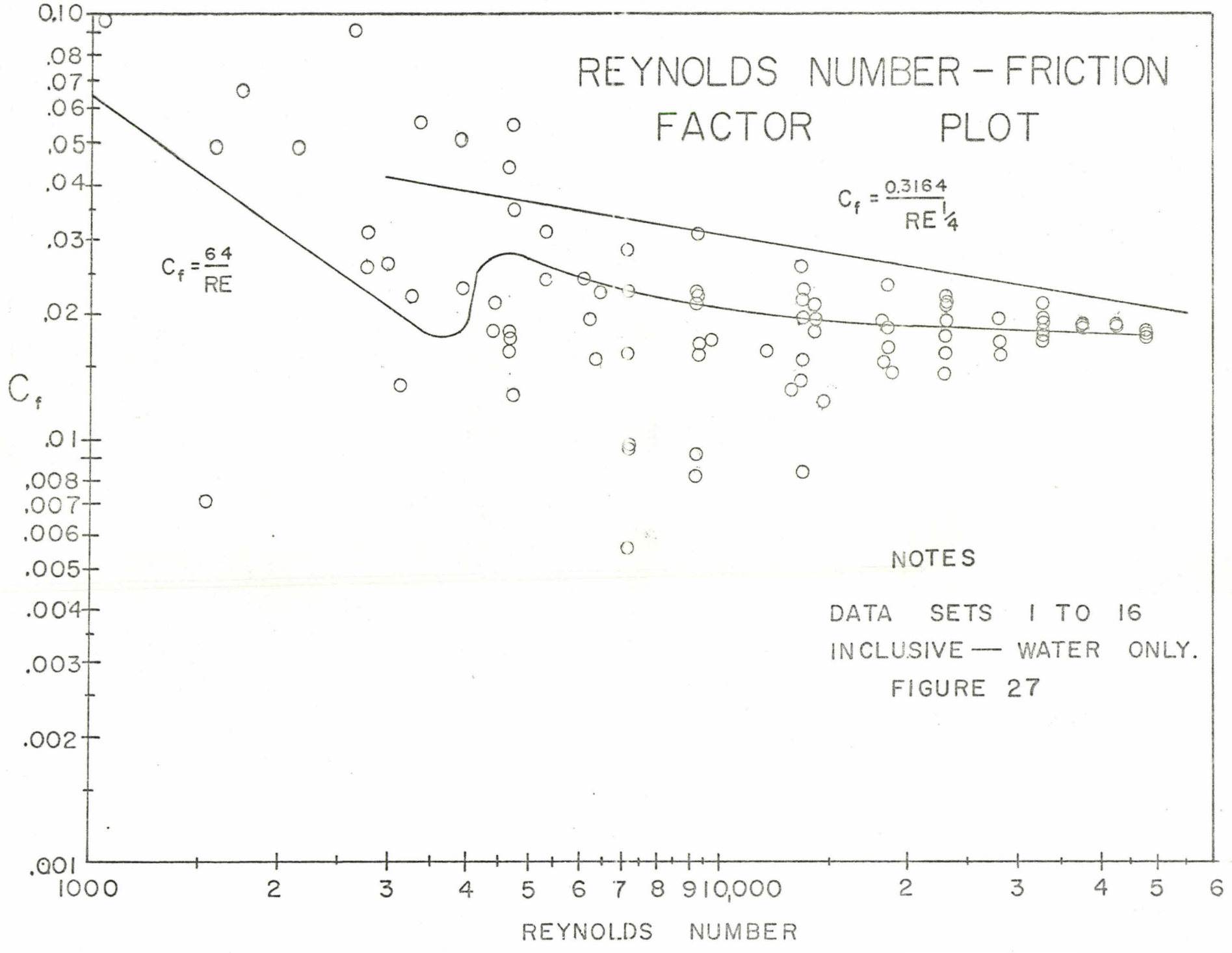
REYNOLDS NUMBER – FRICTION FACTOR PLOT
$C_f = \frac{0.3164}{RE^{1/4}}$
$C_f = \frac{64}{RE}$
C_f
0.10
.08
.07
.06
.05
.04
.03
.02
.01
.008
.007
.006
.005
.004
.003
.002
.001
1000
2
3
4
5
6
7
8
9
10,000
2
3
4
5
6
REYNOLDS NUMBER
NOTES
DATA SETS 1 TO 16 INCLUSIVE — WATER ONLY.

FIGURE 27

From the chapter on errors, Appendix I, it can be seen that very large errors are to be expected at low Reynolds numbers, decreasing exponentially as the Reynolds number increases. The three main sources of this error are the error in the average velocity, the error in the diameter of the pipe, and the error in the pressure drop.

The first error, by careful calibration was reduced to a minimum, and the error in the pipe diameter was simiarly reduced to virtually a negligible amount. However, the error in the pressure drop was difficult to reduce. A special manometer was developed, and is shown in figure 26. The inside diameter of this manometer was three millimeters to ensure that at low angles of inclination the meniscus would not deform, and would maintain the same shape as it had at higher angles. It was found that the temperature difference between the test section and manometer could cause a reading on the manometer when there was no flow. To overcome this the entire manometer assembly, that is manometer plus connecting tubes were enclosed in a water jacket that maintained the temperature close to that found in the test section. However even with these precautions the initial reading could not be eliminated entirely.

To estimate the magnitude of the temperature effects, consider the situation shown in figure 28.

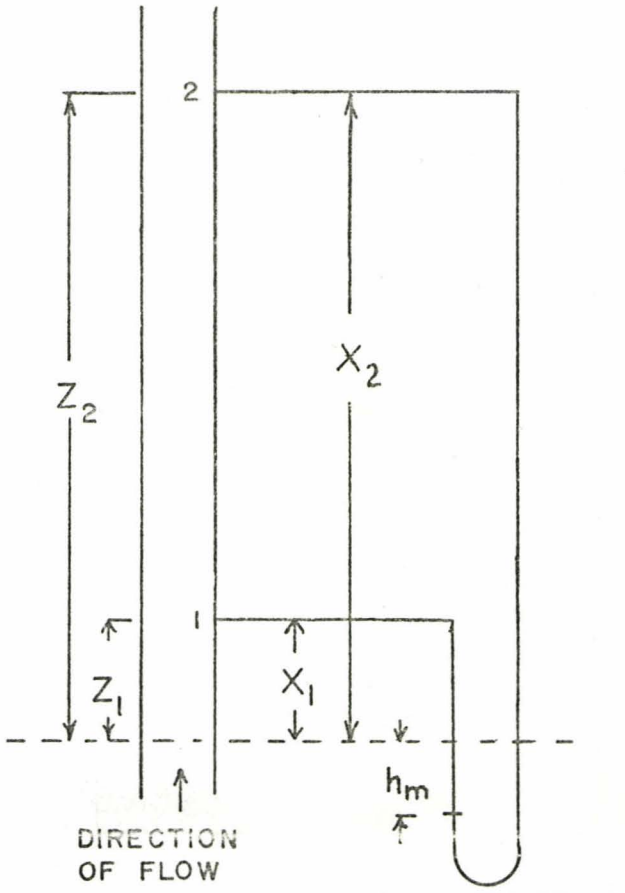

FIGURE 28

Applying the Bernoullis equation between points 1 and 2,

$$\frac{V_1^2}{2g} + \frac{P_1}{\gamma_T} + Z_1 = \frac{V_2^2}{2g} + \frac{P_2}{\gamma_T} + Z_2 + h_f$$

and assuming that $V_1 = V_2$, then;

$$h_f = \frac{P_1 - P_2}{\gamma_T} + (Z_1 - Z_2) \qquad (5.1)$$

Consider now the closed loop, starting from point 1 and going around the manometer to point 2.

$$P_1 + x_1 \gamma_c + h_m \gamma_c - h_m \gamma_m - x_2 \gamma_c = P_2$$

Therefore

$$P_1 - P_2 = \gamma_c (x_2 - x_1) + h_m (\gamma_m - \gamma_c) \tag{5.2}$$

Substituting these results into equation (5.1);

$$h_f = \gamma_c \frac{(x_2 - x_1)}{\gamma_T} + h_m \frac{(\gamma_m - \gamma_c)}{\gamma_T} + (Z_1 - Z_2) \tag{5.3}$$

and letting $Z_1 - Z_2 = \Delta Z$, then;

$$h_f = \Delta Z \left(\frac{\gamma_c}{\gamma_T} - 1\right) + h_m \left(\frac{\gamma_m - \gamma_c}{\gamma_T}\right) \tag{5.4}$$

In order to determine what the no flow manometer reading is, put $h_f = 0$; and let the reading be represented by $(h_m)_0$;

$$(h_m)_0 = \Delta Z \left(\frac{\gamma_T - \gamma_c}{\gamma_m - \gamma_c}\right) \tag{5.5}$$

For a test section length of five feet, and assuming that the manometer and connecting tubes are at room temperature while the test section is at 5°C, then;

$$\gamma_c = 0.99707$$

$$\gamma_T = .99999$$

$$\gamma_m = 1.5934$$

therefore

$$(h_m)_0 = 5.0 \left(\frac{.99999 - .99707}{1.5934 - .99707}\right)$$

$$= 0.0268 \text{ ft of water}$$

Converting this to a manometer reading;

$$h_m = \frac{30.48 \Delta P}{(62.4)(\gamma_m - \gamma_c)\sin \theta} \text{ cm. of fluid.}$$

For the zero reading calculated above

$$\Delta P = 0.0268 \times 62.4 = 1.673 \text{ lb}_F/\text{ft}^2$$

therefore

$$(h_m)_0 = \frac{30.48 \times 1.673}{(62.4)(1.5934 - .99707)(.275)} = 4.98 \text{ cm.}$$

Thus at a manometer inclination of 16° (the usual value thoughout the test) and for carbon tetrachloride under water, a zero reading as large as 5 cm. could be expected.

By adding the water jacket the temperature of the connecting tubes and manometer could be maintained close to that of the test section, and the zero reading could be reduced to approximately 1 to 2 cm., but could not be eliminated entirely because of the heat loss from the water jacket.

To obtain the form of the equation to calculate the pressure drop which incorporates this zero reading, consider the following equation;

$$(h_m)_0 = \Delta Z \left[\frac{\gamma_T - \gamma_c}{\gamma_m - \gamma_c}\right] \tag{5.6}$$

or $$\Delta Z \left(\frac{\gamma_c - \gamma_T}{\gamma_T}\right) = \left(\frac{\gamma_c - \gamma_m}{\gamma_T}\right) (h_m)_0 \tag{5.7}$$

Substituting equation (5.7) into equation (5.4);

$$h_f = \left(\frac{\gamma_c - \gamma_m}{\gamma_T}\right) h_{m_0} + h_m \left(\frac{\gamma_m - \gamma_c}{\gamma_T}\right)$$

or

$$h_f = \left(\frac{\gamma_m - \gamma_c}{\gamma_T}\right) (h_m - h_{m_0})$$

To calculate the friction factor, the head loss from points 1 to 2 is required; then

$$C_f = \frac{hf}{\left(\frac{L}{D}\right) \frac{\rho V^2}{2g_c}}$$

and substituting;

$$C_f = \frac{62.4 \left(\frac{\gamma_m - \gamma_c}{\gamma_T}\right) \frac{(h_m - h_{m_0}) \sin \Theta}{30.48}}{\left(\frac{L}{D}\right) \frac{\rho V^2}{2g_c}}$$

where h_m and h_{m_0} are in centimeters. This equation has been used to calculate the friction factor as a function of the Reynolds number. Figure 27 shows the results obtained for this apparatus.

Using the relationships

$$C_f = \frac{64}{R_e}$$

and $$C_f = \frac{0.3164}{R_e^{1/4}}$$

a deviation plot has been obtained and is compared with the predicted error of Appendix I, (see figure 16).

It can be seen that for laminar flow the results are very poor. However in this region

$$C_f = \frac{64}{R_e}$$

is known to hold rigorously and thus for the purpose of further calculations the pressure drop can be obtained exactly.

At a Reynolds number of 44,000 where because of the large values to be measured the accuracy would be expected to be better than for the low Reynolds number range, the friction factor is still below the expected value. In fact it appears to be about 10% consistently low with a scatter comensurate with the error analysis. This possibly indicates that the flow is somehow altered resulting in a decreased friction factor. In fact the measurements of the diameter of the test section indicate that the test section is barrel-shaped to a slight degree; it is possible that this slight divergence of flow as it enters the test section is responsible for the decreased friction

factor. Because the results appear consistently low it was decided to use the experimental results rather than the Blasius correlation.

Since part of the tests were to be carried out using polymer rather than pure water, and since polymer alters the pressure gradient it was important that a good friction factor, Reynolds number curve for polymer be obtained.

The tests for polymer were carried out in the same manner as those for water, and the friction factor was calculated using the same computer program. The tests were performed for polymer concentrations of 10, 25, 50, 75, and 100 Wppm. The results are shown in figure 29.

Perhaps because the polymer tests were performed at higher Reynolds numbers the error was less, but the scatter in the polymer data appears less than that for water. It is also evident that maximum drag reduction occurs at a concentration of about 50 Wppm.

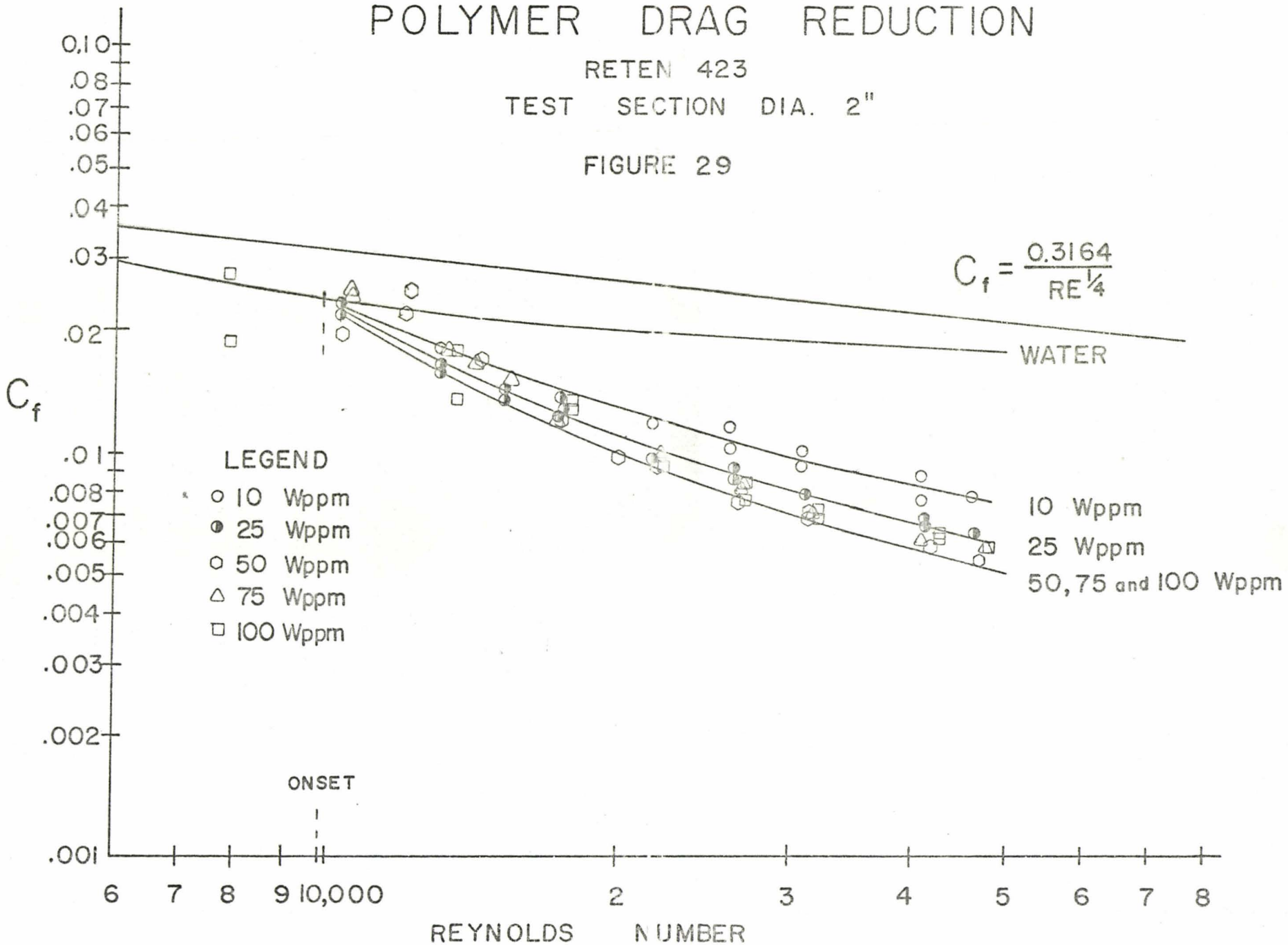
POLYMER DRAG REDUCTION
RETEN 423
TEST SECTION DIA. 2"
FIGURE 29
$C_f = \frac{0.3164}{RE^{1/4}}$
WATER
C_f
LEGEND
10 Wppm
25 Wppm
50 Wppm
75 Wppm
100 Wppm
10 Wppm
25 Wppm
50, 75 and 100 Wppm
ONSET
REYNOLDS NUMBER
0.10
.08
.07
.06
.05
.04
.03
.02
.01
.008
.007
.006
.005
.004
.003
.002
.001
6 7 8 9 10,000 2 3 4 5 6 7 8

APPENDIX VI

PROPERTIES OF THE POLYMER

Part of this experimental study was devoted to the examination of the effects a drag reducing solution has on a sphere hydrodynamically supported within a pipe. The substance used to achieve drag reduction was a polyacrylamide having a trade name Reten 423, and produced by Hercules Inc. This polymer has only recently been developed and therefore some effort was devoted to a study of its properties.

There are many tests that can be performed on the polymer, however those of a chemical nature are exceedingly difficult and tiresome to perform. For the purposes of this study only simple tests that reveal the physical properties of the polymer will be performed. These include firstly determining the change of physical properties of the polymer with time and secondly its rheological categorization, and finally its drag reducing properties in tubes of different sizes.

The instruments used to perform the tests are: a Brookfield cone and plate viscometer model LVT-CP, a capillary tube viscometer (sometimes referred to as a Hoyt Rheometer), and the two inch diameter main test section.

The first property studied was that of variation of drag reducing properties with time. According to that manufacturer several hours should be allowed to elapse between the time the polymer is mixed and used, to allow the polymer molecules to "relax". If the polymer is used immediately after it is mixed it has been observed that its drag reducing properties are not nearly as great as when it has been allowed to stand for several hours.

CAPILLARY TUBE VISCOMETER

FIGURE 30

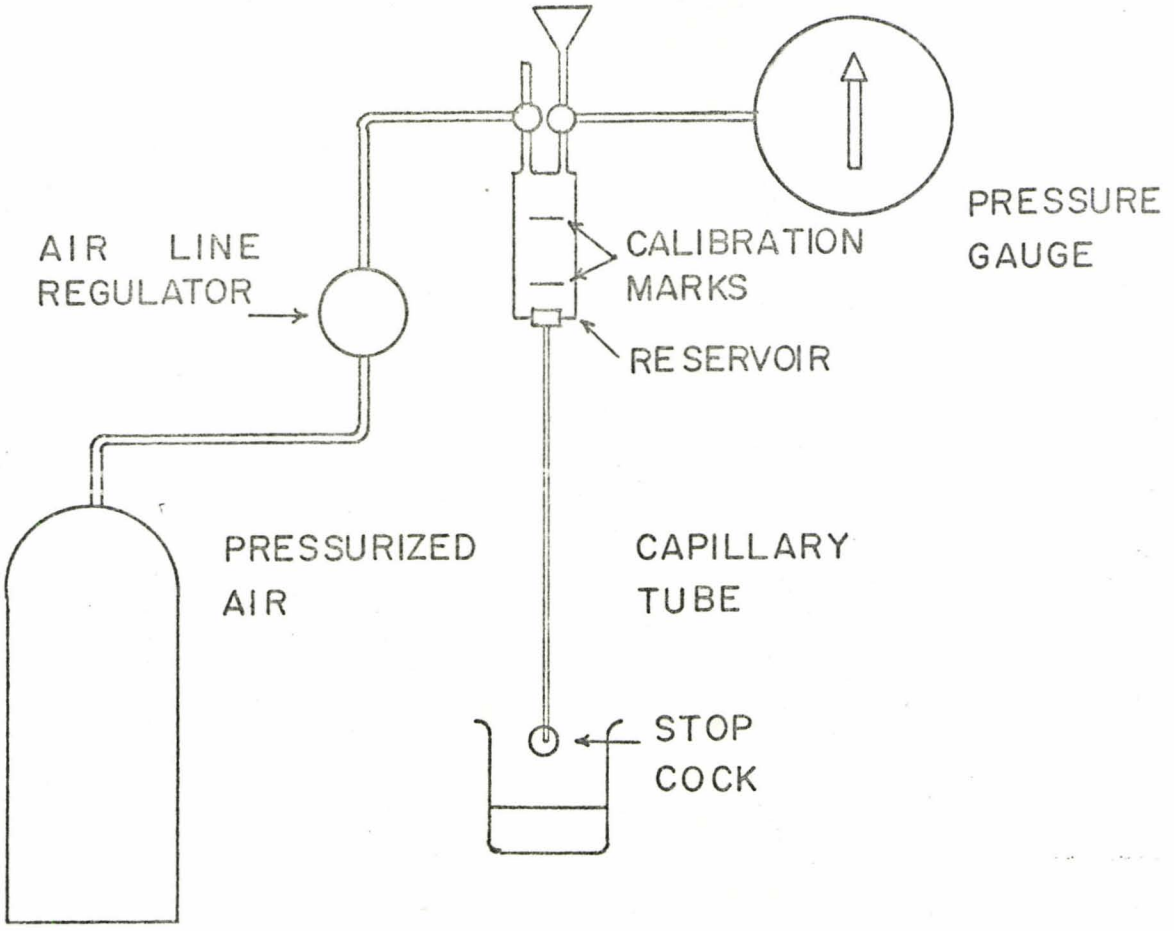

In order to know how long the polymer must be allowed to "relax" a batch was mixed under the usual conditions and samples taken at regular time intervals and the apparent viscosity of each sample measured using the cone and plate viscometer.

This instrument measures the proportionality constant in the equation

$$\tau = \mu \frac{du}{dy} \tag{6.1}$$

which makes the results of the polymer tests somewhat qualitative, in that the above equation is applicable only to laminar flow in Newtonian fluids. However, concentrated polymer solutions are non-Newtonian, that is μ is not a constant. Nevertheless it was felt that if μ were measured at a given shear rate ($\frac{du}{dy}$) = 11.5 sec^{-1}) its values would be an indication of the state of relaxation of the polymer.

Many such tests were performed, and a typical result is shown plotted in figure 31. Different batches varied widely, although the trend indicated in figure 31 was evident in most. In all cases the apparent viscosity dropped sharply in the first hour, climbed again briefly, then dropped and resumed its climb. The peak was generally reached after about six hours after the time of mixing, and maintained. Occasionally the apparent viscosity dropped some time after reaching the peak, although this was not a phenomenon that was always observed. Consequently no batch was used before being aged at least eighteen hours.

The next step was to categorize the rheological character of the concentrated 2000 Wppm polymer solution. To do this the Brookfield cone and plate viscometer was used. A single sample of the solution was taken and its viscosity measured at different shear rates.

APPARENT VISCOSITY TIME GRAPH

RETEN 423 2000 Wppm

BATCH 4

FIGURE 31

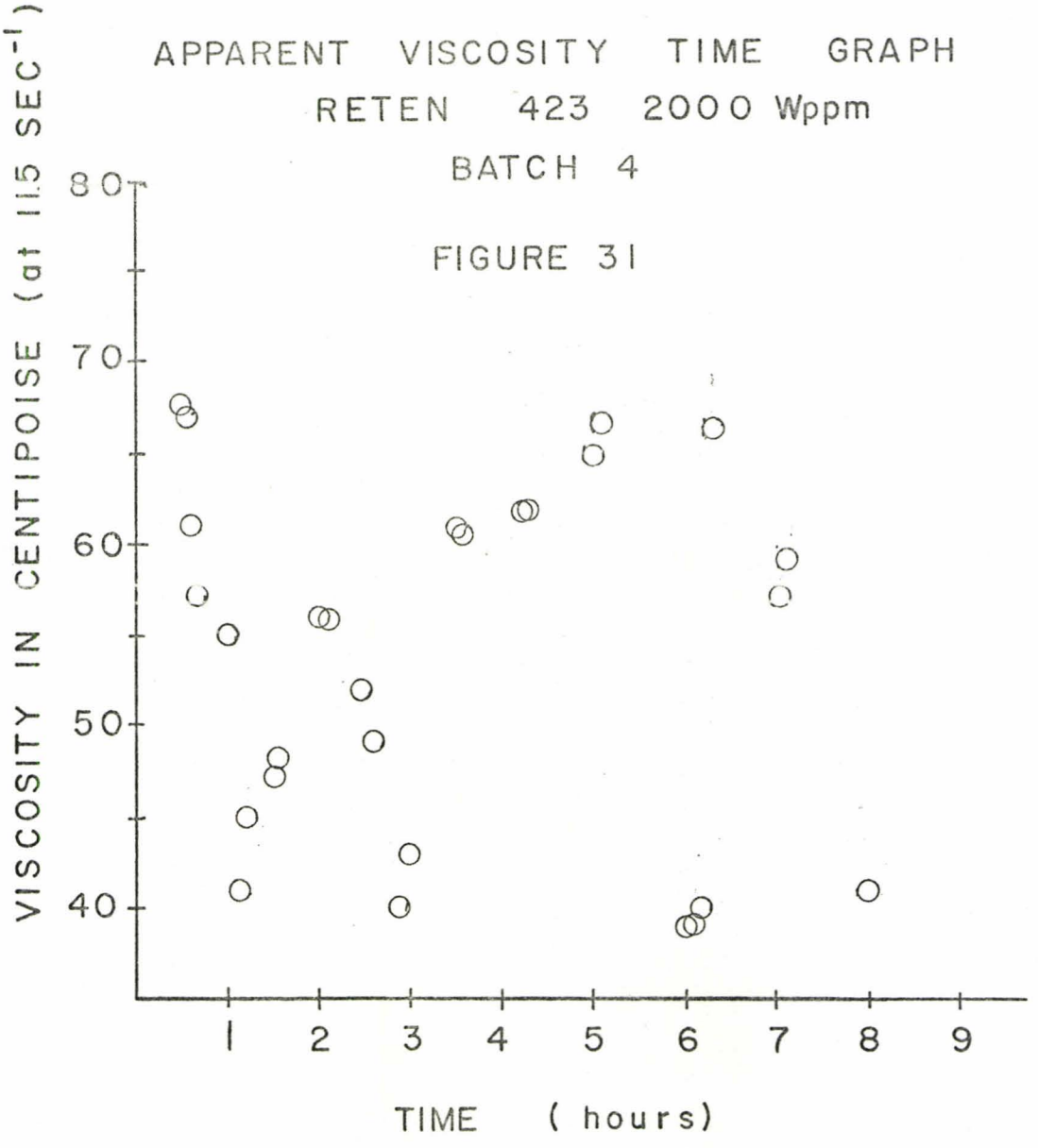

SHEAR STRESS SHEAR RATE

GRAPH

RETEN 423

2000 Wppm

FIGURE 32

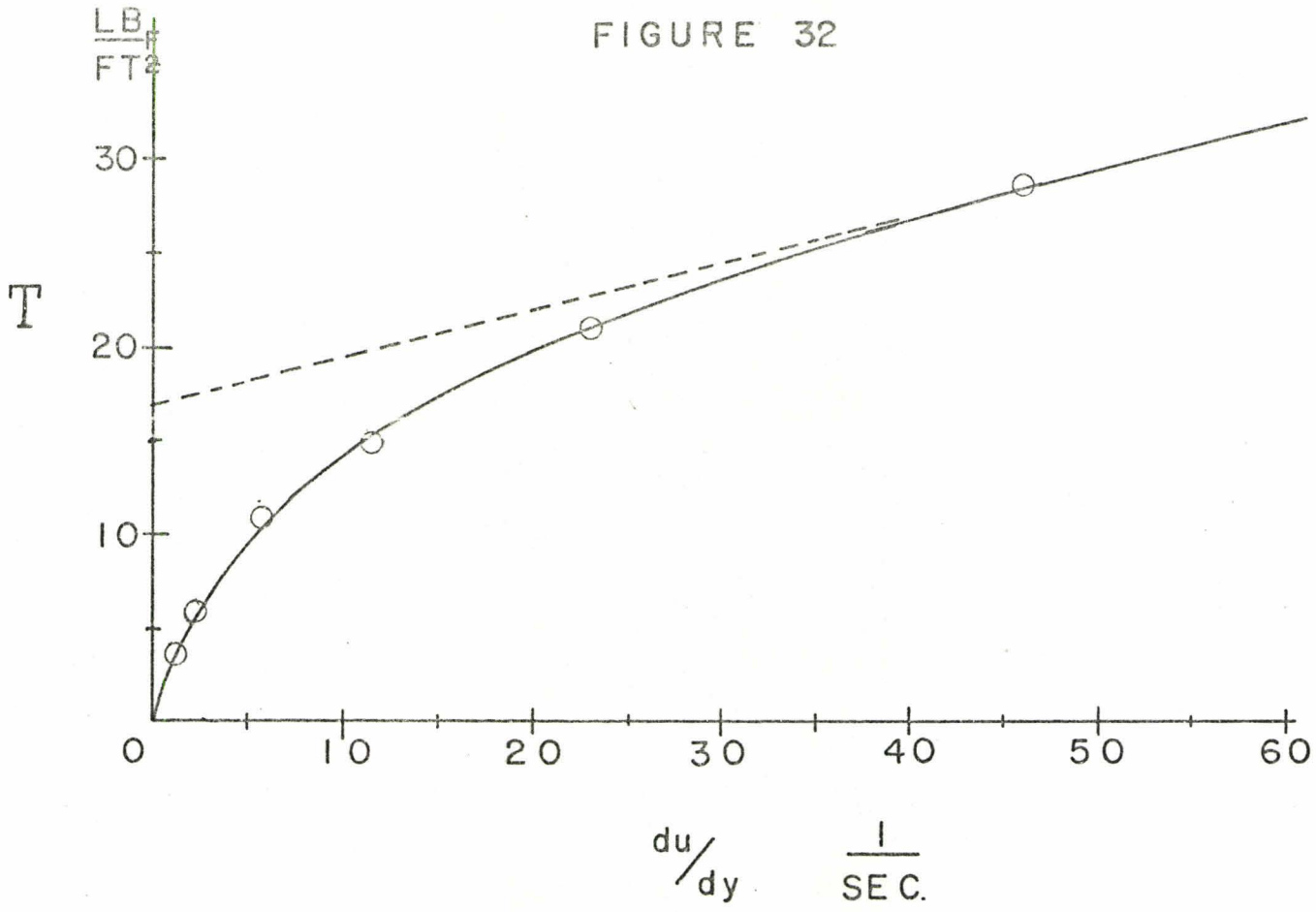

The results are shown in figure 32. It is apparent that concentrated Reten 423 is a pseudo-plastic fluid. At a shear rate of between 35 and 45 sec^{-1}, its shear stress becomes proportional to its shearing rate, but below this value it decreases with increasing shear rate. The viscosity beyond this value becomes $\mu = 0.25\ lb_F\ sec/ft^2$ compared to a water value of $\mu = 2 \times 10^{-5}\ lb_F\ sec/ft^2$.

It has been observed by other authors that polymer solutions exhibit a "diameter-effect" in their drag reducing properties. To determine if this effect occurs with Reten 423 a series of tests were performed using a Hoyt Rheometer similar to the one described in references (33) and (39) and shown in figure 30. The data measured using this instrument is presented in tabular form in tables 9, 10 and 11, and in graphical form in figure 33.

It has been postulated that this diameter effect occurs because of the thinness of the shear layer in capillary tubes, and is therefore completely independent of polymer properties. The results shown in figure 33 seem to bear this out. In figure 33 a comparison between data obtained in a 0.08 inch tube and a 2.0 inch tube show that in the smaller tube, drag reduction commences at lower concentrations and with greater effectiveness and at lower Reynolds numbers than for the much larger tubes. However beyond certain Reynolds numbers the drag reduction in the capillary tube becomes less than that in the test section. This occurence is consistent with an explanation of a thin shear layer that allows the polymer to alter the velocity profile to a greater extent than would occur with a large shear layer.

The final property of interest is one to be derived from the drag reduction data obtained in the two inch diameter test section. Meyer has

FRICTION FACTOR
REYNOLDS NUMBER

RETEN 423 POLYMER

FIGURE 33

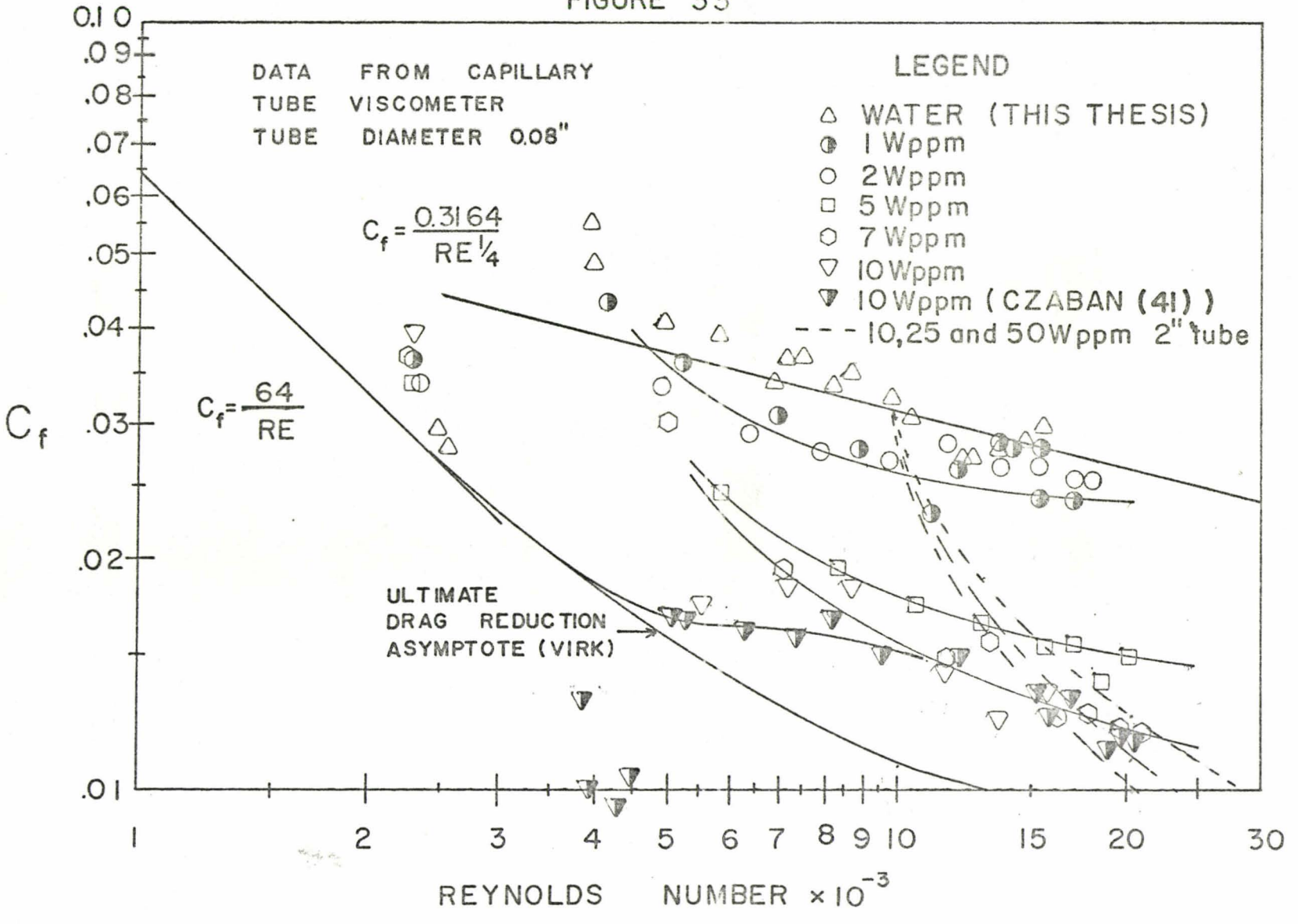

TABLE 9

```
                      PROGRAM TST (INPUT,OUTPUT,TAPE5=INPUT,TAPE6=OUTPUT)
000003                DIMENSION PG(45,10),T(45,10),V(10),VSQ(10),RE(10),DP(10),K1(10)
                     1  K2(10),CF(10)
000003                REAL K,K1,K2,NU,L
000003                INTEGER SETS
                C
000003                K=0.5
000005                D=0.08/12.0
000006                L=1.25
000010                NU=1.06E-5
000011                CONST=(0.0035316*4.0)/(3.14159*D*D)
                C
000014                READ (5,10) SETS
000022             10 FORMAT (I2)
000022                DO 1 I=1,SETS
000024              1 READ (5,2)  (PG(I,J),J=1,10)
000042                DO 3 I=1,SETS
000043              3 READ (5,2) (T(I,J),J=1,10)
000061              2 FORMAT (10F6.2)
                C
000061                WRITE (6,9)
000064              9 FORMAT (1H1,40X,*FRICTION FACTOR-REYNOLDS NUMBER DATA*//)
000064                DO 4 I=1,SETS
000066                DO 5 J=1,10
000067                IF (T(I,J).EQ.0.0) GO TO 11
000073                V(J)=CONST/T(I,J)
000077                VSQ(J)=V(J)*V(J)
000101                RE(J)=V(J)*D/NU
000104                DP(J)=144.0*PG(I,J)+101.4
000111                K1(J)=(DP(J)*4.0*D*32.17)/(2.0*62.4*L*VSQ(J))
000120                K2(J)=((1.0+K)*D)/(L)
000124                CF(J)=K1(J)-K2(J)
000127                GO TO 5
000127             11 CF(J)=0.0
000131                RE(J)=0.0
000132              5 CONTINUE
                C
000134                WRITE (6,6)  I
000142              6 FORMAT (1H0,30X,*DATA SET NUMBER*,4X,I2)
000142                WRITE (6,7)  (RE(J),J=1,10)
000154              7 FORMAT (1H0,10X,*RE*,4X,10E9.2)
000154                WRITE (6,8)  (CF(J),J=1,10)
000166              8 FORMAT (11X,*CF*,4X,10E9.2)
                C
000156              4 CONTINUE
                C
000171                STOP
000173                END

UNUSED COMPILER SPACE
007600
```

TABLE 10

MEASURED DATA

#1		#2		#3		#4		#5		#6		#7		#8	
P	T	P	T	P	T	P	T	P	T	P	T	P	T	P	T
PSIG	SEC	PSIG	SEC	PSIG	SEC	PSIG	SEC	PSIG	SEC	PSIG	SEC	PSIG	SEC	PSIG	SEC
0.0	27.0	0.0	27.3	0.0	27.8	0.0	28.0	0.0	26.3	0.0	28.5	0.0	25.9	0.0	29.5
2.4	16.2	2.1	15.6	2.5	13.0	2.3	11.8	2.1	16.1	2.4	12.7	2.6	14.0	2.7	11.6
4.2	11.2	3.2	12.0	3.5	10.0	5.1	7.8	3.2	12.8	3.5	9.1	3.6	11.8	3.8	8.7
7.0	8.7	5.2	9.2	5.5	8.2	8.4	6.0	5.5	9.4	5.8	7.2	6.0	9.5	5.5	7.4
6.5	9.0	8.0	7.2	8.3	6.6	12.0	5.0	8.5	7.7	8.8	5.6	10.5	6.7	8.5	5.6
9.6	7.9	11.6	5.7	12.3	5.6	11.2	4.2	11.4	6.6	12.1	4.9	15.7	5.6	11.6	4.6
13.6	5.8	15.6	5.2	16.6	4.7	20.6	3.8	16.4	5.2	15.9	4.0	20.2	4.8	16.6	4.0
17.0	5.1	19.6	4.8	20.8	4.2	24.3	3.9	19.5	4.8	19.8	3.6	24.5	4.4		
23.0	4.3	22.8	4.2	24.8	3.8	28.3	3.2	24.0	4.4	23.0	3.3	28.0	4.0		
		25.2	4.0	27.5	3.6			27.7	4.2	27.4	3.1				

The equation for use with the capillary tube viscometer is;

$$\frac{P_1}{\gamma} \frac{V_1^2}{2g} + \Delta Z = \frac{P_2}{\gamma} + \frac{V_2^2}{2g} + \frac{K V_2^2}{2g} + \frac{2 f V_2^2 L}{Dg}$$

where K = 0.5

Tube diameter D = 0.080 inches

Length L = 1.25 ft.

Temperature T = 21°C

Viscosity of water at 21°C $\upsilon = 1.06 \times 10^{-5}$ ft^2/sec

TABLE 11

FRICTION FACTOR--REYNOLDS NUMBER DATA

	DATA SET NUMBER 1							Water		
RE	2.36E+03	3.93E+03	5.68E+03	7.31E+03	7.07E+03	8.60E+03	1.10E+04	1.25E+04	1.48E+04	0.
CF	3.17E-02	5.50E-02	3.96E-02	3.71E-02	3.71E-02	3.57E-02	2.92E-02	2.76E-02	2.59E-02	0.
	DATA SET NUMBER 2							1 Wppm		
RE	2.33E+03	4.08E+03	5.30E+03	6.92E+03	8.34E+03	1.12E+04	1.22E+04	1.33E+04	1.52E+04	1.59E+04
CF	3.26E-02	4.48E-02	3.55E-02	3.07E-02	2.69E-02	2.29E-02	2.61E-02	2.82E-02	2.41E-02	2.41E-02
	DATA SET NUMBER 3							2 Wppm		
RE	2.29E+03	4.89E+03	6.36E+03	7.76E+03	9.54E+03	1.14E+04	1.35E+04	1.52E+04	1.67E+04	1.77E+04
CF	3.41E-02	3.39E-02	2.45E-02	2.43E-02	2.23E-02	2.35E-02	2.16E-02	2.13E-02	2.05E-02	2.03E-02
	DATA SET NUMBER 4							5 Wppm		
RE	2.27E+03	5.39E+03	8.16E+03	1.06E+04	1.27E+04	1.52E+04	1.67E+04	1.87E+04	1.99E+04	0.
CF	3.47E-02	2.44E-02	1.93E-02	1.74E-02	1.66E-02	1.51E-02	1.58E-02	1.44E-02	1.50E-02	0.
	DATA SET NUMBER 5							Water		
RE	2.42E+03	3.95E+03	4.97E+03	6.77E+03	8.26E+03	9.64E+03	1.22E+04	1.33E+04	1.45E+04	1.52E+04
CF	2.97E-02	4.82E-02	4.15E-02	3.44E-02	3.42E-02	3.28E-02	2.78E-02	2.80E-02	2.90E-02	3.08E-02
	DATA SET NUMBER 6							7 Wppm		
RE	2.23E+03	5.01E+03	6.99E+03	8.84E+03	1.14E+04	1.30E+04	1.59E+04	1.77E+04	1.93E+04	2.05E+04
CF	3.62E-02	3.07E-02	1.89E-02	1.81E-02	1.51E-02	1.58E-02	1.26E-02	1.26E-02	1.20E-02	1.29E-02
	DATA SET NUMBER 7							Water		
RE	2.46E+03	4.55E+03	5.39E+03	6.70E+03	9.50E+03	1.14E+04	1.33E+04	1.45E+04	1.59E+04	0.
CF	2.85E-02	4.21E-02	3.84E-02	3.88E-02	3.09E-02	3.18E-02	2.93E-02	2.97E-02	2.75E-02	0.
	DATA SET NUMBER 8							10 Wppm		
RE	2.16E+03	5.49E+03	7.31E+03	8.60E+03	1.14E+04	1.38E+04	1.59E+04	0.	0.	0.
CF	3.94E-02	2.74E-02	1.84E-02	1.83E-02	1.43E-02	1.21E-02	1.34E-02	0.	0.	0.

proposed a law of the wall applicable to polymer such that;

$$u^+ = \frac{1}{k} \ln y^+ + 5.5 + \alpha \ln \left(\frac{u_*}{u_{*0}'}\right) \tag{6.2}$$

where α is a property of the polymer dependant upon concentration and species. Meyer has derived the following modified friction factor relation for Reynolds number large enough that the wall friction exceeds u_{*0}';

$$\frac{1}{\sqrt{f}} = (4 + \frac{\alpha}{2}) \log (R_e\sqrt{f}) - 0.394 - \frac{\alpha}{2} \log \left(\frac{2\, u_{*0}'\, D}{\upsilon}\right) \tag{6.3}$$

F. M. White[25] has collected data for Guar Gum and Polyox WSR 301 showing the variation of α with concentration.

To calculate α it is first necessary to determine u_{*0}' the threshold friction velocity. From figure 29 the threshold value occurs at;

$$R_e = 9750$$

$$C_f = 0.023$$

or $$f = 0.00515$$

Now $u_{*0}' = \sqrt{\frac{\tau_0}{\rho}}$ at onset;

or $$u_{*0}' = \sqrt{\frac{\Delta P R g_c}{2L\rho}} \tag{6.4}$$

By definition

$$C_f = \frac{\Delta P}{(\frac{L}{D}) \frac{\rho V^2}{2g_c}} \tag{6.5}$$

At onset;

$$R_e = \frac{VD}{\upsilon} = 9750$$

therefore

$$u = \frac{9750 \times 1.6885 \times 10^{-5}}{6.1615}$$

$$= 1.019 \text{ ft./sec.}$$

and substituting into (6.5) we have;

$$\Delta P = 0.023 \times \left(\frac{5.0}{.1615}\right) \frac{62.4 \times (1.019)^2}{2 \times 32.2}$$

$$= 0.717 \text{ lb}_F/\text{ft}$$

Thus on substituting into equation (6.4) we can write;

$$u_{*0}' = \left\{\left[\frac{0.717 \left(\frac{.1615}{2}\right) (32.2)}{2 \times 5.0 \times 62.4}\right]\right\}^{1/2}$$

$$= 0.05466 \text{ ft/sec}$$

The value of α can be determined from equation (6.4) by substituting at any value of Reynolds number greater than the threshold value. Letting

$$R_e = 20{,}500$$

$$C_f = 0.010$$

or $$f = 0.0025$$

and substituting into equation (6.3) we have;

$$\frac{1}{\sqrt{.0025}} = (4 + \frac{\alpha}{2}) \log [(20,500) \sqrt{.0025}] - .394$$

$$- \frac{\alpha}{2} \log [\frac{2(.0546)(.1615)}{1.6845 \times 10^{-5}}]$$

Collecting terms and dividing we finally have;

$$\alpha = 83.24$$

This value seems extremely high when compared to the data of White[25] who calculated a maximum value of $\alpha = 11$ for both polyox and Guar Gum. It must be noted however that the threshold value of friction velocity for Reten 423 is extremely low, 0.055 ft/sec compared to 0.23 ft/sec for Guar Gum and 0.08 ft/sec for Polyox WSR 301.

APPENDIX VII

DATA TABLES

```
                      PROGRAM TST (INPUT,OUTPUT,TAPE5=INPUT,TAPE6=OUTPUT)
000003                REAL NU
000003                INTEGER SETS
                C
000003                DIMENSION ZA(40,10),ZRO1(40,10),ZRO2(40,10),V(40,10),SPN(40,10),
                     1 THT(40,10),DS(40),SIG(40),DOPT(100),RRE(100),DPDIF(40,10),
                     2 VSCAV(40,10),COVD(40),BUO(40),GM(40,10),A(40,10,2),DPL(40,10),
                     3 DPM(40,10),FCT(40,10),CRX(40,10),CD(40,10),DPC(40,10),BUO1(40),
                     4 VPR(40,10),XLG(40,10),LJCT(40),XRE(40,10),BLDL(40,10),DPZ(40,10)
                C
000003                COMMON/111/RE(100),DPT(100),D,NU(40),L,RO,NPTS
000003                COMMON/222/LINE(40,7)
                CC
                CCC   DATA INPUT (READ)
                CC
000003                READ (5,1) SETS,N
000013                DO 75 L=1,SETS
000015                SIG(L)=0.0
000016                DS(L)=0.0
000017                DOVD(L)=0.0
000020                BUO(L)=0.0
000021                DO 75 I=1,N
000023                V(L,I)=0.0
000026                GM(L,I)=0.0
000031                SPN(L,I)=0.0
000034                THT(L,I)=0.0
000036             75 CONTINUE
000043                DO 10 L=1,SETS
000045                DO 11 I=1,N
000046                DO 12 K=1,2
000047                READ(5,2) (ZA(K,J),J=1,2)
000062                IF (ZA(1,1).EQ.0.0) GO TO 13
000063             12 CONTINUE
000065                ZRO1(L,I)=ZA(1,2)-ZA(1,1)
000072                ZRO2(L,I)=ZA(2,2)-ZA(2,1)
000076                READ (5,2)  (A(L,I,J),J=1,2)
000114                READ (5,3) V(L,I)
000124                READ (5,4) GM(L,I),SPN(L,I),THT(L,I)
000144             11 CONTINUE
000147             13 READ (5,5) SIG(L),DS(L),NU(L)
000161                READ (5,6) (LINE(L,J),J=1,7)
000175              6 FORMAT (7A10)
000175             10 CONTINUE
000200              1 FORMAT (2I2)
000200              2 FORMAT (2F6.2)
000200              3 FORMAT (F6.2)
000200              4 FORMAT (3F10.4)
000200              5 FORMAT (2F10.4,E10.4)
000200                D=0.16343
000201                RO=62.4
000203                GC=0.99707
000204                GT=0.99999
000206                DL=4.0
000207                DO 200 I=1,N
                CC
```

```
000211      200 LJCT(I)=I
000214          READ (5,72) NPTS
000222       72 FORMAT (I2)
000222          DO 41 I=1,NPTS
000224       41 READ (5,40) RRE(I),DDPT(I)
000236          READ (5,42) XPL,YPL,XACT,YACT
000251       40 FORMAT (2F6.2)
000251       42 FORMAT (4F20.2)
            C
            CC      CONVERT DIGITIZER DATA TO ACTUAL VALUES
            C
000251          SFX1=XPL/(ALOG(XACT)-ALOG(1000.0))
000260          SFY1=YPL/(ALOG(YACT)-ALOG(0.001))
000266          WRITE (6,70)
000271       70 FORMAT (23X,*REYNOLDS NUMBER*,5X,*FRICTION FACTOR*//)
000271          DO 43 I=1,NPTS
000273          RE(I)=EXP((RRE(I)/SFX1)+ALOG(1000.0))
000303          DPT(I)=EXP((DDPT(I)/SFY1)+ALOG(0.001))
000314          WRITE (6,44) RE(I),DPT(I)
000324       44 FORMAT (20X,2E15.5)
000324       43 CONTINUE
            C
            CC
            CC      INITIALIZE PROGRAM   PRELIMINARY CALCULATIONS
            C
000327          DO 20 L=1,SETS
000330          DS(L)=DS(L)/12.0
000332          IF (L.GT.26) D=0.1615
000336          DO 20 I=1,N
000340          FCT(L,I)=0.0
000343          CRX(L,I)=0.0
000346          CD(L,I)=0.0
000351          DPDIF(L,I)=0.0
000353          DPC(L,I)=0.0
000356          VSQAV(L,I)=0.0
000360          DPL(L,I)=0.0
000363          DPM(L,I)=0.0
000365          VPR(L,I)=0.0
000370          XLG(L,I)=0.0
000372          XRE(L,I)=0.0
000375          DPZ(L,I)=0.0
000377          BLDL(L,I)=0.0
            C
000402          IF (V(L,I).EQ.0.0) GO TO 20
000404          FCT(L,I)=((GM(L,I)-GC)/GT)*THT(L,I)/30.48
000415          V(L,I)=V(L,I)*(0.1605*4.0)/(3.14159*D*D*60.0)
            C
000425       20 CONTINUE
000432          D=0.16343
            C
            CC      CORRECT FOR THERMAL NON ZERO
            C
000434          DO 21 L=1,SETS
000435          DO 21 I=1,N
000436          IF (V(L,I).EQ.0.0) GO TO 21
000441          CRX(L,I)=(ZRO1(L,I)+ZRO2(L,I))/2.0
000450       21 CONTINUE
```

```
      C
      C       CALCULATE PRESSURE DROP ACROSS CAPSULE ETC
      C
000455            DO 30 L=1,SETS
000457            IF (L.LE.26) GO TO 310
000461            D=0.1615
000463            DL=5.0
      C
000464        310 DOVD(L)=DS(L)/D
000467            BUO(L)=(SIG(L)-RO)/RO
000471            BUO1(L)=(SIG(L)-RO)/SIG(L)
000474            DO 31 I=1,N
      C
000475            IF (V(L,I).EQ.0.0) GO TO 31
000500            DPC(L,I)=((A(L,I,2)-A(L,I,1))-CRX(L,I))*RO*FCT(L,I)
000512            VSQAV(L,I)=V(L,I)*V(L,I)
000514            CALL INTERP (V(L,I),L,DPM(L,I),BLDL(L,I),XRE(L,I))
000521            DPDIF(L,I)=DPC(L,I)-DPM(L,I)
000530            CD(L,I)=(4.0/3.0)*(DS(L)*32.17/VSQAV(L,I))*((SIG(L)-RO)/RO)
000543            VPR(L,I)=VSQAV(L,I)/(BUO(L)*D)
000550            XLG(L,I)=DPDIF(L,I)/(BUO(L)*D)
000554            DPZ(L,I)=1.0+(DL/(SPN(L,I)*DS(L)))*((DPC(L,I)/BLDL(L,I))-1.0)
000567         31 CONTINUE
000572         30 CONTINUE
      C
      CC
      C
      C                    OUTPUT PORTION OF PROGRAM
      C
000574            DO 50 L=1,SETS
000576            DS(L)=DS(L)*12.0
000600            WRITE (6,51) (LINE(L,J),J=1,7)
000614         51 FORMAT (H1,20X,7A10)
      C
000614            WRITE (6,52) DS(L),SIG(L)
000624         52 FORMAT (H0,10X,*SPHERE DIAMETER*,F10.5,25X,*SPHERE DENSITY LB PER
                1FT..3*,F10.5//)
000624            WRITE (6,62) DOVD(L)
000632         62 FORMAT (10X,*D OVER D RATIO*,5X,F10.5)
000632            WRITE (6,65) NU(L)
000640         65 FORMAT (10X,*VISCOSITY*,10X,E10.3)
000640            WRITE (6,63)  BUO(L)
000646         63 FORMAT (10X,*(SIGMA-RO)/RO*,6X,F10.5)
000646            WRITE (6,80)  BUO1(L)
000654         80 FORMAT (10X,*SIGMA-RO/SIGMA*,5X,F10.5//)
000654            WRITE (6,400)
000660        400 FORMAT (H0,20X,*MANOMETER READING (CM)*,10X,*ZERO 1*,10X,*ZERO 2*)
000660            DO 401 I=1,N
000662            WRITE (6,402)  (A(L,I,J),J=1,2),ZRO1(L,I),ZRO2(L,I)
000705        402 FORMAT (25X,F5.2,5X,F5.2,13X,F5.2,11X,F5.2)
000705        401 CONTINUE
000710            WRITE (6,311)    (LJCT(I),I=1,N)
000722        311 FORMAT (H0,17X,10I9)
000722            WRITE (6,53 ) (GM(L,I),I=1,N)
000737         53 FORMAT (10X,*MAN. GM*,5X,10E9.2)
000737            WRITE (6,55)  (SPN(L,I),I=1,N)
000754         55 FORMAT (10X,*SPHERE NO*,3X,10E9.2)
000754            WRITE (6,54) (V(L,I),I=1,N)
```

```
000771         54 FORMAT (10X,*(V-AV)*6X,10E9.2)
000771            WRITE (6,59) (VSDAV(L,I),I=1,N)
001006         59 FORMAT (10X,*(V-AV)-SD*,3X,10E9.2)
001006            WRITE (6,61) (CD(L,I),I=1,N)
001023         61 FORMAT (10X,*DRAG COEFF*,2X,10E9.2)
001023            WRITE (6,203) (XRE(L,I),I=1,N)
001040        203 FORMAT (10X,*RE*,10X,10E9.2)
001040            WRITE (6,58) (DPC(L,I),I=1,N)
001055         58 FORMAT (10X,*DELTA-PM*,4X,10E9.2)
001055            WRITE (6,60) (DPDIF(L,I),I=1,N)
001072         60 FORMAT (10X*DPM-DPL*,5X,10E9.2)
001072            WRITE (6,84)  (VPR(L,I),I=1,N)
001107         84 FORMAT (10X,*V.V/K*,7X,10E9.2)
001107            WRITE (6,85)  (XLG(L,I),I=1,N)
001124         85 FORMAT (10X,*DPM-DPL/K*,3X,10E9.2)
001124            WRITE (6,56) (THT(L,I),I=1,N)
001141         56 FORMAT (10X,*MAN. THETA*,2X,10E9.2)
001141            WRITE (6,57) (CRX(L,I),I=1,N)
001156         57 FORMAT (10X,*(ZR1+ZR2)/2*,1X,10E9.2)
001156            WRITE (6,350)  (DPZ(L,I),I=1,N)
001173        350 FORMAT (10X,*PR1*,9X,10E9.2)
001173            WRITE (6,201)  (BLDL(L,I),I=1,N)
001210        201 FORMAT (10X,*DPL-BLASIUS*,1X,10E9.2)
001210            WRITE (6,403)
001214        403 FORMAT (H0,40X,*K=D.(SIG-R0)/R0*)
001214         50 CONTINUE
          C
          C
001217            STOP
001221            END

UNUSED COMPILER SPACE
015700
```

```
                SUBROUTINE INTERP(V,LX,DH,DH1,CLR)
      C
000010          REAL NU
000010          COMMON/111/RE(100),DPT(100),D,NU(40),L,RO,NPTS
      C
000010          DL=4.0
000011          D=0.16343
000012          IF (LX.LE.26) GO TO 50
000015          DL=5.0
000016          D=0.1615
000020       50 CLR=V*D/NU(LX)
000022          IF (CLR.LE.2500.0) GO TO 130
      C
000025          DO 100 I=1,NPTS
000026          IF (CLR.LE.RE(I)) GO TO 110
000031      100 CONTINUE
      C
000033          WRITE (6,120) LX
000040      120 FORMAT (10X,*DATA NOT IN RANGE*,5X,*SET NUMBER*,5X,I2//)
000040          DH=0.00
000044          GO TO 500
      C
000044      110 I=I-1
000046          CF=(DPT(I)-DPT(I+1))*((CLR-RE(I))/(RE(I+1)-RE(I)))+DPT(I+1)
000055          DH=(CF*DL*RO*V*V)/(D*2.0*32.17)
000063          CF1=0.316/(CLR)**0.25
000067          DH1=(CF1*DL*RO*V*V)/(D*2.0*32.17)
000076          GO TO 500
000076      130 DH=(32.0*DL*RO*V*V)/(32.17*D*CLR)
000104          DH1=DH
      C
000105      500 RETURN
000106          END

UNUSED COMPILER SPACE
023200
```

SET 1 1.875 STEEL SINGLE SPHERE

SPHERE DIAMETER 1.87500 SPHERE DENSITY LB PER FT..3 499.51000

D OVER D RATIO .95607
VISCOSITY 1.539E-05
(SIGMA-RO)/RO 7.00497
SIGMA-RO/SIGMA .87508

MANOMETER READING (CM)		ZERO 1	ZERO 2
8.08	65.30	1.43	1.86
8.05	65.38	1.86	1.93
8.00	65.10	1.93	1.62

	1	2	3	4	5	6	7	8	9	10
MAN. GM	1.59E+00	1.59E+00	1.59E+00	0.	0.	0.	0.	0.	0.	0.
SPHERE NO	1.00E+00	1.00E+00	1.00E+00	0.	0.	0.	0.	0.	0.	0.
(V-AV)	7.14E-01	7.14E-01	4.59E-01	0.	0.	0.	0.	0.	0.	0.
(V-AV)-SO	5.10E-01	5.10E-01	2.11E-01	0.	0.	0.	0.	0.	0.	0.
DRAG COEFF	9.21E+01	9.21E+01	2.23E+02	0.	0.	0.	0.	0.	0.	0.
RE	7.58E+03	7.58E+03	4.88E+03	0.	0.	0.	0.	0.	0.	0.
DELTA-PM	4.05E+01	4.04E+01	4.03E+01	0.	0.	0.	0.	0.	0.	0.
DPM-DPL	4.02E+01	4.01E+01	4.02E+01	0.	0.	0.	0.	0.	0.	0.
V.V/K	4.45E-01	4.45E-01	1.84E-01	0.	0.	0.	0.	0.	0.	0.
DPM-DPL/K	3.51E+01	3.50E+01	3.51E+01	0.	0.	0.	0.	0.	0.	0.
MAN. THETA	6.02E-01	6.02E-01	6.02E-01	0.	0.	0.	0.	0.	0.	0.
(ZR1+ZR2)/2	1.64E+00	1.89E+00	1.77E+00	0.	0.	0.	0.	0.	0.	0.
PR1	2.51E+03	2.50E+03	5.43E+03	0.	0.	0.	0.	0.	0.	0.
DPL-BLASIUS	4.10E-01	4.10E-01	1.89E-01	0.	0.	0.	0.	0.	0.	0.

K=D.(SIG-RO)/RO

SET 2 1.749 STEEL SINGLE SPHERE

SPHERE DIAMETER 1.74900 SPHERE DENSITY LB PER FT..3 503.50000

D OVER D RATIO	.89182
VISCOSITY	1.637E-05
(SIGMA-RO)/RO	7.06891
SIGMA-RO/SIGMA	.87607

MANOMETER READING (CM)		ZERO 1	ZERO 2
13.70	56.80	.96	.96

	1	2	3	4	5	6	7	8	9	10
MAN. GM	1.59E+00	0.	0.	0.	0.	0.	0.	0.	0.	0.
SPHERE NO	1.00E+00	0.	0.	0.	0.	0.	0.	0.	0.	0.
(V-AV)	6.69E-01	0.	0.	0.	0.	0.	0.	0.	0.	0.
(V-AV)-SC	4.48E-01	0.	0.	0.	0.	0.	0.	0.	0.	0.
DRAG COEFF	9.86E+01	0.	0.	0.	0.	0.	0.	0.	0.	0.
RE	6.68E+03	0.	0.	0.	0.	0.	0.	0.	0.	0.
DELTA-PM	3.10E+01	0.	0.	0.	0.	0.	0.	0.	0.	0.
DPM-DPL	3.07E+01	0.	0.	0.	0.	0.	0.	0.	0.	0.
V.V/K	3.88E-01	0.	0.	0.	0.	0.	0.	0.	0.	0.
DPM-DPL/K	2.66E+01	0.	0.	0.	0.	0.	0.	0.	0.	0.
MAN. THETA	6.09E-01	0.	0.	0.	0.	0.	0.	0.	0.	0.
(ZR1+ZR2)/2	9.60E-01	0.	0.	0.	0.	0.	0.	0.	0.	0.
PR1	2.26E+03	0.	0.	0.	0.	0.	0.	0.	0.	0.
DPL-BLASIUS	3.72E-01	0.	0.	0.	0.	0.	0.	0.	0.	0.

K=D.(SIG-RO)/RO

SET 3 1.625 STEEL UP TO 2 IN LINE

SPHERE DIAMETER 1.62500 SPHERE DENSITY LB PER FT..3 506.80000

D OVER D RATIO	.82859
VISCOSITY	1.539E-05
(SIGMA-RO)/RO	7.12179
SIGMA-RO/SIGMA	.87687

MANOMETER READING (CM)		ZERO 1	ZERO 2
18.31	56.37	.87	1.52
29.56	36.60	.10	.10

	1	2	3	4	5	6	7	8	9	10
MAN. GM	1.59E+00	1.35E+01	0.	0.	0.	0.	0.	0.	0.	0.
SPHERE NO	1.00E+00	2.00E+00	0.	0.	0.	0.	0.	0.	0.	0.
(V-AV)	1.50E+00	2.35E+00	0.	0.	0.	0.	0.	0.	0.	0.
(V-AV)-SQ	2.25E+00	5.51E+00	0.	0.	0.	0.	0.	0.	0.	0.
DRAG COEFF	1.84E+01	7.51E+00	0.	0.	0.	0.	0.	0.	0.	0.
RE	1.59E+04	2.49E+04	0.	0.	0.	0.	0.	0.	0.	0.
DELTA-PM	2.70E+01	5.67E+01	0.	0.	0.	0.	0.	0.	0.	0.
DPM-DPL	2.59E+01	5.41E+01	0.	0.	0.	0.	0.	0.	0.	0.
V.V/K	1.93E+00	4.73E+00	0.	0.	0.	0.	0.	0.	0.	0.
DPM-DPL/K	2.22E+01	4.65E+01	0.	0.	0.	0.	0.	0.	0.	0.
MAN. THETA	6.05E-01	3.17E-01	0.	0.	0.	0.	0.	0.	0.	0.
(ZR1+ZR2)/2	1.20E+00	1.00E-01	0.	0.	0.	0.	0.	0.	0.	0.
PR1	5.03E+02	2.41E+02	0.	0.	0.	0.	0.	0.	0.	0.
DPL-BLASIUS	1.50E+00	3.29E+00	0.	0.	0.	0.	0.	0.	0.	0.

K=D.(SIG-RO)/RO

SET 4 1.497 STEEL UP TO 5 IN LINE

SPHERE DIAMETER 1.49700 SPHERE DENSITY LB PER FT..3 513.50000

D OVER D RATIO	.76332
VISCOSITY	1.716E-05
(SIGMA-RO)/RO	7.22917
SIGMA-RO/SIGMA	.87848

MANOMETER READING (CM)		ZERO 1	ZERO 2
17.70	55.65	1.70	1.40
30.15	36.00	.10	.10
30.20	35.90	.10	.10
30.10	36.00	.10	.10
28.80	37.35	.10	.10
28.80	37.35	.07	.10
27.34	38.80	.08	.10
27.38	38.78	.07	.08
25.90	40.25	.06	.06
25.90	41.90	.08	.03

	1	2	3	4	5	6	7	8	9	10
MAN. GM	1.59E+00	1.35E+01	1.35E+01	1.35E+01	1.35E+01	1.35E+01	1.35E+01	1.35E+01	1.35E+01	1.35E+01
SPHERE NO	1.00E+00	2.00E+00	2.00E+00	2.00E+00	3.00E+00	3.00E+00	4.00E+00	4.00E+00	5.00E+00	5.00E+00
(V-AV)	3.20E+00	3.62E+00	3.52E+00	3.62E+00	3.67E+00	3.57E+00	3.95E+00	3.95E+00	4.38E+00	4.38E+00
(V-AV)-SQ	1.02E+01	1.31E+01	1.24E+01	1.31E+01	1.35E+01	1.27E+01	1.56E+01	1.56E+01	1.92E+01	1.92E+01
DRAG COEFF	3.78E+00	2.95E+00	3.12E+00	2.95E+00	2.67E+00	3.03E+00	2.48E+00	2.48E+00	2.01E+00	2.01E+00
RE	3.05E+04	3.45E+04	3.35E+04	3.45E+04	3.50E+04	3.40E+04	3.77E+04	3.77E+04	4.18E+04	4.18E+04
DELTA-PM	2.65E+01	4.66E+01	4.54E+01	4.70E+01	6.85E+01	6.86E+01	9.22E+01	9.18E+01	1.16E+02	1.29E+02
DPM-DPL	2.20E+01	4.09E+01	4.00E+01	4.13E+01	6.26E+01	6.30E+01	8.55E+01	8.52E+01	1.08E+02	1.21E+02
V.V/K	8.67E+00	1.11E+01	1.05E+01	1.11E+01	1.14E+01	1.08E+01	1.32E+01	1.32E+01	1.63E+01	1.63E+01
DPM-DPL/K	1.86E+01	3.46E+01	3.38E+01	3.49E+01	5.30E+01	5.34E+01	7.24E+01	7.21E+01	9.10E+01	1.02E+02
MAN. THETA	6.02E-01	3.16E-01	3.16E-01	3.16E-01	3.16E-01	3.16E-01	3.16E-01	3.16E-01	3.16E-01	3.16E-01
(ZR1+ZR2)/2	1.55E+00	1.00E-01	1.00E-01	1.00E-01	1.00E-01	8.50E-02	9.00E-02	7.50E-02	6.00E-02	5.50E-02
PR1	1.15E+02	8.85E+01	9.10E+01	8.94E+01	8.94E+01	9.45E+01	8.08E+01	8.05E+01	6.83E+01	7.68E+01
DPL-BLASIUS	5.82E+00	7.22E+00	6.87E+00	7.22E+00	7.39E+00	7.04E+00	8.41E+00	8.41E+00	1.01E+01	1.01E+01

K=D.(SIG-RO)/RO

SET 5 1.497 STEEL A CONTINUATION OF SET 4

SPHERE DIAMETER 1.49700 SPHERE DENSITY LB PER FT..3 513.50000

D OVER D RATIO	.76332
VISCOSITY	1.716E-05
(SIGMA-RO)/RO	7.22917
SIGMA-RO/SIGMA	.87848

MANOMETER READING (CM)		ZERO 1	ZERO 2
21.55	44.65	.05	.05
21.50	44.55	.09	.05
21.95	44.14	.11	.09

	1	2	3	4	5	6	7	8	9	10
MAN. GM	1.35E+01	1.35E+01	1.35E+01	0.	0.	0.	0.	0.	0.	0.
SPHERE NO	6.00E+00	6.00E+00	6.00E+00	0.	0.	0.	0.	0.	0.	0.
(V-AV)	4.14E+00	4.14E+00	4.07E+00	0.	0.	0.	0.	0.	0.	0.
(V-AV)-SQ	1.72E+01	1.72E+01	1.65E+01	0.	0.	0.	0.	0.	0.	0.
DRAG COEFF	2.25E+00	2.25E+00	2.34E+00	0.	0.	0.	0.	0.	0.	0.
RE	3.95E+04	3.95E+04	3.87E+04	0.	0.	0.	0.	0.	0.	0.
DELTA-PM	1.87E+02	1.86E+02	1.79E+02	0.	0.	0.	0.	0.	0.	0.
DPM-DPL	1.80E+02	1.79E+02	1.72E+02	0.	0.	0.	0.	0.	0.	0.
V.V/K	1.45E+01	1.45E+01	1.40E+01	0.	0.	0.	0.	0.	0.	0.
DPM-DPL/K	1.52E+02	1.51E+02	1.46E+02	0.	0.	0.	0.	0.	0.	0.
MAN. THETA	3.16E-01	3.16E-01	3.16E-01	0.	0.	0.	0.	0.	0.	0.
(ZR1+ZR2)/2	5.00E-02	7.00E-02	1.00E-01	0.	0.	0.	0.	0.	0.	0.
PR1	1.05E+02	1.05E+02	1.04E+02	0.	0.	0.	0.	0.	0.	0.
DPL-BLASIUS	9.14E+00	9.14E+00	8.84E+00	0.	0.	0.	0.	0.	0.	0.

K=D.(SIG-RO)/RO

SET 6 1.375 STEEL SINGLE SPHERES

SPHERE DIAMETER 1.37500 SPHERE DENSITY LB PER FT..3 520.50000

D OVER D RATIO	.70112
VISCOSITY	1.539E-05
(SIGMA-RO)/RO	7.34135
SIGMA-RO/SIGMA	.88012

MANOMETER READING (CM)		ZERO 1	ZERO 2
19.78	54.00	1.83	1.39
19.50	54.00	1.39	2.08
19.30	53.95	2.08	2.10

	1	2	3	4	5	6	7	8	9	10
MAN. GM	1.59E+00	1.59E+00	1.59E+00	0.	0.	0.	0.	0.	0.	0.
SPHERE NO	1.00E+00	1.00E+00	1.00E+00	0.	0.	0.	0.	0.	0.	0.
(V-AV)	3.93E+00	3.93E+00	3.93E+00	0.	0.	0.	0.	0.	0.	0.
(V-AV)-SQ	1.54E+01	1.54E+01	1.54E+01	0.	0.	0.	0.	0.	0.	0.
DRAG COEFF	2.34E+00	2.34E+00	2.34E+00	0.	0.	0.	0.	0.	0.	0.
RE	4.17E+04	4.17E+04	4.17E+04	0.	0.	0.	0.	0.	0.	0.
DELTA-PM	2.38E+01	2.39E+01	2.37E+01	0.	0.	0.	0.	0.	0.	0.
DPM-DPL	1.71E+01	1.72E+01	1.70E+01	0.	0.	0.	0.	0.	0.	0.
V.V/K	1.29E+01	1.29E+01	1.29E+01	0.	0.	0.	0.	0.	0.	0.
DPM-DPL/K	1.42E+01	1.43E+01	1.42E+01	0.	0.	0.	0.	0.	0.	0.
MAN. THETA	6.02E-01	6.02E-01	6.02E-01	0.	0.	0.	0.	0.	0.	0.
(ZR1+ZR2)/2	1.61E+00	1.74E+00	2.09E+00	0.	0.	0.	0.	0.	0.	0.
PR1	6.84E+01	6.89E+01	6.83E+01	0.	0.	0.	0.	0.	0.	0.
DPL-BLASIUS	8.11E+00	8.11E+00	8.11E+00	0.	0.	0.	0.	0.	0.	0.

K=D.(SIG-RO)/RO

SET 7 1.250 STEEL SINGLE SPHERE

SPHERE DIAMETER 1.25000 SPHERE DENSITY LB PER FT..3 535.80000

D OVER D RATIO .63738
VISCOSITY 1.539E-05
(SIGMA-RO)/RO 7.58654
SIGMA-RO/SIGMA .88354

MANOMETER READING (CM)		ZERO 1	ZERO 2
20.95	52.33	1.79	1.13
20.98	52.33	1.13	1.23

	1	2	3	4	5	6	7	8	9	10
MAN. GM	1.59E+00	1.59E+00	0.	0.	0.	0.	0.	0.	0.	0.
SPHERE NO	1.00E+00	1.00E+00	0.	0.	0.	0.	0.	0.	0.	0.
(V-AV)	4.38E+00	4.41E+00	0.	0.	0.	0.	0.	0.	0.	0.
(V-AV)-SQ	1.92E+01	1.95E+01	0.	0.	0.	0.	0.	0.	0.	0.
DRAG COEFF	1.76E+00	1.74E+00	0.	0.	0.	0.	0.	0.	0.	0.
RE	4.65E+04	4.69E+04	0.	0.	0.	0.	0.	0.	0.	0.
DELTA-PM	2.19E+01	2.20E+01	0.	0.	0.	0.	0.	0.	0.	0.
DPM-DPL	1.37E+01	1.38E+01	0.	0.	0.	0.	0.	0.	0.	0.
V.V/K	1.55E+01	1.57E+01	0.	0.	0.	0.	0.	0.	0.	0.
DPM-DPL/K	1.11E+01	1.11E+01	0.	0.	0.	0.	0.	0.	0.	0.
MAN. THETA	6.03E-01	6.03E-01	0.	0.	0.	0.	0.	0.	0.	0.
(ZR1+ZR2)/2	1.46E+00	1.18E+00	0.	0.	0.	0.	0.	0.	0.	0.
PR1	4.82E+01	4.78E+01	0.	0.	0.	0.	0.	0.	0.	0.
DPL-BLASIUS	9.81E+00	9.93E+00	0.	0.	0.	0.	0.	0.	0.	0.

K=D.(SIG-RO)/RO

SET 8 1.00 STEEL SINGLE SPHERES

SPHERE DIAMETER 1.00000 SPHERE DENSITY LB PER FT..3 513.50000

D OVER D RATIO	.50990
VISCOSITY	1.539E-05
(SIGMA-RO)/RO	7.22917
SIGMA-RO/SIGMA	.87848

MANOMETER READING (CM)		ZERO 1	ZERO 2
23.60	49.50	1.62	1.20
23.50	49.60	1.16	1.77

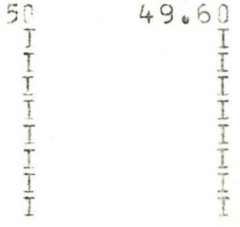

	1	2	3	4	5	6	7	8	9	10
MAN. GM	1.59E+00	1.59E+00	0.	0.	0.	0.	0.	0.	0.	0.
SPHERE NO	1.00E+00	1.00E+00	0.	0.	0.	0.	0.	0.	0.	0.
(V-AV)	4.93E+00	4.92E+00	0.	0.	0.	0.	0.	0.	0.	0.
(V-AV)-SQ	2.44E+01	2.42E+01	0.	0.	0.	0.	0.	0.	0.	0.
DRAG COEFF	1.06E+00	1.07E+00	0.	0.	0.	0.	0.	0.	0.	0.
RE	5.24E+04	5.22E+04	0.	0.	0.	0.	0.	0.	0.	0.
DELTA-PM	1.76E+01	1.77E+01	0.	0.	0.	0.	0.	0.	0.	0.
DPM-DPL	7.35E+00	7.53E+00	0.	0.	0.	0.	0.	0.	0.	0.
V.V/K	2.06E+01	2.05E+01	0.	0.	0.	0.	0.	0.	0.	0.
DPM-DPL/K	6.22E+00	6.37E+00	0.	0.	0.	0.	0.	0.	0.	0.
MAN. THETA	5.92E-01	5.92E-01	0.	0.	0.	0.	0.	0.	0.	0.
(ZR1+ZR2)/2	1.41E+00	1.47E+00	0.	0.	0.	0.	0.	0.	0.	0.
PR1	2.28E+01	2.36E+01	0.	0.	0.	0.	0.	0.	0.	0.
DPL-BLASIUS	1.21E+01	1.20E+01	0.	0.	0.	0.	0.	0.	0.	0.

K=D.(SIG-RO)/RO

SET 9 7/8 STEEL SINGLE SPHERES

SPHERE DIAMETER .87500 SPHERE DENSITY LB PER FT..3 482.50000

D OVER D RATIO .44616
VISCOSITY 1.584E-05
(SIGMA-RO)/RO 6.73237
SIGMA-RO/SIGMA .87067

MANOMETER READING (CM)		ZERO 1	ZERO 2
25.85	47.60	1.62	1.30
25.85	47.75	1.31	1.63

	1	2	3	4	5	6	7	8	9	10
MAN. GM	1.59E+00	1.59E+00	0.	0.	0.	0.	0.	0.	0.	0.
SPHERE NO	1.00E+00	1.00E+00	0.	0.	0.	0.	0.	0.	0.	0.
(V-AV)	4.89E+00	4.88E+00	0.	0.	0.	0.	0.	0.	0.	0.
(V-AV)-SO	2.39E+01	2.38E+01	0.	0.	0.	0.	0.	0.	0.	0.
DRAG COEFF	8.81E-01	8.85E-01	0.	0.	0.	0.	0.	0.	0.	0.
RE	5.04E+04	5.03E+04	0.	0.	0.	0.	0.	0.	0.	0.
DELTA-PM	1.50E+01	1.51E+01	0.	0.	0.	0.	0.	0.	0.	0.
DPM-DPL	4.98E+00	5.13E+00	0.	0.	0.	0.	0.	0.	0.	0.
V.V/K	2.17E+01	2.16E+01	0.	0.	0.	0.	0.	0.	0.	0.
DPM-DPL/K	4.53E+00	4.66E+00	0.	0.	0.	0.	0.	0.	0.	0.
MAN. THETA	6.09E-01	6.09E-01	0.	0.	0.	0.	0.	0.	0.	0.
(ZR1+ZR2)/2	1.46E+00	1.47E+00	0.	0.	0.	0.	0.	0.	0.	0.
PR1	1.48E+01	1.55E+01	0.	0.	0.	0.	0.	0.	0.	0.
DPL-BLASIUS	1.20E+01	1.19E+01	0.	0.	0.	0.	0.	0.	0.	0.

K=D.(SIG-RO)/RO

SET 10 3/4 STEEL SINGLE SPHERES

SPHERE DIAMETER .75000 SPHERE DENSITY LB PER FT..3 482.00000

D OVER D RATIO .38243
VISCOSITY 1.584E-05
(SIGMA-RO)/RO 6.72436
SIGMA-RO/SIGMA .87054

MANOMETER READING (CM) ZERO 1 ZERO 2

26.93 46.37 1.27 1.19
27.05 46.48 1.19 1.59

	1	2	3	4	5	6	7	8	9	10
MAN. GM	1.59E+00	1.59E+00	0.	0.	0.	0.	0.	0.	0.	0.
SPHERE NO	1.00E+00	1.00E+00	0.	0.	0.	0.	0.	0.	0.	0.
(V-AV)	4.81E+00	4.81E+00	0.	0.	0.	0.	0.	0.	0.	0.
(V-AV)-SQ	2.32E+01	2.32E+01	0.	0.	0.	0.	0.	0.	0.	0.
DRAG COEFF	7.78E-01	7.78E-01	0.	0.	0.	0.	0.	0.	0.	0.
RE	4.97E+04	4.97E+04	0.	0.	0.	0.	0.	0.	0.	0.
DELTA-PM	1.34E+01	1.33E+01	0.	0.	0.	0.	0.	0.	0.	0.
DPM-DPL	3.76E+00	3.64E+00	0.	0.	0.	0.	0.	0.	0.	0.
V.V/K	2.11E+01	2.11E+01	0.	0.	0.	0.	0.	0.	0.	0.
DPM-DPL/K	3.43E+00	3.31E+00	0.	0.	0.	0.	0.	0.	0.	0.
MAN. THETA	6.09E-01	6.09E-01	0.	0.	0.	0.	0.	0.	0.	0.
(ZR1+ZR2)/2	1.23E+00	1.39E+00	0.	0.	0.	0.	0.	0.	0.	0.
PR1	1.08E+01	1.01E+01	0.	0.	0.	0.	0.	0.	0.	0.
DPL-BLASIUS	1.16E+01	1.16E+01	0.	0.	0.	0.	0.	0.	0.	0.

K=D.(SIG-RO)/RO

SET 11 5/8 STEEL SINGLE SPHERES

SPHERE DIAMETER .62500 SPHERE DENSITY LB PER FT..3 482.30000

D OVER D RATIO	.31869
VISCOSITY	1.539E-05
(SIGMA-RO)/RO	6.72917
SIGMA-RO/SIGMA	.87062

MANOMETER READING (CM)		ZERO 1	ZERO 2
27.85	45.40	1.27	1.23
27.90	45.45	1.23	1.88

	1	2	3	4	5	6	7	8	9	10
MAN. GM	1.59E+00	1.59E+00	0.	0.	0.	0.	0.	0.	0.	0.
SPHERE NO	1.00E+00	1.00E+00	0.	0.	0.	0.	0.	0.	0.	0.
(V-AV)	4.72E+00	4.72E+00	0.	0.	0.	0.	0.	0.	0.	0.
(V-AV)-SQ	2.22E+01	2.22E+01	0.	0.	0.	0.	0.	0.	0.	0.
DRAG COEFF	6.76E-01	6.76E-01	0.	0.	0.	0.	0.	0.	0.	0.
RE	5.01E+04	5.01E+04	0.	0.	0.	0.	0.	0.	0.	0.
DELTA-PM	1.20E+01	1.18E+01	0.	0.	0.	0.	0.	0.	0.	0.
DPM-DPL	2.74E+00	2.51E+00	0.	0.	0.	0.	0.	0.	0.	0.
V.V/K	2.02E+01	2.02E+01	0.	0.	0.	0.	0.	0.	0.	0.
DPM-DPL/K	2.49E+00	2.29E+00	0.	0.	0.	0.	0.	0.	0.	0.
MAN. THETA	6.09E-01	6.09E-01	0.	0.	0.	0.	0.	0.	0.	0.
(ZR1+ZR2)/2	1.25E+00	1.56E+00	0.	0.	0.	0.	0.	0.	0.	0.
PR1	6.96E+00	5.41E+00	0.	0.	0.	0.	0.	0.	0.	0.
DPL-BLASIUS	1.12E+01	1.12E+01	0.	0.	0.	0.	0.	0.	0.	0.

K=D.(SIG-RO)/RO

SET 12 1/2 STEEL SINGLE SPHERES

SPHERE DIAMETER .50000 SPHERE DENSITY LB PER FT..3 484.00000

D OVER D RATIO	.25495
VISCOSITY	1.539E-05
(SIGMA-RO)/RO	6.75641
SIGMA-RO/SIGMA	.87107

MANOMETER READING (CM)

29.00
29.15

44.28
44.15

ZERO 1

1.45
1.25

ZERO 2

1.25
1.44

	1	2	3	4	5	6	7	8	9	10
MAN. GM	1.59E+00	1.59E+00	0.	0.	0.	0.	0.	0.	0.	0.
SPHERE NO	1.00E+00	1.00E+00	0.	0.	0.	0.	0.	0.	0.	0.
(V-AV)	4.43E+00	4.38E+00	0.	0.	0.	0.	0.	0.	0.	0.
(V-AV)-SQ	1.96E+01	1.92E+01	0.	0.	0.	0.	0.	0.	0.	0.
DRAG COEFF	6.15E-01	6.29E-01	0.	0.	0.	0.	0.	0.	0.	0.
RE	4.71E+04	4.65E+04	0.	0.	0.	0.	0.	0.	0.	0.
DELTA-PM	1.03E+01	1.01E+01	0.	0.	0.	0.	0.	0.	0.	0.
DPM-DPL	1.95E+00	1.94E+00	0.	0.	0.	0.	0.	0.	0.	0.
V.V/K	1.78E+01	1.74E+01	0.	0.	0.	0.	0.	0.	0.	0.
DPM-DPL/K	1.76E+00	1.76E+00	0.	0.	0.	0.	0.	0.	0.	0.
MAN. THETA	6.09E-01	6.09E-01	0.	0.	0.	0.	0.	0.	0.	0.
(ZR1+ZR2)/2	1.35E+00	1.35E+00	0.	0.	0.	0.	0.	0.	0.	0.
PR1	3.58E+00	3.51E+00	0.	0.	0.	0.	0.	0.	0.	0.
DPL-BLASIUS	1.00E+01	9.81E+00	0.	0.	0.	0.	0.	0.	0.	0.

K=D.(SIG-RO)/RO

SET 13 3/8 STEEL SINGLE SPHERES

SPHERE DIAMETER .37500 SPHERE DENSITY LB PER FT..3 485.00000

D OVER D RATIO .19121
VISCOSITY 1.539E-05
(SIGMA-RO)/RO 6.77244
SIGMA-RO/SIGMA .87134

MANOMETER READING (CM) ZERO 1 ZERO 2
33.00 42.70 1.19 1.38

	1	2	3	4	5	6	7	8	9	10
MAN. GM	1.59E+00	0.	0.	0.	0.	0.	0.	0.	0.	0.
SPHERE NO	1.00E+00	0.	0.	0.	0.	0.	0.	0.	0.	0.
(V-AV)	4.11E+00	0.	0.	0.	0.	0.	0.	0.	0.	0.
(V-AV)-SQ	1.69E+01	0.	0.	0.	0.	0.	0.	0.	0.	0.
DRAG COEFF	5.37E-01	0.	0.	0.	0.	0.	0.	0.	0.	0.
RE	4.37E+04	0.	0.	0.	0.	0.	0.	0.	0.	0.
DELTA-PM	6.20E+00	0.	0.	0.	0.	0.	0.	0.	0.	0.
DPM-DPL	-8.91E-01	0.	0.	0.	0.	0.	0.	0.	0.	0.
V.V/K	1.53E+01	0.	0.	0.	0.	0.	0.	0.	0.	0.
DPM-DPL/K	-8.05E-01	0.	0.	0.	0.	0.	0.	0.	0.	0.
MAN. THETA	6.09E-01	0.	0.	0.	0.	0.	0.	0.	0.	0.
(ZR1+ZR2)/2	1.28E+00	0.	0.	0.	0.	0.	0.	0.	0.	0.
PR1	-3.65E+01	0.	0.	0.	0.	0.	0.	0.	0.	0.
DPL-BLASIUS	8.78E+00	0.	0.	0.	0.	0.	0.	0.	0.	0.

K=D.(SIG-RO)/RO

SET 14 1.740 PLASTIC UP TO 5 IN LINE FREE FLOATING

SPHERE DIAMETER 1.74000 SPHERE DENSITY LB PER FT..3 73.69000

D OVER D RATIO .88723
VISCOSITY 1.637E-05
(SIGMA-RO)/RO .18093
SIGMA-RO/SIGMA .15321

MANOMETER READING (CM)		ZERO 1	ZERO 2
32.97	40.00	6.43	6.67
32.79	40.17	6.67	7.08
31.02	41.98	8.90	9.48
27.40	45.71	10.63	10.70
24.40	48.70	9.62	10.50
24.97	48.17	10.50	11.00
23.50	49.60	11.10	10.62
21.00	52.08	10.62	12.30
I	I	I	I
I	I	I	I

	1	2	3	4	5	6	7	8	9	10
MAN. GM	1.59E+00	1.59E+00	1.59E+00	1.59E+00	1.59E+00	1.59E+00	1.59E+00	1.59E+00	0.	0.
SPHERE NO	1.00E+00	1.00E+00	2.00E+00	3.00E+01	4.00E+00	4.00E+00	4.00E+00	5.00E+00	0.	0.
(V-AV)	1.17E-01	1.20E-01	1.26E-01	1.53E-01	1.59E-01	1.42E-01	1.52E-01	1.53E-01	0.	0.
(V-AV)-SO	1.38E-02	1.44E-02	1.59E-02	2.34E-02	2.54E-02	2.00E-02	2.30E-02	2.34E-02	0.	0.
DRAG COEFF	8.18E+01	7.83E+01	7.06E+01	4.81E+01	4.43E+01	5.62E+01	4.89E+01	4.81E+01	0.	0.
RE	1.17E+03	1.20E+03	1.26E+03	1.53E+03	1.59E+03	1.41E+03	1.52E+03	1.53E+03	0.	0.
DELTA-PM	7.08E-02	7.45E-02	2.54E-01	1.10E+00	2.04E+00	1.79E+00	2.19E+00	2.81E+00	0.	0.
DPM-DPL	5.30E-02	5.62E-02	2.35E-01	1.07E+00	2.02E+00	1.76E+00	2.16E+00	2.79E+00	0.	0.
V.V/K	4.65E-01	4.86E-01	5.39E-01	7.92E-01	8.59E-01	6.78E-01	7.79E-01	7.92E-01	0.	0.
DPM-DPL/K	1.79E+00	1.90E+00	7.93E+00	3.63E+01	6.82E+01	5.96E+01	7.31E+01	9.44E+01	0.	0.
MAN. THETA	1.22E-01	1.22E-01	1.18E-01	1.18E-01	1.18E-01	1.18E-01	1.18E-01	1.18E-01	0.	0.
(ZR1+ZR2)/2	6.55E+00	6.87E+00	9.19E+00	1.07E+01	1.01E+01	1.07E+01	1.09E+01	1.15E+01	0.	0.
PR1	8.28E+01	8.61E+01	1.69E+02	4.34E+01	5.75E+02	5.66E+02	6.47E+02	6.62E+02	0.	0.
DPL-BLASIUS	1.79E-02	1.82E-02	1.92E-02	2.33E-02	2.43E-02	2.15E-02	2.31E-02	2.33E-02	0.	0.

K=D.(SIG-RO)/RO

SET 15 1.475 PLASTIC UP TO 4 IN LINE FREE FLOATING

SPHERE DIAMETER 1.47500 SPHERE DENSITY LB PER FT..3 73.32000

D OVER D RATIO .75211
VISCOSITY 1.637E-05
(SIGMA-RO)/RO .17500
SIGMA-RO/SIGMA .14894

MANOMETER READING (CM)		ZERO 1	ZERO 2
32.89	40.02	6.86	4.60
32.91	40.01	4.60	5.76
34.64	36.25	.65	1.08
33.71	36.73	.91	1.10
33.92	37.09	.68	1.17
33.90	37.12	1.17	1.30
33.00	38.00	.84	1.18
33.04	38.00	1.09	3.60
33.12	37.90	.49	1.15
I	I	I	I

	1	2	3	4	5	6	7	8	9	10
MAN. GM	1.59E+00	1.59E+00	1.59E+00	1.59E+00	1.59E+00	1.59E+00	1.59E+00	1.59E+00	1.59E+00	0.
SPHERE NO	1.00E+00	1.00E+00	1.00E+00	2.00E+00	2.00E+00	2.00E+00	4.00E+00	4.00E+00	4.00E+00	0.
(V-AV)	2.61E-01	2.49E-01	2.74E-01	2.96E-01	4.07E-01	4.04E-01	4.20E-01	4.21E-01	3.19E-01	0.
(V-AV)-SQ	6.83E-02	6.18E-02	7.52E-02	8.75E-02	1.65E-01	1.63E-01	1.76E-01	1.77E-01	1.02E-01	0.
DRAG COEFF	1.35E+01	1.49E+01	1.23E+01	1.05E+01	5.58E+00	5.65E+00	5.24E+00	5.21E+00	9.08E+00	0.
RE	2.61E+03	2.48E+03	2.74E+03	2.95E+03	4.06E+03	4.04E+03	4.19E+03	4.20E+03	3.18E+03	0.
DELTA-PM	2.01E-01	2.75E-01	2.84E-01	7.69E-01	8.62E-01	7.62E-01	1.52E+00	9.98E-01	1.51E+00	0.
DPM-DPL	1.61E-01	2.37E-01	2.41E-01	7.23E-01	7.87E-01	6.88E-01	1.44E+00	9.18E-01	1.46E+00	0.
V.V/K	2.39E+00	2.16E+00	2.63E+00	3.06E+00	5.79E+00	5.71E+00	6.15E+00	6.19E+00	3.55E+00	0.
DPM-DPL/K	5.62E+00	8.30E+00	8.41E+00	2.53E+01	2.75E+01	2.40E+01	5.05E+01	3.21E+01	5.10E+01	0.
MAN. THETA	1.18E-01	1.18E-01	3.16E-01	3.16E-01	3.17E-01	3.17E-01	3.16E-01	3.16E-01	3.16E-01	0.
(ZR1+ZR2)/2	5.73E+00	5.18E+00	8.65E-01	1.00E+00	9.25E-01	1.24E+00	1.01E+00	2.35E+00	8.20E-01	0.
PR1	5.95E+01	2.05E+02	8.72E+01	1.25E+02	7.49E+01	6.53E+01	6.84E+01	4.21E+01	1.14E+02	0.
DPL-BLASIUS	7.17E-02	3.78E-02	7.79E-02	8.91E-02	1.55E-01	1.54E-01	1.64E-01	1.65E-01	1.01E-01	0.

K=D.(SIG-RO)/RO

SET 16 1.740 PLASTIC UP TO 4 IN LINE TWO DIAMETERS APART

SPHERE DIAMETER 1.74000 SPHERE DENSITY LB PER FT..3 73.69000

D OVER D RATIO .88723
VISCOSITY 1.689E-05
(SIGMA-RO)/RO .18093
SIGMA-RO/SIGMA .15321

MANOMETER READING (CM)		ZERO 1	ZERO 2
32.97	40.00	6.43	6.67
32.79	40.17	6.67	7.08
33.72	37.62	1.60	1.65
33.60	37.77	1.61	1.65
33.68	37.71	1.65	1.60
33.68	37.72	1.60	1.66
32.29	38.98	1.83	1.87
32.20	39.08	1.87	-1.20
32.32	39.00	1.38	1.64
31.50	39.62	1.26	1.43

	1	2	3	4	5	6	7	8	9	10
MAN. GM	1.59E+00	1.59E+00	1.59E+00	1.59E+00	1.59E+00	1.59E+00	1.59E+00	1.59E+00	1.59E+00	1.59E+00
SPHERE NO	1.00E+00	1.00E+00	2.00E+00	2.00E+00	2.00E+00	2.00E+00	3.00E+00	3.00E+00	3.00E+00	4.00E+00
(V-AV)	1.17E-01	1.20E-01	1.22E-01	1.17E-01	1.20E-01	1.13E-01	1.19E-01	1.19E-01	1.19E-01	1.21E-01
(V-AV)-SQ	1.38E-02	1.44E-02	1.50E-02	1.38E-02	1.44E-02	1.29E-02	1.41E-02	1.41E-02	1.41E-02	1.47E-02
DRAG COEFF	8.18E+01	7.83E+01	7.51E+01	8.18E+01	7.83E+01	8.74E+01	8.00E+01	8.00E+01	8.00E+01	7.67E+01
RE	1.14E+03	1.16E+03	1.18E+03	1.14E+03	1.16E+03	1.10E+03	1.15E+03	1.15E+03	1.15E+03	1.17E+03
DELTA-PM	7.08E-02	7.45E-02	8.73E-01	9.75E-01	9.23E-01	9.25E-01	1.86E+00	2.51E+00	1.98E+00	2.60E+00
DPM-DPL	5.24E-02	5.57E-02	8.54E-01	9.56E-01	9.04E-01	9.07E-01	1.84E+00	2.49E+00	1.97E+00	2.58E+00
V.V/K	4.65E-01	4.86E-01	5.07E-01	4.65E-01	4.86E-01	4.36E-01	4.76E-01	4.76E-01	4.76E-01	4.96E-01
DPM-DPL/K	1.77E+00	1.88E+00	2.89E+01	3.23E+01	3.06E+01	3.07E+01	6.22E+01	8.43E+01	6.65E+01	8.73E+01
MAN. THETA	1.22E-01	1.22E-01	3.17E-01	3.17E-01	3.17E-01	3.17E-01	3.17E-01	3.17E-01	3.17E-01	3.17E-01
(ZR1+ZR2)/2	6.55E+00	6.87E+00	1.63E+00	1.63E+00	1.63E+00	1.63E+00	1.85E+00	3.35E-01	1.51E+00	1.35E+00
PR1	7.95E+01	8.26E+01	6.14E+02	7.17E+02	6.64E+02	7.03E+02	9.09E+02	1.23E+03	9.72E+02	9.37E+02
DPL-BLASIUS	1.84E-02	1.88E-02	1.92E-02	1.84E-02	1.88E-02	1.78E-02	1.86E-02	1.86E-02	1.86E-02	1.90E-02

K=D.(SIG-RO)/RO

SET 17 1.740 PLASTIC A CONTINUATION OF SET 16

SPHERE DIAMETER 1.74000 SPHERE DENSITY LB PER FT..3 73.69000

D OVER D RATIO	.88723
VISCOSITY	1.689E-05
(SIGMA-RO)/RO	.18093
SIGMA-RO/SIGMA	.15321

MANOMETER READING (CM)		ZERO 1	ZERO 2
31.86	39.39	1.34	1.30
31.70	39.48	1.20	1.34
31.77	39.43	1.30	1.34
30.79	40.60	1.41	1.45
30.98	40.40	1.45	1.77
30.98	40.49	1.28	1.60
29.32	42.06	.64	1.79
29.35	42.07	1.79	1.82
29.40	42.00	1.82	1.83
I	I	I	I

	1	2	3	4	5	6	7	8	9	10
MAN. GM	1.59E+00	1.59E+00	1.59E+00	1.59E+00	1.59E+00	1.59E+00	1.59E+00	1.59E+00	1.59E+00	0.
SPHERE NO	4.00E+00	4.00E+00	4.00E+00	5.00E+00	5.00E+00	5.00E+00	6.00E+00	6.00E+00	6.00E+00	0.
(V-AV)	1.19E-01	1.20E-01	1.20E-01	1.17E-01	1.19E-01	1.17E-01	1.17E-01	1.19E-01	1.17E-01	0.
(V-AV)-SQ	1.41E-02	1.44E-02	1.44E-02	1.38E-02	1.41E-02	1.38E-02	1.38E-02	1.41E-02	1.38E-02	0.
DRAG COEFF	8.00E+01	7.83E+01	7.83E+01	8.18E+01	8.00E+01	8.18E+01	8.18E+01	8.00E+01	8.18E+01	0.
RE	1.15E+03	1.16E+03	1.16E+03	1.14E+03	1.15E+03	1.14E+03	1.14E+03	1.15E+03	1.14E+03	0.
DELTA-PM	2.41E+00	2.50E+00	2.43E+00	3.22E+00	3.00E+00	3.10E+00	4.42E+00	4.19E+00	4.14E+00	0.
DPM-DPL	2.39E+00	2.48E+00	2.41E+00	3.20E+00	2.98E+00	3.08E+00	4.40E+00	4.17E+00	4.12E+00	0.
V.V/K	4.76E-01	4.86E-01	4.86E-01	4.65E-01	4.76E-01	4.65E-01	4.65E-01	4.76E-01	4.65E-01	0.
DPM-DPL/K	8.08E+01	8.39E+01	8.17E+01	1.08E+02	1.01E+02	1.04E+02	1.49E+02	1.41E+02	1.39E+02	0.
MAN. THETA	3.17E-01	3.17E-01	3.17E-01	3.17E-01	3.17E-01	3.17E-01	3.17E-01	3.17E-01	3.17E-01	0.
(ZR1+ZR2)/2	1.32E+00	1.27E+00	1.32E+00	1.43E+00	1.61E+00	1.44E+00	1.21E+00	1.80E+00	1.83E+00	0.
PR1	8.86E+02	9.10E+02	8.86E+02	9.59E+02	8.84E+02	9.24E+02	1.10E+03	1.03E+03	1.03E+03	0.
DPL-BLASIUS	1.86E-02	1.88E-02	1.88E-02	1.84E-02	1.86E-02	1.84E-02	1.84E-02	1.86E-02	1.84E-02	0.

K=D.(SIG-RO)/RO

SET 18 1.475 PLASTIC UP TO 5 IN LINE AT TWO DIAMETERS APART

SPHERE DIAMETER 1.47500 SPHERE DENSITY LB PER FT..3 73.32000

D OVER D RATIO .75211
VISCOSITY 1.689E-05
(SIGMA-RO)/RO .17500
SIGMA-RO/SIGMA .14894

MANOMETER READING (CM)		ZERO 1	ZERO 2
32.91	40.01	.60	5.76
34.15	36.91	1.38	1.63
33.60	37.59	1.51	1.77
33.00	37.20	1.77	1.79
32.60	38.32	1.74	1.92
32.68	38.26	1.68	1.91
32.62	38.33	1.76	1.84
32.39	38.89	1.35	1.81
32.17	39.00	1.80	1.89
32.29	38.94	1.40	1.83

	1	2	3	4	5	6	7	8	9	10
MAN. GM	1.59E+00	1.59E+00	1.59E+00	1.59E+00	1.59E+00	1.59E+00	1.59E+00	1.59E+00	1.59E+00	1.59E+00
SPHERE NO	1.00E+00	2.00E+00	3.00E+00	3.00E+00	4.00E+00	4.00E+00	4.00E+00	5.00E+00	5.00E+00	5.00E+00
(V-AV)	2.49E-01	2.68E-01	2.72E-01	2.75E-01	2.70E-01	2.86E-01	2.91E-01	2.93E-01	3.05E-01	2.87E-01
(V-AV)-SQ	6.18E-02	7.17E-02	7.38E-02	7.59E-02	7.31E-02	8.16E-02	8.45E-02	8.60E-02	9.29E-02	8.23E-02
DRAG COEFF	1.49E+01	1.29E+01	1.25E+01	1.22E+01	1.26E+01	1.13E+01	1.09E+01	1.07E+01	9.93E+00	1.12E+01
RE	2.41E+03	2.59E+03	2.63E+03	2.67E+03	2.62E+03	2.76E+03	2.81E+03	2.84E+03	2.95E+03	2.78E+03
DELTA-PM	5.62E-01	4.84E-01	9.06E-01	9.33E-01	1.50E+00	1.46E+00	1.51E+00	1.90E+00	1.92E+00	1.93E+00
DPM-DPL	5.23E-01	4.40E-01	8.63E-01	8.88E-01	1.46E+00	1.41E+00	1.46E+00	1.85E+00	1.87E+00	1.89E+00
V.V/K	2.16E+00	2.51E+00	2.58E+00	2.65E+00	2.56E+00	2.85E+00	2.96E+00	3.01E+00	3.25E+00	2.88E+00
DPM-DPL/K	1.83E+01	1.54E+01	3.02E+01	3.11E+01	5.10E+01	4.94E+01	5.10E+01	6.46E+01	6.55E+01	6.59E+01
MAN. THETA	1.18E-01	3.19E-01	3.19E-01	3.19E-01	3.19E-01	3.19E-01	3.19E-01	3.19E-01	3.19E-01	3.17E-01
(ZR1+ZR2)/2	3.18E+00	1.50E+00	1.64E+00	1.78E+00	1.83E+00	1.79E+00	1.80E+00	1.58E+00	1.84E+00	1.62E+00
PR1	4.37E+02	8.92E+01	1.17E+02	1.18E+02	1.52E+02	1.34E+02	1.34E+02	1.34E+02	1.27E+02	1.42E+02
DPL-BLASIUS	3.90E-02	7.54E-02	7.73E-02	7.92E-02	7.66E-02	8.44E-02	8.71E-02	8.84E-02	9.45E-02	8.51E-02

K=D.(SIG-RO)/RO

SET 19 A CONTINUATION OF SET 18 6 IN LINE 2D

SPHERE DIAMETER 1.47500 SPHERE DENSITY LB PER FT..3 73.32000

D OVER D RATIO .75211
VISCOSITY 1.689E-05
(SIGMA-RO)/RO .17500
SIGMA-RO/SIGMA .14894

MANOMETER READING (CM)		ZERO 1	ZERO 2
31.28	39.80	1.71	1.92
31.28	39.85	1.92	1.92
31.30	39.85	1.88	1.95

	1	2	3	4	5	6	7	8	9	10
MAN. GM	1.59E+00	1.59E+00	1.59E+00	0.	0.	0.	0.	0.	0.	0.
SPHERE NO	6.00E+00	6.00E+00	6.00E+00	0.	0.	0.	0.	0.	0.	0.
(V-AV)	2.91E-01	3.01E-01	3.05E-01	0.	0.	0.	0.	0.	0.	0.
(V-AV)-SQ	8.45E-02	9.06E-02	9.29E-02	0.	0.	0.	0.	0.	0.	0.
DRAG COEFF	1.09E+01	1.02E+01	9.93E+00	0.	0.	0.	0.	0.	0.	0.
RE	2.81E+03	2.91E+03	2.95E+03	0.	0.	0.	0.	0.	0.	0.
DELTA-PM	2.57E+00	2.55E+00	2.55E+00	0.	0.	0.	0.	0.	0.	0.
DPM-DPL	2.53E+00	2.50E+00	2.50E+00	0.	0.	0.	0.	0.	0.	0.
V.V/K	2.96E+00	3.17E+00	3.25E+00	0.	0.	0.	0.	0.	0.	0.
DPM-DPL/K	8.83E+01	8.75E+01	8.73E+01	0.	0.	0.	0.	0.	0.	0.
MAN. THETA	3.17E-01	3.17E-01	3.17E-01	0.	0.	0.	0.	0.	0.	0.
(ZR1+ZR2)/2	1.82E+00	1.92E+00	1.91E+00	0.	0.	0.	0.	0.	0.	0.
PR1	1.56E+02	1.45E+02	1.42E+02	0.	0.	0.	0.	0.	0.	0.
DPL-BLASIUS	8.71E-02	9.25E-02	9.45E-02	0.	0.	0.	0.	0.	0.	0.

K=D.(SIG-RO)/RO

SET 20 1.236 PLASTIC SINGLE SPHERES

SPHERE DIAMETER 1.23600 SPHERE DENSITY LB PER FT..3 72.26000

D OVER D PATIO .63024
VISCOSITY 1.637E-05
(SIGMA-RO)/RO .15801
SIGMA-RO/SIGMA .13645

MANOMETER READING (CM)		ZERO 1	ZERO 2
32.64	42.60	6.91	6.78
32.64	43.30	6.78	6.32

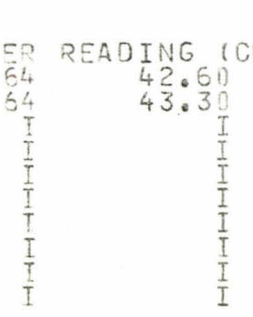

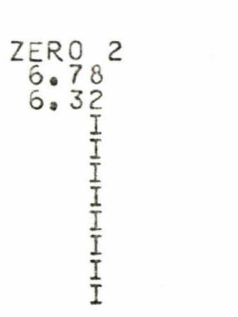

	1	2	3	4	5	6	7	8	9	10
MAN. GM	1.59E+00	1.59E+00	0.	0.	0.	0.	0.	0.	0.	0.
SPHERE NO	1.00E+00	1.00E+00	0.	0.	0.	0.	0.	0.	0.	0.
(V-AV)	5.15E-01	5.10E-01	0.	0.	0.	0.	0.	0.	0.	0.
(V-AV)-SC	2.65E-01	2.60E-01	0.	0.	0.	0.	0.	0.	0.	0.
DRAG COEFF	2.63E+00	2.68E+00	0.	0.	0.	0.	0.	0.	0.	0.
RE	5.14E+03	5.09E+03	0.	0.	0.	0.	0.	0.	0.	0.
DELTA-PM	4.47E-01	5.89E-01	0.	0.	0.	0.	0.	0.	0.	0.
DPM-DPL	2.94E-01	4.28E-01	0.	0.	0.	0.	0.	0.	0.	0.
V.V/K	1.03E+01	1.01E+01	0.	0.	0.	0.	0.	0.	0.	0.
DPM-DPL/K	1.14E+01	1.66E+01	0.	0.	0.	0.	0.	0.	0.	0.
MAN. THETA	1.18E-01	1.18E-01	0.	0.	0.	0.	0.	0.	0.	0.
(ZR1+ZR2)/2	6.85E+00	6.55E+00	0.	0.	0.	0.	0.	0.	0.	0.
PR1	3.60E+01	6.12E+01	0.	0.	0.	0.	0.	0.	0.	0.
DPL-BLASIUS	2.35E-01	2.31E-01	0.	0.	0.	0.	0.	0.	0.	0.

K=D.(SIG-RO)/RO

SET 21 0.981 PLASTIC SINGLE SPHERES

SPHERE DIAMETER .98100 SPHERE DENSITY LB PER FT..3 62.78000

D OVER D RATIO .50021
VISCOSITY 1.637E-05
(SIGMA-RO)/RO .00609
SIGMA-RO/SIGMA .00605

MANOMETER READING (CM) ZERO 1 ZERO 2

32.50 40.34 6.82 6.09
32.39 40.40 6.14 6.40

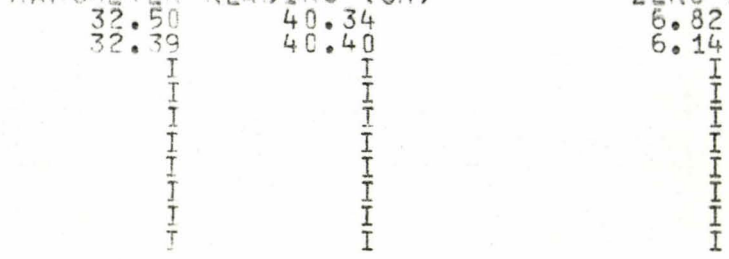

	1	2	3	4	5	6	7	8	9	10
MAN. GM	1.59E+00	1.59E+00	0.	0.	0.	0.	0.	0.	0.	0.
SPHERE NO	1.00E+00	1.00E+00	0.	0.	0.	0.	0.	0.	0.	0.
(V-AV)	7.65E-01	7.65E-01	0.	0.	0.	0.	0.	0.	0.	0.
(V-AV)-SQ	5.85E-01	5.85E-01	0.	0.	0.	0.	0.	0.	0.	0.
DRAG COEFF	3.65E-02	3.65E-02	0.	0.	0.	0.	0.	0.	0.	0.
RE	7.64E+03	7.64E+03	0.	0.	0.	0.	0.	0.	0.	0.
DELTA-PM	1.99E-01	2.49E-01	0.	0.	0.	0.	0.	0.	0.	0.
DPM-DPL	-1.63E-01	-1.12E-01	0.	0.	0.	0.	0.	0.	0.	0.
V.V/K	5.88E+02	5.88E+02	0.	0.	0.	0.	0.	0.	0.	0.
DPM-DPL/K	-1.63E+02	-1.12E+02	0.	0.	0.	0.	0.	0.	0.	0.
MAN. THETA	1.18E-01	1.18E-01	0.	0.	0.	0.	0.	0.	0.	0.
(ZR1+ZR2)/2	6.46E+00	6.27E+00	0.	0.	0.	0.	0.	0.	0.	0.
PR1	-2.72E+01	-2.19E+01	0.	0.	0.	0.	0.	0.	0.	0.
DPL-BLASIUS	4.70E-01	4.70E-01	0.	0.	0.	0.	0.	0.	0.	0.

K=D.(SIG-RO)/RO

SET 22 0.969 PLASTIC SINGLE SPHERES

SPHERE DIAMETER .96900 SPHERE DENSITY LB PER FT..3 73.92000

D OVER D RATIO .49410
VISCOSITY 1.637E-05
(SIGMA-RO)/RO .18462
SIGMA-RO/SIGMA .15584

MANOMETER READING (CM) ZERO 1 ZERO 2

34.55 36.34 .27 .69
34.66 36.28 .70 .57

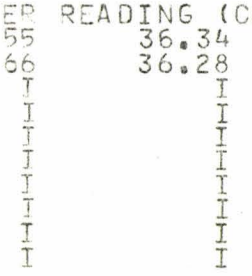

	1	2	3	4	5	6	7	8	9	10
MAN. GM	1.59E+00	1.59E+00	0.	0.	0.	0.	0.	0.	0.	0.
SPHERE NO	1.00E+00	1.00E+00	0.	0.	0.	0.	0.	0.	0.	0.
(V-AV)	7.97E-01	7.82E-01	0.	0.	0.	0.	0.	0.	0.	0.
(V-AV)-SQ	6.35E-01	6.11E-01	0.	0.	0.	0.	0.	0.	0.	0.
DRAG COEFF	1.01E+00	1.05E+00	0.	0.	0.	0.	0.	0.	0.	0.
RE	7.96E+03	7.80E+03	0.	0.	0.	0.	0.	0.	0.	0.
DELTA-PM	5.08E-01	3.82E-01	0.	0.	0.	0.	0.	0.	0.	0.
DPM-DPL	1.24E-01	1.29E-03	0.	0.	0.	0.	0.	0.	0.	0.
V.V/K	2.11E+01	2.03E+01	0.	0.	0.	0.	0.	0.	0.	0.
DPM-DPL/K	4.12E+00	4.27E-02	0.	0.	0.	0.	0.	0.	0.	0.
MAN. THETA	3.21E-01	3.21E-01	0.	0.	0.	0.	0.	0.	0.	0.
(ZR1+ZR2)/2	4.80E-01	6.35E-01	0.	0.	0.	0.	0.	0.	0.	0.
PR1	1.35E+00	-9.73E+00	0.	0.	0.	0.	0.	0.	0.	0.
DPL-BLASIUS	5.04E-01	4.88E-01	0.	0.	0.	0.	0.	0.	0.	0.

K=D.(SIG-RO)/RO

SET 23 0.879 PLASTIC SINGLE SPHERES

SPHERE DIAMETER .87900 SPHERE DENSITY LB PER FT..3 70.33000

D OVER D RATIO .44820
VISCOSITY 1.637E-05
(SIGMA-RO)/RO .12708
SIGMA-RO/SIGMA .11275

MANOMETER READING (CM) ZERO 1 ZERO 2

32.47 40.35 6.64 6.40
32.39 40.40 6.40 6.51

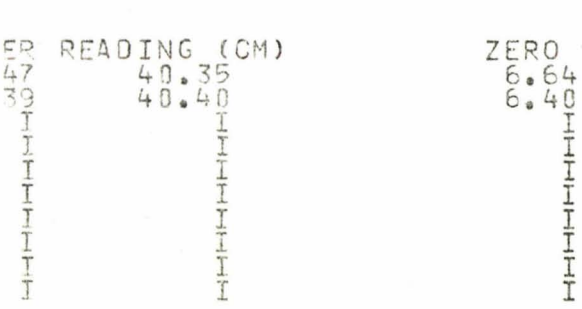

	1	2	3	4	5	6	7	8	9	10
MAN. GM	1.59E+00	1.59E+00	0.	0.	0.	0.	0.	0.	0.	0.
SPHERE NO	1.00E+00	1.00E+00	0.	0.	0.	0.	0.	0.	0.	0.
(V-AV)	6.76E-01	6.76E-01	0.	0.	0.	0.	0.	0.	0.	0.
(V-AV)-SQ	4.57E-01	4.57E-01	0.	0.	0.	0.	0.	0.	0.	0.
DRAG COEFF	8.74E-01	8.74E-01	0.	0.	0.	0.	0.	0.	0.	0.
RE	6.75E+03	6.75E+03	0.	0.	0.	0.	0.	0.	0.	0.
DELTA-PM	1.95E-01	2.23E-01	0.	0.	0.	0.	0.	0.	0.	0.
DPM-DPL	-1.06E-01	-7.79E-02	0.	0.	0.	0.	0.	0.	0.	0.
V.V/K	2.20E+01	2.20E+01	0.	0.	0.	0.	0.	0.	0.	0.
DPM-DPL/K	-5.10E+00	-3.75E+00	0.	0.	0.	0.	0.	0.	0.	0.
MAN. THETA	1.18E-01	1.18E-01	0.	0.	0.	0.	0.	0.	0.	0.
(ZR1+ZR2)/2	6.52E+00	6.45E+00	0.	0.	0.	0.	0.	0.	0.	0.
PR1	-2.54E+01	-2.14E+01	0.	0.	0.	0.	0.	0.	0.	0.
DPL-BLASIUS	3.78E-01	3.78E-01	0.	0.	0.	0.	0.	0.	0.	0.

K=D.(SIG-RO)/RO

SET 24 0.742 PLASTIC SINGLE SPHERES

SPHERE DIAMETER .74200 SPHERE DENSITY LB PER FT..3 72.63000

D OVER D RATIO	.37835
VISCOSITY	1.637E-05
(SIGMA-RO)/RO	.16394
SIGMA-RO/SIGMA	.14085

MANOMETER READING (CM)		ZERO 1	ZERO 2
34.70	36.19	.63	.60
34.68	36.20	.60	.60

	1	2	3	4	5	6	7	8	9	10
MAN. GM	1.59E+00	1.59E+00	0.	0.	0.	0.	0.	0.	0.	0.
SPHERE NO	1.00E+00	1.00E+00	0.	0.	0.	0.	0.	0.	0.	0.
(V-AV)	7.33E-01	7.18E-01	0.	0.	0.	0.	0.	0.	0.	0.
(V-AV)-SQ	5.38E-01	5.15E-01	0.	0.	0.	0.	0.	0.	0.	0.
DRAG COEFF	8.09E-01	8.44E-01	0.	0.	0.	0.	0.	0.	0.	0.
RE	7.32E+03	7.17E+03	0.	0.	0.	0.	0.	0.	0.	0.
DELTA-PM	3.39E-01	3.57E-01	0.	0.	0.	0.	0.	0.	0.	0.
DPM-DPL	2.98E-04	2.14E-02	0.	0.	0.	0.	0.	0.	0.	0.
V.V/K	2.01E+01	1.92E+01	0.	0.	0.	0.	0.	0.	0.	0.
DPM-DPL/K	1.11E-02	8.00E-01	0.	0.	0.	0.	0.	0.	0.	0.
MAN. THETA	3.21E-01	3.21E-01	0.	0.	0.	0.	0.	0.	0.	0.
(ZR1+ZR2)/2	6.15E-01	6.00E-01	0.	0.	0.	0.	0.	0.	0.	0.
PR1	-1.33E+01	-8.76E+00	0.	0.	0.	0.	0.	0.	0.	0.
DPL-BLASIUS	4.36E-01	4.20E-01	0.	0.	0.	0.	0.	0.	0.	0.

K=D.(SIG-RO)/RO

SET 25 0.616 PLASTIC SINGLE SPHERES

SPHERE DIAMETER .61600 SPHERE DENSITY LB PER FT..3 72.82000

D OVER D RATIO	.31410
VISCOSITY	1.637E-05
(SIGMA-RO)/RO	.16699
SIGMA-RO/SIGMA	.14309

MANOMETER READING (CM)		ZERO 1	ZERO 2
32.85	39.87	5.68	5.95
32.42	40.24	6.20	6.24

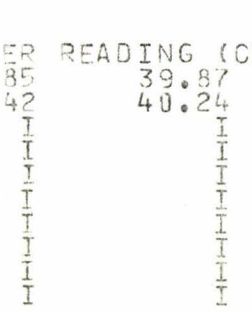

	1	2	3	4	5	6	7	8	9	10
MAN. GM	1.59E+00	1.59E+00	0.	0.	0.	0.	0.	0.	0.	0.
SPHERE NO	1.00E+00	1.00E+00	0.	0.	0.	0.	0.	0.	0.	0.
(V-AV)	6.44E-01	6.73E-01	0.	0.	0.	0.	0.	0.	0.	0.
(V-AV)-SQ	4.15E-01	4.53E-01	0.	0.	0.	0.	0.	0.	0.	0.
DRAG COEFF	8.87E-01	8.11E-01	0.	0.	0.	0.	0.	0.	0.	0.
RE	6.43E+03	6.72E+03	0.	0.	0.	0.	0.	0.	0.	0.
DELTA-PM	1.73E-01	2.29E-01	0.	0.	0.	0.	0.	0.	0.	0.
DPM-DPL	-1.05E-01	-6.86E-02	0.	0.	0.	0.	0.	0.	0.	0.
V.V/K	1.52E+01	1.66E+01	0.	0.	0.	0.	0.	0.	0.	0.
DPM-DPL/K	-3.85E+00	-2.51E+00	0.	0.	0.	0.	0.	0.	0.	0.
MAN. THETA	1.18E-01	1.18E-01	0.	0.	0.	0.	0.	0.	0.	0.
(ZR1+ZR2)/2	5.81E+00	6.22E+00	0.	0.	0.	0.	0.	0.	0.	0.
PR1	-3.82E+01	-2.93E+01	0.	0.	0.	0.	0.	0.	0.	0.
DPL-BLASIUS	3.47E-01	3.76E-01	0.	0.	0.	0.	0.	0.	0.	0.

K=D.(SIG-RO)/RO

SET 26 0.608 PLASTIC SINGLE SPHERES

SPHERE DIAMETER .60800 SPHERE DENSITY LB PER FT..3 71.33000

D OVER D RATIO .31002
VISCOSITY 1.637E-05
(SIGMA-RO)/RO .14311
SIGMA-RO/SIGMA .12519

MANOMETER READING (CM)		ZERO 1	ZERO 2
34.88	36.12	.63	.61
34.89	36.13	.61	.60

	1	2	3	4	5	6	7	8	9	10
MAN. GM	1.59E+00	1.59E+00	0.	0.	0.	0.	0.	0.	0.	0.
SPHERE NO	1.00E+00	1.00E+00	0.	0.	0.	0.	0.	0.	0.	0.
(V-AV)	6.57E-01	6.57E-01	0.	0.	0.	0.	0.	0.	0.	0.
(V-AV)-SQ	4.31E-01	4.31E-01	0.	0.	0.	0.	0.	0.	0.	0.
DRAG COEFF	7.21E-01	7.21E-01	0.	0.	0.	0.	0.	0.	0.	0.
RE	6.56E+03	6.56E+03	0.	0.	0.	0.	0.	0.	0.	0.
DELTA-PM	2.40E-01	2.46E-01	0.	0.	0.	0.	0.	0.	0.	0.
DPM-DPL	-5.06E-02	-4.48E-02	0.	0.	0.	0.	0.	0.	0.	0.
V.V/K	1.84E+01	1.84E+01	0.	0.	0.	0.	0.	0.	0.	0.
DPM-DPL/K	-2.16E+00	-1.91E+00	0.	0.	0.	0.	0.	0.	0.	0.
MAN. THETA	3.21E-01	3.21E-01	0.	0.	0.	0.	0.	0.	0.	0.
(ZR1+ZR2)/2	6.20E-01	6.05E-01	0.	0.	0.	0.	0.	0.	0.	0.
PR1	-2.51E+01	-2.39E+01	0.	0.	0.	0.	0.	0.	0.	0.
DPL-BLASIUS	3.60E-01	3.60E-01	0.	0.	0.	0.	0.	0.	0.	0.

K=D.(SIG-RO)/RO

SET 27 1.740 PLASTIC UP TO 9 IN LINE D APART

SPHERE DIAMETER 1.74000 SPHERE DENSITY LB PER FT..3 78.79000

D OVER D RATIO .89783
VISCOSITY 1.743E-05
(SIGMA-RO)/RO .26266
SIGMA-RO/SIGMA .20802

MANOMETER READING (CM)		ZERO 1	ZERO 2
34.42	36.53	.65	1.78
34.33	36.60	1.78	1.96
34.30	36.68	1.96	1.92
34.78	36.46	.79	1.65
34.60	36.56	1.60	1.73
34.57	36.62	1.73	1.80
34.55	36.68	1.78	-3.16
33.75	37.43	1.79	2.14
33.50	37.65	2.14	2.13
33.55	37.64	2.06	2.21

	1	2	3	4	5	6	7	8	9	10
MAN. GM	1.59E+00	1.59E+00	1.59E+00	1.59E+00	1.59E+00	1.59E+00	1.59E+00	1.59E+00	1.59E+00	1.59E+00
SPHERE NO	1.00E+00	1.00E+00	1.00E+00	1.00E+00	1.00E+00	1.00E+00	1.00E+00	2.00E+00	2.00E+00	2.00E+00
(V-AV)	6.92E-02	6.92E-02	6.92E-02	9.40E-02	9.92E-02	9.92E-02	9.79E-02	1.33E-01	1.33E-01	1.35E-01
(V-AV)-SQ	4.79E-03	4.79E-03	4.79E-03	8.84E-03	9.85E-03	9.85E-03	9.59E-03	1.77E-02	1.77E-02	1.81E-02
DRAG COEFF	3.41E+02	3.41E+02	3.41E+02	1.85E+02	1.66E+02	1.66E+02	1.70E+02	9.21E+01	9.21E+01	9.03E+01
RE	6.41E+02	6.41E+02	6.41E+02	8.71E+02	9.19E+02	9.19E+02	9.07E+02	1.23E+03	1.23E+03	1.25E+03
DELTA-PM	3.42E-01	1.53E-01	1.68E-01	1.77E-01	1.13E-01	1.09E-01	1.08E+00	6.58E-01	7.73E-01	7.50E-01
DPM-DPL	3.27E-01	1.38E-01	1.54E-01	1.57E-01	9.26E-02	8.88E-02	1.06E+00	6.31E-01	7.46E-01	7.22E-01
V.V/K	1.13E-01	1.13E-01	1.13E-01	2.08E-01	2.32E-01	2.32E-01	2.26E-01	4.18E-01	4.18E-01	4.26E-01
DPM-DPL/K	7.72E+00	3.26E+00	3.62E+00	3.70E+00	2.18E+00	2.09E+00	2.50E+01	1.49E+01	1.76E+01	1.70E+01
MAN. THETA	3.16E-01	3.16E-01	3.16E-01	3.17E-01	3.17E-01	3.17E-01	3.17E-01	3.17E-01	3.17E-01	3.17E-01
(ZR1+ZR2)/2	1.21E+00	1.87E+00	1.94E+00	1.22E+00	1.67E+00	1.76E+00	-6.90E-01	1.97E+00	2.14E+00	2.13E+00
PR1	7.87E+02	3.33E+02	3.70E+02	2.79E+02	1.56E+02	1.50E+02	1.80E+03	3.94E+02	4.66E+02	4.47E+02
DPL-BLASIUS	1.44E-02	1.44E-02	1.44E-02	1.95E-02	2.06E-02	2.06E-02	2.03E-02	2.76E-02	2.76E-02	2.79E-02

K=D.(SIG-RO)/RO

SET 28 A CONTINUATION OF 27

SPHERE DIAMETER 1.74000 SPHERE DENSITY LB PER FT..3 78.79000

D OVER D RATIO	.89783
VISCOSITY	1.743E-05
(SIGMA-RO)/RO	.26266
SIGMA-RO/SIGMA	.20802

MANOMETER READING (CM)		ZERO 1	ZERO 2
33.68	37.58	1.92	2.14
32.80	38.58	2.09	2.29
33.37	38.00	2.29	2.30
32.51	38.80	2.12	2.30
32.60	38.75	2.30	2.27
31.51	40.43	1.90	2.11
31.30	40.50	2.11	2.06
31.38	40.45	1.84	1.90
30.70	41.00	1.90	2.02
31.50	40.33	2.00	2.09

	1	2	3	4	5	6	7	8	9	10
MAN. GM	1.59E+00	1.59E+00	1.59E+00	1.59E+00	1.59E+00	1.59E+00	1.59E+00	1.59E+00	1.59E+00	1.59E+00
SPHERE NO	2.00E+00	3.00E+00	3.00E+00	3.00E+00	3.00E+00	4.00E+00	4.00E+00	4.00E+00	4.00E+00	4.00E+00
(V-AV)	1.32E-01	1.59E-01	1.58E-01	1.59E-01	1.59E-01	1.78E-01	1.79E-01	1.70E-01	1.70E-01	1.71E-01
(V-AV)-SQ	1.74E-02	2.54E-02	2.50E-02	2.54E-02	2.54E-02	3.15E-02	3.20E-02	2.88E-02	2.88E-02	2.93E-02
DRAG COEFF	9.39E+01	6.44E+01	6.54E+01	6.44E+01	6.44E+01	5.18E+01	5.10E+01	5.67E+01	5.67E+01	5.58E+01
RE	1.22E+03	1.48E+03	1.46E+03	1.48E+03	1.48E+03	1.65E+03	1.66E+03	1.57E+03	1.57E+03	1.58E+03
DELTA-PM	7.18E-01	1.38E+00	8.96E-01	1.57E+00	1.48E+00	2.65E+00	2.73E+00	2.76E+00	3.20E+00	2.60E+00
DPM-DPL	6.90E-01	1.34E+00	8.63E-01	1.53E+00	1.45E+00	2.62E+00	2.69E+00	2.73E+00	3.17E+00	2.57E+00
V.V/K	4.10E-01	5.98E-01	5.89E-01	5.98E-01	5.98E-01	7.44E-01	7.54E-01	6.79E-01	6.79E-01	6.90E-01
DPM-DPL/K	1.63E+01	3.17E+01	2.04E+01	3.61E+01	3.42E+01	6.17E+01	6.35E+01	6.43E+01	7.46E+01	6.06E+01
MAN. THETA	3.17E-01	3.17E-01	3.17E-01	3.17E-01	3.17E-01	3.17E-01	3.17E-01	3.17E-01	3.17E-01	3.17E-01
(ZR1+ZR2)/2	2.03E+00	2.19E+00	2.29E+00	2.21E+00	2.28E+00	2.00E+00	2.08E+00	1.87E+00	1.96E+00	2.04E+00
PR1	4.36E+02	4.69E+02	3.04E+02	5.34E+02	5.05E+02	6.13E+02	6.27E+02	6.69E+02	7.76E+02	6.25E+02
DPL-BLASIUS	2.74E-02	3.31E-02	3.28E-02	3.31E-02	3.31E-02	3.68E-02	3.71E-02	3.52E-02	3.52E-02	3.55E-02

K=D.(SIG-RO)/RO

SET 29 A CONTINUATION OF SET 28

SPHERE DIAMETER 1.74000 SPHERE DENSITY LB PER FT..3 78.79000

D OVER D RATIO .89783
VISCOSITY 1.716E-05
(SIGMA-RO)/RO .26266
SIGMA-RO/SIGMA .20802

MANOMETER READING (CM)		ZERO 1	ZERO 2
29.39	42.20	1.79	2.20
29.55	42.05	2.12	2.22
29.60	42.06	2.22	2.25
27.31	44.10	1.82	2.21
27.53	43.85	2.21	2.38
27.38	43.95	2.21	2.31
27.55	43.88	2.13	2.30
25.53	45.80	1.08	1.10
25.30	46.00	1.03	1.10
25.70	45.60	1.10	1.00

	1	2	3	4	5	6	7	8	9	10
MAN. GM	1.59E+00	1.59E+00	1.59E+00	1.59E+00	1.59E+00	1.59E+00	1.59E+00	1.59E+00	1.59E+00	1.59E+00
SPHERE NO	5.00E+00	5.00E+00	5.00E+00	6.00E+00	6.00E+00	6.00E+00	6.00E+00	7.00E+00	7.00E+00	7.00E+00
(V-AV)	1.96E-01	1.96E-01	1.96E-01	2.00E-01	2.04E-01	1.97E-01	1.98E-01	1.80E-01	2.13E-01	2.12E-01
(V-AV)-SQ	3.84E-02	3.84E-02	3.84E-02	3.99E-02	4.15E-02	3.89E-02	3.94E-02	3.25E-02	4.53E-02	4.48E-02
DRAG COEFF	4.26E+01	4.26E+01	4.26E+01	4.09E+01	3.94E+01	4.20E+01	4.15E+01	5.03E+01	3.61E+01	3.65E+01
RE	1.84E+03	1.84E+03	1.84E+03	1.88E+03	1.92E+03	1.86E+03	1.87E+03	1.70E+03	2.00E+03	1.99E+03
DELTA-PM	4.15E+00	3.96E+00	3.92E+00	5.67E+00	5.58E+00	5.49E+00	5.42E+00	7.36E+00	7.54E+00	7.23E+00
DPM-DPL	4.11E+00	3.92E+00	3.88E+00	5.63E+00	5.54E+00	5.45E+00	5.38E+00	7.32E+00	7.49E+00	7.19E+00
V.V/K	9.04E-01	9.04E-01	9.04E-01	9.41E-01	9.78E-01	9.17E-01	9.29E-01	7.66E-01	1.07E+00	1.05E+00
DPM-DPL/K	9.69E+01	9.25E+01	9.16E+01	1.33E+02	1.26E+02	1.29E+02	1.27E+02	1.73E+02	1.77E+02	1.70E+02
MAN. THETA	3.17E-01	3.17E-01	3.17E-01	3.17E-01	3.17E-01	3.17E-01	3.17E-01	3.17E-01	3.17E-01	3.17E-01
(ZR1+ZR2)/2	2.00E+00	2.17E+00	2.24E+00	2.01E+00	2.09E+00	2.26E+00	2.22E+00	1.09E+00	1.06E+00	1.05E+00
PR1	7.10E+02	6.78E+02	6.71E+02	7.94E+02	7.79E+02	7.79E+02	7.64E+02	9.82E+02	8.50E+02	8.21E+02
DPL-BLASIUS	4.00E-02	4.00E-02	4.00E-02	4.08E-02	4.16E-02	4.02E-02	4.05E-02	3.68E-02	4.34E-02	4.32E-02

K=D.(SIG-RO)/RO

SET 30 A CONTINUATION OF SET 29

SPHERE DIAMETER 1.74000 SPHERE DENSITY LB PER FT..3 78.79000

D OVER D RATIO .89783
VISCOSITY 1.689E-05
(SIGMA-RO)/RO .26266
SIGMA-RO/SIGMA .20802

MANOMETER READING (CM)		ZERO 1	ZERO 2
26.25	45.45	1.09	1.06
24.48	46.74	.68	.89
24.50	46.80	.70	1.04
22.55	48.68	.83	.77
22.55	48.64	.77	.77

	1	2	3	4	5	6	7	8	9	10
MAN. GM	1.59E+00	1.59E+00	1.59E+00	1.59E+00	1.59E+00	0.	0.	0.	0.	0.
SPHERE NO	7.00E+00	8.00E+00	8.00E+00	9.00E+00	9.00E+00	0.	0.	0.	0.	0.
(V-AV)	1.82E-01	2.12E-01	2.13E-01	2.23E-01	2.23E-01	0.	0.	0.	0.	0.
(V-AV)-SO	3.29E-02	4.48E-02	4.53E-02	4.99E-02	4.99E-02	0.	0.	0.	0.	0.
DRAG COEFF	4.96E+01	3.65E+01	3.61E+01	3.28E+01	3.28E+01	0.	0.	0.	0.	0.
RE	1.74E+03	2.02E+03	2.04E+03	2.14E+03	2.14E+03	0.	0.	0.	0.	0.
DELTA-PM	6.96E+00	8.24E+00	8.22E+00	9.72E+00	9.72E+00	0.	0.	0.	0.	0.
DPM-DPL	6.92E+00	8.20E+00	8.18E+00	9.68E+00	9.67E+00	0.	0.	0.	0.	0.
V.V/K	7.77E-01	1.05E+00	1.07E+00	1.18E+00	1.18E+00	0.	0.	0.	0.	0.
DPM-DPL/K	1.63E+02	1.93E+02	1.93E+02	2.28E+02	2.28E+02	0.	0.	0.	0.	0.
MAN. THETA	3.17E-01	3.17E-01	3.17E-01	3.17E-01	3.17E-01	0.	0.	0.	0.	0.
(ZR1+ZR2)/2	1.07E+00	7.85E-01	8.70E-01	8.00E-01	7.70E-01	0.	0.	0.	0.	0.
PR1	9.36E+02	8.33E+02	8.26E+02	8.27E+02	8.27E+02	0.	0.	0.	0.	0.
DPL-BLASIUS	3.65E-02	4.25E-02	4.28E-02	4.49E-02	4.49E-02	0.	0.	0.	0.	0.

K=D.(SIG-RO)/RO

SET 31 1.478 PLASTIC UP TO 10 IN LINE 0 APART

SPHERE DIAMETER 1.47800 SPHERE DENSITY LB PER FT..3 77.43000

D OVER D RATIO	.76264
VISCOSITY	1.716E-05
(SIGMA-RO)/RO	.24087
SIGMA-RO/SIGMA	.19411

MANOMETER READING (CM)		ZERO 1	ZERO 2
35.35	36.50	.90	.90
35.39	36.54	.89	.98
35.38	36.48	.98	.98
34.30	36.96	.48	1.50
33.80	37.48	1.49	1.90
33.50	37.78	1.10	1.90
33.48	37.75	1.90	1.82
33.50	37.70	1.82	2.09
32.15	39.40	2.13	2.04
32.00	39.59	2.04	2.00

	1	2	3	4	5	6	7	8	9	10
MAN. GM	1.59E+00	1.59E+00	1.59E+00	1.59E+00	1.59E+00	1.59E+00	1.59E+00	1.59E+00	1.59E+00	1.59E+00
SPHERE NO	1.00E+00	1.00E+00	1.00E+00	2.00E+00	2.00E+00	3.00E+00	3.00E+00	3.00E+00	4.00E+00	4.00E+00
(V-AV)	2.26E-01	2.17E-01	2.22E-01	4.36E-01	3.94E-01	4.81E-01	4.44E-01	4.51E-01	5.69E-01	5.93E-01
(V-AV)-SQ	5.10E-02	4.70E-02	4.93E-02	1.90E-01	1.55E-01	2.31E-01	1.97E-01	2.03E-01	3.24E-01	3.51E-01
DRAG COEFF	2.49E+01	2.71E+01	2.58E+01	6.69E+00	8.13E+00	5.51E+00	6.46E+00	6.27E+00	3.93E+00	3.62E+00
RE	2.13E+03	2.04E+03	2.09E+03	4.11E+03	3.71E+03	4.52E+03	4.18E+03	4.24E+03	5.36E+03	5.58E+03
DELTA-PM	9.60E-02	8.25E-02	4.61E-02	6.41E-01	7.62E-01	1.07E+00	9.25E-01	8.62E-01	1.98E+00	2.14E+00
DPM-DPL	4.98E-02	3.83E-02	7.42E-04	5.32E-01	6.69E-01	9.30E-01	8.12E-01	7.45E-01	1.69E+00	1.82E+00
V.V/K	1.31E+00	1.21E+00	1.27E+00	4.89E+00	4.00E+00	5.94E+00	5.07E+00	5.22E+00	8.33E+00	9.04E+00
DPM-DPL/K	1.28E+00	9.84E-01	1.91E-02	1.37E+01	1.72E+01	2.39E+01	2.09E+01	1.92E+01	4.34E+01	4.68E+01
MAN. THETA	3.17E-01	3.17E-01	3.17E-01	3.17E-01	3.17E-01	3.17E-01	3.17E-01	3.17E-01	3.17E-01	3.17E-01
(ZR1+ZR2)/2	9.00E-01	9.35E-01	9.80E-01	9.90E-01	1.69E+00	1.50E+00	1.86E+00	1.96E+00	2.08E+00	2.02E+00
PR1	4.49E+01	3.61E+01	1.66E+00	3.84E+01	6.25E+01	4.15E+01	4.13E+01	3.63E+01	4.68E+01	4.71E+01
DPL-BLASIUS	4.61E-02	4.42E-02	4.53E-02	2.25E-01	1.89E-01	2.67E-01	2.33E-01	2.39E-01	3.59E-01	3.86E-01

K=D.(SIG-RO)/RO

SET 32 A CONTINUATION OF SET 31

SPHERE DIAMETER 1.47800 SPHERE DENSITY LB PER FT..3 77.43000

D OVER D RATIO .76264
VISCOSITY 1.689E-05
(SIGMA-RO)/RO .24087
SIGMA-RO/SIGMA .19411

MANOMETER READING (CM)	ZERO 1	ZERO 2
32.00	39.50	1.62	2.12
30.98	40.50	2.05	2.20
31.20	40.35	2.20	2.14
31.00	40.49	2.14	2.02
30.96	40.50	2.02	2.04
29.78	41.48	1.77	2.18
29.78	41.47	2.18	2.16
29.77	41.44	2.16	2.23
28.70	42.57	2.06	2.10
28.65	42.50	1.80	1.95

	1	2	3	4	5	6	7	8	9	10
MAN. GM	1.59E+00	1.59E+00	1.59E+00	1.59E+00	1.59E+00	1.59E+00	1.59E+00	1.59E+00	1.59E+00	1.59E+00
SPHERE NO	4.00E+00	5.00E+00	5.00E+00	5.00E+00	5.00E+00	6.00E+00	6.00E+00	6.00E+00	7.00E+00	7.00E+00
(V-AV)	6.10E-01	6.54E-01	6.67E-01	6.70E-01	6.61E-01	7.12E-01	6.84E-01	6.78E-01	7.09E-01	7.23E-01
(V-AV)-SQ	3.72E-01	4.28E-01	4.45E-01	4.49E-01	4.37E-01	5.06E-01	4.68E-01	4.59E-01	5.03E-01	5.23E-01
DRAG COEFF	3.42E+00	2.97E+00	2.86E+00	2.84E+00	2.91E+00	2.51E+00	2.72E+00	2.77E+00	2.53E+00	2.43E+00
RE	5.83E+03	6.26E+03	6.38E+03	6.41E+03	6.32E+03	6.81E+03	6.54E+03	6.48E+03	6.78E+03	6.92E+03
DELTA-PM	2.16E+00	2.84E+00	2.68E+00	2.84E+00	2.88E+00	3.73E+00	3.65E+00	3.64E+00	4.53E+00	4.60E+00
DPM-DPL	1.83E+00	2.46E+00	2.30E+00	2.46E+00	2.51E+00	3.31E+00	3.25E+00	3.25E+00	4.10E+00	4.17E+00
V.V/K	9.56E+00	1.10E+01	1.14E+01	1.15E+01	1.12E+01	1.30E+01	1.20E+01	1.18E+01	1.29E+01	1.35E+01
DPM-DPL/K	4.71E+01	6.33E+01	5.92E+01	6.33E+01	6.46E+01	8.50E+01	8.37E+01	8.34E+01	1.06E+02	1.07E+02
MAN. THETA	3.17E-01	3.17E-01	3.17E-01	3.17E-01	3.17E-01	3.17E-01	3.17E-01	3.17E-01	3.17E-01	3.17E-01
(ZR1+ZR2)/2	1.87E+00	2.13E+00	2.17E+00	2.08E+00	2.03E+00	1.98E+00	2.17E+00	2.20E+00	2.08E+00	1.87E+00
PR1	4.52E+01	4.33E+01	3.89E+01	4.14E+01	4.32E+01	4.20E+01	4.43E+01	4.49E+01	4.51E+01	4.42E+01
DPL-BLASIUS	4.04E-01	4.57E-01	4.73E-01	4.76E-01	4.65E-01	5.29E-01	4.94E-01	4.86E-01	5.26E-01	5.44E-01

K=D.(SIG-RO)/RO

SET 33 A CONTINUATION OF SET 32

SPHERE DIAMETER 1.47800 SPHERE DENSITY LB PER FT..3 77.43000

D OVER D RATIO .76264
VISCOSITY 1.689E-05
(SIGMA-RO)/RO .24087
SIGMA-RO/SIGMA .19411

MANOMETER READING (CM)	ZERO 1	ZERO 2
29.49	2.20	2.30
28.65	1.80	1.95
27.54	1.85	1.83
27.55	1.83	1.88
26.14	1.81	1.80
26.50	1.80	1.80
25.49	.95	1.18
25.30	.96	2.14
I	I	I
I	I	I

	1	2	3	4	5	6	7	8	9	10
MAN. GM	1.59E+00	1.59E+00	1.59E+00	1.59E+00	1.59E+00	1.59E+00	1.59E+00	1.59E+00	0.	0.
SPHERE NO	6.00E+00	7.00E+00	8.00E+00	8.00E+00	9.00E+00	9.00E+00	1.00E+01	1.00E+01	0.	0.
(V-AV)	6.92E-01	7.12E-01	7.52E-01	7.40E-01	7.12E-01	7.31E-01	7.31E-01	7.39E-01	0.	0.
(V-AV)-SQ	4.79E-01	5.06E-01	5.66E-01	5.48E-01	5.06E-01	5.35E-01	5.35E-01	5.46E-01	0.	0.
DRAG COEFF	2.66E+00	2.51E+00	2.25E+00	2.32E+00	2.51E+00	2.38E+00	2.38E+00	2.33E+00	0.	0.
RE	6.62E+03	6.81E+03	7.19E+03	7.08E+03	6.81E+03	6.99E+03	6.99E+03	7.07E+03	0.	0.
DELTA-PM	3.82E+00	4.60E+00	5.46E+00	5.45E+00	6.38E+00	6.26E+00	7.41E+00	7.31E+00	0.	0.
DPM-DPL	3.42E+00	4.17E+00	5.01E+00	5.00E+00	5.96E+00	5.82E+00	6.97E+00	6.87E+00	0.	0.
V.V/K	1.23E+01	1.30E+01	1.45E+01	1.41E+01	1.30E+01	1.37E+01	1.37E+01	1.40E+01	0.	0.
DPM-DPL/K	8.80E+01	1.07E+02	1.29E+02	1.29E+02	1.53E+02	1.50E+02	1.79E+02	1.76E+02	0.	0.
MAN. THETA	3.17E-01	3.17E-01	3.17E-01	3.17E-01	3.17E-01	3.17E-01	3.17E-01	3.17E-01	0.	0.
(ZR1+ZR2)/2	2.25E+00	1.87E+00	1.84E+00	1.85E+00	1.80E+00	1.80E+00	1.06E+00	1.55E+00	0.	0.
PR1	4.55E+01	4.56E+01	4.34E+01	4.47E+01	5.09E+01	4.73E+01	5.11E+01	4.94E+01	0.	0.
DPL-BLASIUS	5.04E-01	5.29E-01	5.83E-01	5.67E-01	5.29E-01	5.55E-01	5.55E-01	5.65E-01	0.	0.

K=D.(SIG-RO)/RO

SET 34 1.235 PLASTIC UP TO 12 IN LINE D APART

SPHERE DIAMETER 1.23500 SPHERE DENSITY LB PER FT..3 80.15000

D OVER D RATIO	.63725
VISCOSITY	1.689E-05
(SIGMA-RO)/RO	.28446
SIGMA-RO/SIGMA	.22146

MANOMETER READING (CM)		ZERO 1	ZERO 2
35.36	36.21	.39	.39
35.30	36.30	.40	.40
35.26	36.31	.40	.40
34.60	37.22	1.88	1.88
34.80	38.00	.30	.87
34.80	38.04	.85	.96
33.78	38.07	.96	1.00
32.20	39.11	-.12	.98
33.40	38.38	.98	1.00
33.40	38.35	1.00	1.02

	1	2	3	4	5	6	7	8	9	10
MAN. GM	1.59E+00	1.59E+00	1.59E+00	1.59E+00	1.59E+00	1.59E+00	1.59E+00	1.59E+00	1.59E+00	1.59E+00
SPHERE NO	1.00E+00	1.00E+00	1.00E+00	2.00E+00	3.00E+00	3.00E+00	3.00E+00	4.00E+00	4.00E+00	4.00E+00
(V-AV)	4.51E-01	4.57E-01	4.60E-01	5.50E-01	8.42E-01	8.49E-01	8.55E-01	1.04E+00	1.02E+00	1.02E+00
(V-AV)-SQ	2.03E-01	2.09E-01	2.11E-01	3.02E-01	7.09E-01	7.20E-01	7.32E-01	1.09E+00	1.04E+00	1.04E+00
DRAG COEFF	6.19E+00	6.01E+00	5.94E+00	4.15E+00	1.77E+00	1.74E+00	1.72E+00	1.16E+00	1.21E+00	1.21E+00
RE	4.31E+03	4.37E+03	4.40E+03	5.26E+03	8.06E+03	8.12E+03	8.18E+03	9.97E+03	9.75E+03	9.75E+03
DELTA-PM	1.77E-01	2.30E-01	2.49E-01	2.84E-01	1.00E+00	8.96E-01	1.27E+00	2.49E+00	1.53E+00	1.51E+00
DPM-DPL	6.03E-02	1.10E-01	1.28E-01	2.03E-02	4.59E-01	3.42E-01	7.06E-01	1.70E+00	7.83E-01	7.63E-01
V.V/K	4.42E+00	4.55E+00	4.60E+00	6.58E+00	1.54E+01	1.57E+01	1.59E+01	2.36E+01	2.26E+01	2.26E+01
DPM-DPL/K	1.31E+00	2.39E+00	2.78E+00	4.41E-01	1.00E+01	7.45E+00	1.54E+01	3.70E+01	1.70E+01	1.66E+01
MAN. THETA	3.17E-01	3.17E-01	3.17E-01	3.17E-01	3.17E-01	3.17E-01	3.17E-01	3.17E-01	3.17E-01	3.17E-01
(ZR1+ZR2)/2	3.90E-01	4.00E-01	4.00E-01	1.88E+00	5.85E-01	9.05E-01	9.80E-01	4.30E-01	9.90E-01	1.01E+00
PR1	-1.15E+01	-1.68E+00	1.65E+00	-2.80E+00	7.68E+00	4.96E+00	1.30E+01	1.81E+01	7.58E+00	7.35E+00
DPL-BLASIUS	2.38E-01	2.44E-01	2.46E-01	3.37E-01	7.10E-01	7.20E-01	7.30E-01	1.03E+00	9.93E-01	9.93E-01

K=D.(SIG-RO)/RO

SET 35 A CONTINUATION OF SET 34

SPHERE DIAMETER 1.23500 SPHERE DENSITY LB PER FT..3 80.15000

D OVER D RATIO .63725
VISCOSITY 1.689E-05
(SIGMA-RO)/RO .28446
SIGMA-RO/SIGMA .22146

MANOMETER READING (CM)		ZERO 1	ZERO 2
31.64	39.82	1.41	1.44
31.64	39.80	1.41	1.44
31.64	39.80	1.44	1.46
30.80	40.65	1.49	1.52
30.75	46.64	1.52	1.52
36.62	40.80	1.57	1.60
29.93	41.50	1.31	1.45
29.92	41.50	1.00	1.52
30.08	41.40	1.52	1.50
29.85	42.00	1.56	1.70

	1	2	3	4	5	6	7	8	9	10
MAN. GM	1.59E+00	1.59E+00	1.59E+00	1.59E+00	1.59E+00	1.59E+00	1.59E+00	1.59E+00	1.59E+00	1.59E+00
SPHERE NO	5.00E+00	5.00E+00	5.00E+00	6.00E+00	6.00E+00	6.00E+00	7.00E+00	7.00E+00	7.00E+00	8.00E+00
(V-AV)	1.13E+00	1.14E+00	1.13E+00	1.21E+00	1.20E+00	1.19E+00	1.23E+00	1.21E+00	1.22E+00	1.27E+00
(V-AV)-SQ	1.27E+00	1.31E+00	1.28E+00	1.46E+00	1.45E+00	1.43E+00	1.52E+00	1.46E+00	1.50E+00	1.60E+00
DRAG COEFF	9.86E-01	9.62E-01	9.84E-01	8.59E-01	8.68E-01	8.80E-01	8.28E-01	8.61E-01	8.37E-01	7.83E-01
RE	1.08E+04	1.09E+04	1.08E+04	1.16E+04	1.15E+04	1.14E+04	1.18E+04	1.16E+04	1.17E+04	1.21E+04
DELTA-PM	2.59E+00	2.58E+00	2.58E+00	3.20E+00	5.52E+00	9.96E-01	3.91E+00	3.96E+00	3.77E+00	4.04E+00
DPM-DPL	1.69E+00	1.65E+00	1.67E+00	2.19E+00	4.51E+00	6.26E-03	2.89E+00	2.95E+00	2.76E+00	2.95E+00
V.V/K	2.77E+01	2.84E+01	2.78E+01	3.18E+01	3.15E+01	3.11E+01	3.30E+01	3.18E+01	3.27E+01	3.49E+01
DPM-DPL/K	3.67E+01	3.59E+01	3.63E+01	4.76E+01	9.82E+01	1.36E-01	6.29E+01	6.42E+01	6.00E+01	6.42E+01
MAN. THETA	3.17E-01	3.17E-01	3.17E-01	3.17E-01	3.17E-01	3.17E-01	3.17E-01	3.17E-01	3.17E-01	3.17E-01
(ZR1+ZR2)/2	1.43E+00	1.43E+00	1.45E+00	1.50E+00	1.52E+00	1.58E+00	1.38E+00	1.26E+00	1.51E+00	1.63E+00
PR1	1.25E+01	1.20E+01	1.24E+01	1.23E+01	2.66E+01	-9.42E-01	1.37E+01	1.46E+01	1.32E+01	1.18E+01
DPL-BLASIUS	1.19E+00	1.21E+00	1.19E+00	1.34E+00	1.33E+00	1.31E+00	1.38E+00	1.34E+00	1.37E+00	1.45E+00

K=D.(SIG-RO)/RO

SET 36 A CONTINUATION OF SET 35

SPHERE DIAMETER 1.23500 SPHERE DENSITY LB PER FT..3 80.15000

D OVER D RATIO .63725
VISCOSITY 1.689E-05
(SIGMA-RO)/RO .28446
SIGMA-RO/SIGMA .22146

MANOMETER READING (CM)	ZERO 1	ZERO 2
29.85	42.00	1.70	1.70
29.70	42.00	1.70	1.69
28.29	43.05	1.12	1.84
28.28	43.01	1.36	1.45
28.30	43.02	1.45	1.44
28.55	42.94	1.44	1.51
27.90	43.43	1.10	1.30
27.80	43.50	1.21	1.19
27.90	43.40	1.19	1.30
27.40	43.90	1.10	1.23

	1	2	3	4	5	6	7	8	9	10
MAN. GM	1.59E+00	1.59E+00	1.59E+00	1.59E+00	1.59E+00	1.59E+00	1.59E+00	1.59E+00	1.59E+00	1.59E+00
SPHERE NO	8.00E+00	8.00E+00	9.00E+00	9.00E+00	9.00E+00	9.00E+00	1.00E+01	1.00E+01	1.00E+01	1.10E+01
(V-AV)	1.27E+00	1.25E+00	1.23E+00	1.25E+00	1.27E+00	1.25E+00	1.24E+00	1.21E+00	1.22E+00	1.22E+00
(V-AV)-SQ	1.60E+00	1.57E+00	1.52E+00	1.56E+00	1.60E+00	1.57E+00	1.54E+00	1.46E+00	1.48E+00	1.50E+00
DRAG COEFF	7.83E-01	8.01E-01	8.28E-01	8.06E-01	7.83E-01	7.99E-01	8.18E-01	8.59E-01	8.48E-01	8.37E-01
RE	1.21E+04	1.20E+04	1.18E+04	1.19E+04	1.21E+04	1.20E+04	1.19E+04	1.16E+04	1.16E+04	1.17E+04
DELTA-PM	4.01E+00	4.07E+00	5.10E+00	5.11E+00	5.09E+00	4.96E+00	5.50E+00	5.57E+00	5.47E+00	5.89E+00
DPM-DPL	2.92E+00	3.01E+00	4.08E+00	4.06E+00	4.00E+00	3.89E+00	4.46E+00	4.55E+00	4.48E+00	4.88E+00
V.V/K	3.49E+01	3.41E+01	3.30E+01	3.39E+01	3.49E+01	3.42E+01	3.34E+01	3.18E+01	3.22E+01	3.27E+01
DPM-DPL/K	6.36E+01	6.55E+01	8.88E+01	8.84E+01	8.72E+01	8.47E+01	9.72E+01	9.90E+01	9.75E+01	1.06E+02
MAN. THETA	3.17E-01	3.17E-01	3.17E-01	3.17E-01	3.17E-01	3.17E-01	3.17E-01	3.17E-01	3.17E-01	3.17E-01
(ZR1+ZR2)/2	1.70E+00	1.69E+00	1.48E+00	1.41E+00	1.45E+00	1.48E+00	1.20E+00	1.20E+00	1.25E+00	1.16E+00
PR1	1.17E+01	1.23E+01	1.55E+01	1.51E+01	1.46E+01	1.44E+01	1.53E+01	1.64E+01	1.58E+01	1.56E+01
DPL-BLASIUS	1.45E+00	1.42E+00	1.38E+00	1.41E+00	1.45E+00	1.42E+00	1.40E+00	1.34E+00	1.35E+00	1.37E+00

K=D.(SIG-RO)/RO

SET 37 A CONTINUATION OF SET 36

SPHERE DIAMETER 1.23500 SPHERE DENSITY LB PER FT..3 80.15000

D OVER D RATIO .63725
VISCOSITY 1.689E-05
(SIGMA-RO)/RO .28446
SIGMA-RO/SIGMA .22146

MANOMETER READING (CM)	ZERO 1	ZERO 2
27.50	1.23	1.22
26.65	.90	1.01
26.65	1.01	1.13

	1	2	3	4	5	6	7	8	9	10
MAN. GM	1.59E+00	1.59E+00	1.59E+00	0.	0.	0.	0.	0.	0.	0.
SPHERE NO	1.10E+01	1.20E+01	1.20E+01	0.	0.	0.	0.	0.	0.	0.
(V-AV)	1.22E+00	1.23E+00	1.24E+00	0.	0.	0.	0.	0.	0.	0.
(V-AV)-SQ	1.48E+00	1.52E+00	1.54E+00	0.	0.	0.	0.	0.	0.	0.
DRAG COEFF	8.46E-01	8.28E-01	8.18E-01	0.	0.	0.	0.	0.	0.	0.
RE	1.17E+04	1.18E+04	1.19E+04	0.	0.	0.	0.	0.	0.	0.
DELTA-PM	5.80E+00	6.53E+00	6.49E+00	0.	0.	0.	0.	0.	0.	0.
DPM-DPL	4.80E+00	5.51E+00	5.46E+00	0.	0.	0.	0.	0.	0.	0.
V.V/K	3.23E+01	3.30E+01	3.34E+01	0.	0.	0.	0.	0.	0.	0.
DPM-DPL/K	1.05E+02	1.20E+02	1.19E+02	0.	0.	0.	0.	0.	0.	0.
MAN. THETA	3.17E-01	3.17E-01	3.17E-01	0.	0.	0.	0.	0.	0.	0.
(ZR1+ZR2)/2	1.23E+00	9.55E-01	1.07E+00	0.	0.	0.	0.	0.	0.	0.
PR1	1.55E+01	1.61E+01	1.58E+01	0.	0.	0.	0.	0.	0.	0.
DPL-BLASIUS	1.36E+00	1.38E+00	1.40E+00	0.	0.	0.	0.	0.	0.	0.

K=D.(SIG-RO)/RO

```
                PROGRAM TST (INPUT,OUTPUT,TAPE5=INPUT,TAPE6=OUTPUT)
000003          REAL NU
000003          INTEGER SETS
          C
000003          DIMENSION ZA(40,10),ZRO1(40,10),ZRO2(40,10),V(40,10),
                1 THT(40,10),DPDIF(40,10),VSQAV(40,10),GM(40,10),A(40,10,2),DPL(
                2 40,10),DPM(40,10),FCT(40,10),CRX(40,10),CD(40,10),DPC(40,10),
                3 VPR(40,10),XLG(40,10),LJCT(40),XRE(40,10),DS(40,10),SIG(40,10),
                4 DDPT(5,100),RRE(5,100),DOVD(40,10),BUO(40,10),BUO1(40,10)
                5 ,ID(100),IX(100),IY(100)
          C
000003          COMMON/111/RE(5,100),DPT(5,100),D,NU(40),RO,NPTS(6)
000003          COMMON/222/LINE(40,7)
000003          COMMON/333/ISUB(5)
          C
          C     DATA INPUT (READ)
          C
          C
000003          READ (5,1) SETS,N
000013          DO 75 L=1,SETS
000015          DO 75 I=1,N
000016          SIG (L,I)=0.0
000021          DS(L,I)=0.0
000024          DOVD(L,I)=0.0
000027          BUO(L,I)=0.0
000031          V(L,I)=0.0
000034          GM(L,I)=0.0
000036          THT(L,I)=0.0
000041       75 CONTINUE
000046          DO 10 L=1,SETS
000047          DO 11 I=1,N
000050          DO 12 K=1,2
000051          READ(5,2) (ZA(K,J),J=1,2)
000064          IF (ZA(1,1).EQ.0.0) GO TO 13
000065       12 CONTINUE
000067          ZRO1(L,I)=ZA(1,2)-ZA(1,1)
000074          ZRO2(L,I)=ZA(2,2)-ZA(2,1)
000100          READ (5,2)  (A(L,I,J),J=1,2)
000116          READ (5,3) V(L,I)
000126          READ (5,4) DS(L,I),THT(L,I),GM(L,I),SIG(L,I)
000152       11 CONTINUE
000155       13 READ (5,5) NU(L)
000163          READ (5,6) (LINE(L,J),J=1,7)
000177        6 FORMAT (7A10)
000177       10 CONTINUE
000202        1 FORMAT (2I2)
000202        2 FORMAT (2F6.2)
000202        3 FORMAT (F6.2)
000202        4 FORMAT (4F10.5)
000202        5 FORMAT (E10.4)
000202          D=0.1615
000203          RO=62.4
000205          GC=0.99707
000206          GT=0.99999
000210          DL=5.0
000211          DO 200 I=1,N
          C
```

```
      C     READ DIGITIZER DATA
      C
000213  200 LJCT(I)=I
000216      K=1
000217      NN=500
000220  340 DO 300 I=1,NN
000222      IF (NN.EQ.1) GO TO 310
000224      READ (5,305) ID(I),IX(I),IY(I)
000235  305 FORMAT (3I10)
000235      IF (IX(I).EQ.0) GO TO 320
000237      RRE(K,I)=FLOAT(IX(I))/100.0
000244      DDPT(K,I)=FLOAT(IY(I))/100.0
000252  300 CONTINUE
000254  320 K=K+1
000256      ISUB(K-1)=I-1
000260      IF (K.GE.5) GO TO 330
000262      GO TO 340
000263  330 NN=1
000264      GO TO 340
000265  310 READ(5,42) XPL,YPL,XACT,YACT
000301   42 FORMAT (4F20.2)
      C
      C     CONVERT DIGITIZER DATA TO ACTUAL VALUES
      C
000301      SFX1=XPL/(ALOG(XACT)-ALOG(1000.0))
000310      SFY1=YPL/(ALOG(YACT)-ALOG(0.001))
000316      DO 43 I=1,4
000317      WRITE (6,70)
000322   70 FORMAT (60X,*RE*,20X,*CF*//)
000322      KK=ISUB(I)
000324      DO 43 J=1,KK
000326      RE(I,J)=EXP((RRE(I,J)/SFX1)+ALOG(1000.0))
000342      DPT(I,J)=EXP((DDPT(I,J)/SFY1)+ALOG(0.001))
000355      WRITE (6,46) RE(I,J),DPT(I,J)
000367   46 FORMAT (45X,2E20.5)
000367   43 CONTINUE
      C
      C
      C     INITIALIZE PROGRAM   PRELIMINARY CALCULATIONS
      C
000374      DO 20 L=1,SETS
000375      DO 20 I=1,N
000376      DS(L,I)=DS(L,I)/12.0
000402      FCT(L,I)=0.0
000405      CRX(L,I)=0.0
000410      CD(L,I)=0.0
000413      DPDIF(L,I)=0.0
000415      DPC(L,I)=0.0
000420      VSQAV(L,I)=0.0
000422      DPL(L,I)=0.0
000425      DPM(L,I)=0.0
000427      VPR(L,I)=0.0
000432      XLG(L,I)=0.0
000434      XRE(L,I)=0.0
      C
000437      IF (V(L,I).EQ.0.0) GO TO 20
000441      FCT(L,I)=((GM(L,I)-GC)/GT)*THT(L,I)/30.48
000452      V(L,I)=V(L,I)*(0.1605*4.0)/(3.14159*D*3*60.0)
```

```
      C
000462       20 CONTINUE
      C
      C     CORRECT FOR THERMAL NON ZERO
      C
000467        DO 21 L=1,SETS
000471        DO 21 I=1,N
000472        IF (V(L,I).EQ.0.0) GO TO 21
000475        CRX(L,I)=(ZRO1(L,I)+ZRO2(L,I))/2.0
000504       21 CONTINUE
      C
      C     CALCULATE PRESSURE DROP ACROSS CAPSULE ETC
      C
000511        DO 30 L=1,SETS
000513        DO 31 I=1,N
      C
000514        IF (V(L,I).EQ.0.0) GO TO 31
000517        DOVD(L,I)=DS(L,I)/D
000524        BUO(L,I)=(SIG(L,I)-RO)/RO
000530        BUO1(L,I)=(SIG(L,I)-RO)/SIG(L,I)
000533        DPC(L,I)=((A(L,I,2)-A(L,I,1))-CRX(L,I))*RO*FCT(L,I)
000542        VSQAV(L,I)=V(L,I)*V(L,I)
000544        CALL INTERP (V(L,I),L,DPM(L,I),XRE(L,I))
000550        DPDIF(L,I)=DPC(L,I)-DPM(L,I)
000557        CD(L,I)=(4.0/3.0)*(DS(L,I)*32.17/VSQAV(L,I))*((SIG(L,I)-RO)/RO)
000573        VPR(L,I)=VSQAV(L,I)/(BUO(L,I)*D)
000600        XLG(L,I)=DPDIF(L,I)/(BUO(L,I)*D)
000603       31 CONTINUE
000606       30 CONTINUE
      C
      C
      C                  OUTPUT PORTION OF PROGRAM
      C
000610        DO 50 L=1,SETS
000612        DS(L,I)=DS(L,I)*12.0
000616        WRITE (6,51) (LINE(L,J),J=1,7)
000632       51 FORMAT (H1,20X,7A10)
      C
000632        WRITE (6,65) NU(L)
000640       65 FORMAT (H0,10X,*VISCOSITY (FT..2)/SEC*,5X,10E10.3//)
000640        WRITE (6,400)
000644      400 FORMAT (H0,20X,*MANOMETER READING (CM)*,10X,*ZERO 1*,10X,*ZERO 2*)
000644        DO 401 I=1,N
000646        WRITE (6,402) (A(L,I,J),J=1,2),ZRO1(L,I),ZRO2(L,I)
000671      402 FORMAT (25X,F5.2,5X,F5.2,13X,F5.2,11X,F5.2)
000671      401 CONTINUE
000674        WRITE (6,201)  (LJCT(I),I=1,N)
000706      201 FORMAT (H0,17X,10I9)
000706        WRITE (6,62)  (DOVD(L,I),I=1,N)
000723       62 FORMAT (10X,*D/D*,9X,10E9.2)
000723        WRITE (6,63) (BUO(L,I),I=1,N)
000740       63 FORMAT (10X,*SIGMA-RO/RO*,1X,10E9.2)
000740        WRITE (6,54) (V(L,I),I=1,N)
000755       54 FORMAT (10X,*(V-AV)*,6X,10E9.2)
000755        WRITE (6,59) (VSQAV(L,I),I=1,N)
000772       59 FORMAT (10X,*(V-AV)..2*,3X,10E9.2)
000772        WRITE (6,61) (CD(L,I),I=1,N)
001007       61 FORMAT (10X,*DRAG COEFF*,2X,10E9.2)
```

```
001007           WRITE (6,203) (XRE(L,I),I=1,N)
001024       203 FORMAT (10X,*RE*,10X,10E9.2)
001024           WRITE (6,58) (DPC(L,I),I=1,N)
001041        58 FORMAT (10X,*DPM*,9X,10E9.2)
001041           WRITE (6,60) (DPDTE(L,I),I=1,N)
001056        60 FORMAT (10X,*DPM-DPL*,5X,10E9.2)
001056           WRITE (6,84)  (VPR(L,I),I=1,N)
001073        84 FORMAT (10X,*(V-AV)..2/K*,1X,10E9.2)
001073           WRITE (6,85)  (XLG(L,I),I=1,N)
001110        85 FORMAT (10X,*DPM-DPL/K*,3X,10E9.2)
001110           WRITE (6,53 ) (GM(L,I),I=1,N)
001125        53 FORMAT (10X,*MAN. GM*,5X,10E9.2)
001125           WRITE (6,56) (THT(L,I),I=1,N)
001142        56 FORMAT (10X,*MAN. THETA*,2X,10E9.2)
001142           WRITE (6,57) (CRX(L,I),I=1,N)
001157        57 FORMAT (10X,*(ZR1+ZR2)/2*,1X,10E9.2)
001157           WRITE (6,403)
001163       403 FORMAT (H0,40X,*K=D.(SIG-RO)/RO*)
001163        50 CONTINUE
         C
         C
001166           STOP
001170           END

UNUSED COMPILER SPACE
017100
```

```
                SUBROUTINE INTERP  (V,L,DH,CLR)
      C
000007          REAL NU
000007          COMMON/111/RE(5,100),DPT(5,100),D,NU(40),RO,NPTS(6)
000007          COMMON/333/ISUB(5)
      C
000007          IF (L.GE.10) GO TO 200
000011          DL=5.0
000013          D=0.1615
000014       50 CLR=V*D/NU(L)
000017          IF (CLR.LE.2500.0) GO TO 130
000021          IF (CLR.LT.9400.0) K=1
000024          IF (CLR.LT.9400.0) GO TO 230
      C
000026          IF (L-5) 210,210,220
000030      210 K=3
000031          GO TO 230
000032      220 K=4
000033      230 J=ISUB(K)
000035          DO 100 I=1,J
000037          IF (CLR.LE.RE(K,I)) GO TO 110
000043      100 CONTINUE
      C
000045          WRITE (6,120) L
000053      120 FORMAT (10X,*DATA NOT IN RANGE*,5X,*SET NUMBER*,5X,I2//)
000053          DH=0.00
000056          GO TO 500
      C
000057      110 I=I-1
000061          CF=(DPT(K,I)-DPT(K,I+1))*((CLR-RE(K,I))/(RE(K,I+1)-RE(K,I)))+DPT(K
               1,I+1)
000075          DH=(CF*DL*RO*V*V)/(D*2.0*32.17)
000103          GO TO 500
000104      130 DH=(32.0*DL*RO*V*V)/(32.17*D*CLR)
000113          GO TO 500
      C
000113      200 WRITE (6,300)
000117      300 FORMAT (2X,*CF DATA EXCEEDED*//)
000117      500 RETURN
000120          END

UNUSED COMPILER SPACE
023000
```

DATA SET 1 SINGLE STEEL SPHERES IN 25 WPPM POLYMER

VISCOSITY (FT..2)/SEC 1.744E-05

MANOMETER READING (CM)		ZERO 1	ZERO 2
17.91	52.66	1.29	1.31
18.63	51.80	1.21	1.29
18.49	51.98	1.10	1.21
21.03	49.28	.02	.99
21.05	49.33	-.14	.02
23.35	46.93	-.27	-.32
23.42	46.92	-.34	-.27
27.59	42.58	.10	-.27
27.52	42.61	-.22	-.27
24.58	45.10	.27	0.00

	1	2	3	4	5	6	7	8	9	10
D/D	7.74E-01	7.74E-01	7.74E-01	7.09E-01	7.09E-01	6.45E-01	6.45E-01	5.16E-01	5.16E-01	3.87E-01
SIGMA-RO/RO	7.23E+00	7.23E+00	7.23E+00	7.34E+00	7.34E+00	7.59E+00	7.59E+00	7.23E+00	7.23E+00	6.72E+00
(V-AV)	2.79E+00	3.06E+00	3.06E+00	3.98E+00	3.92E+00	4.60E+00	4.59E+00	4.77E+00	4.71E+00	4.60E+00
(V-AV)..2	7.81E+00	9.35E+00	9.35E+00	1.59E+01	1.54E+01	2.11E+01	2.11E+01	2.28E+01	2.22E+01	2.12E+01
DRAG COEFF	4.96E+00	4.14E+00	4.14E+00	2.27E+00	2.35E+00	1.60E+00	1.61E+00	1.13E+00	1.17E+00	8.52E-01
RE	2.59E+04	2.83E+04	2.83E+04	3.69E+04	3.63E+04	4.26E+04	4.25E+04	4.42E+04	4.36E+04	4.26E+04
DPM	2.35E+01	2.25E+01	2.28E+01	1.97E+01	2.01E+01	1.69E+01	1.69E+01	1.07E+01	1.09E+01	6.87E+00
DPM-DPL	2.14E+01	2.01E+01	2.04E+01	1.62E+01	1.68E+01	1.29E+01	1.28E+01	6.53E+00	6.58E+00	2.81E+00
(V-AV)..2/K	6.69E+00	8.01E+00	8.01E+00	1.34E+01	1.30E+01	1.73E+01	1.72E+01	1.95E+01	1.90E+01	1.95E+01
DPM-DPL/K	1.83E+01	1.72E+01	1.74E+01	1.37E+01	1.41E+01	1.05E+01	1.05E+01	5.59E+00	5.63E+00	2.59E+00
MAN. GM	1.59E+00	1.59E+00	1.59E+00	1.59E+00	1.59E+00	1.59E+00	1.59E+00	1.59E+00	1.59E+00	1.59E+00
MAN. THETA	5.76E-01	5.76E-01	5.76E-01	5.81E-01	5.81E-01	5.81E-01	5.81E-01	5.82E-01	5.82E-01	2.77E-01
(ZR1+ZR2)/2	1.30E+00	1.25E+00	1.16E+00	5.05E-01	-6.00E-02	-2.95E-01	-3.05E-01	-8.50E-02	-2.45E-01	1.35E-01

K=D.(SIG-RO)/RO

DATA SET 2 SINGLE STEEL SPHERES IN 25 WPPM POLYMER

VISCOSITY (FT..2)/SEC 1.744E-05

MANOMETER READING (CM)		ZERO 1	ZERO 2
26.40	43.25	.90	-.11
27.80	41.50	.82	-.60
29.42	40.12	3.28	-.24

	1	2	3	4	5	6	7	8	9	10
D/D	3.22E-01	2.58E-01	1.93E-01	0.	0.	0.	0.	0.	0.	0.
SIGMA-RO/RO	6.73E+00	6.76E+00	6.77E+00	0.	0.	0.	0.	0.	0.	0.
(V-AV)	4.45E+00	4.33E+00	3.87E+00	0.	0.	0.	0.	0.	0.	0.
(V-AV)..2	1.98E+01	1.88E+01	1.50E+01	0.	0.	0.	0.	0.	0.	0.
DRAG COEFF	7.60E-01	6.43E-01	6.06E-01	0.	0.	0.	0.	0.	0.	0.
RE	4.12E+04	4.01E+04	3.58E+04	0.	0.	0.	0.	0.	0.	0.
DPM	5.55E+00	4.69E+00	3.17E+00	0.	0.	0.	0.	0.	0.	0.
DPM-DPL	1.62E+00	8.47E-01	-3.55E-02	0.	0.	0.	0.	0.	0.	0.
(V-AV)..2/K	1.82E+01	1.72E+01	1.37E+01	0.	0.	0.	0.	0.	0.	0.
DPM-DPL/K	1.49E+00	7.76E-01	-3.25E-02	0.	0.	0.	0.	0.	0.	0.
MAN. GM	1.59E+00	1.59E+00	1.59E+00	0.	0.	0.	0.	0.	0.	0.
MAN. THETA	2.77E-01	2.84E-01	2.84E-01	0.	0.	0.	0.	0.	0.	0.
(ZR1+ZR2)/2	3.95E-01	1.10E-01	1.52E+00	0.	0.	0.	0.	0.	0.	0.

K=D.(SIG-RO)/RO

DATA SET 4 25 WPPM POLYMER

VISCOSITY (FT..2)/SEC 1.744E-05

MANOMETER READING (CM)		ZERO 1	ZERO 2
29.50	40.70	1.80	1.08
29.78	40.42	1.85	1.11
30.04	40.16	.16	.10
28.81	41.39	1.10	.66
28.29	41.91	1.70	1.02
27.17	43.03	.96	.57
27.30	42.90	.60	.36
26.59	43.61	1.31	.78
25.81	44.39	.98	.58
25.38	44.82	1.42	.86

	1	2	3	4	5	6	7	8	9	10
D/D	1.93E-01	1.93E-01	1.93E-01	2.58E-01	2.58E-01	3.22E-01	3.22E-01	3.22E-01	3.87E-01	3.87E-01
SIGMA-RO/RO	7.67E+01	7.67E+01	7.67E+01	6.76E+00	6.76E+00	6.73E+00	6.73E+00	6.73E+00	6.72E+00	6.72E+00
(V-AV)	3.94E+00	3.87E+00	3.75E+00	4.11E+00	4.38E+00	4.53E+00	4.38E+00	4.59E+00	4.65E+00	4.78E+00
(V-AV)..2	1.55E+01	1.50E+01	1.41E+01	1.69E+01	1.92E+01	2.05E+01	1.92E+01	2.11E+01	2.16E+01	2.29E+01
DRAG COEFF	6.63E+00	6.85E+00	7.30E+00	7.14E-01	6.29E-01	7.34E-01	7.85E-01	7.13E-01	8.35E-01	7.88E-01
RE	3.65E+04	3.59E+04	3.48E+04	3.81E+04	4.06E+04	4.19E+04	4.05E+04	4.25E+04	4.30E+04	4.43E+04
DPM	3.37E+00	3.16E+00	3.45E+00	4.04E+00	4.23E+00	5.21E+00	5.22E+00	5.52E+00	6.15E+00	6.32E+00
DPM-DPL	1.32E-02	-5.09E-02	2.81E-01	5.04E-01	4.52E-01	1.11E+00	1.45E+00	1.47E+00	1.97E+00	2.11E+00
(V-AV)..2/K	1.25E+00	1.21E+00	1.14E+00	1.55E+01	1.76E+01	1.88E+01	1.76E+01	1.94E+01	1.99E+01	2.11E+01
DPM-DPL/K	1.07E-03	-4.10E-03	2.27E-02	4.62E-01	4.14E-01	1.02E+00	1.34E+00	1.35E+00	1.81E+00	1.94E+00
MAN. GM	1.59E+00	1.59E+00	1.59E+00	1.59E+00	1.59E+00	1.59E+00	1.59E+00	1.59E+00	1.59E+00	1.59E+00
MAN. THETA	2.84E-01	2.84E-01	2.84E-01	2.84E-01	2.84E-01	2.84E-01	2.84E-01	2.84E-01	2.84E-01	2.84E-01
(ZR1+ZR2)/2	1.44E+00	1.48E+00	1.30E-01	8.80E-01	1.36E+00	7.65E-01	4.80E-01	1.05E+00	7.80E-01	1.14E+00

K=D.(SIG-RO)/RO

DATA SET 5 25 WPPM POLYMER

VISCOSITY (FT..2)/SEC 1.744E-05

MANOMETER READING (CM)		ZERO 1	ZERO 2
21.34	48.86	1.52	.92
19.47	50.73	1.64	.98
18.41	51.79	1.66	1.00
12.12	58.08	.92	.56
12.24	57.96	1.62	.98
9.79	60.41	1.10	.66
33.65	36.55	.02	.02
33.72	36.48	.04	.02
33.78	36.42	.03	.02
33.61	36.59	-.05	-1.85

	1	2	3	4	5	6	7	8	9	10
D/D	5.16E-01	5.16E-01	5.16E-01	6.45E-01	6.45E-01	6.45E-01	7.09E-01	7.09E-01	7.09E-01	7.72E-01
SIGMA-RO/RO	7.23E+00	7.23E+00	7.23E+00	7.59E+00	7.59E+00	7.59E+00	7.34E+00	7.34E+00	7.34E+00	7.23E+00
(V-AV)	4.65E+00	4.61E+00	4.75E+00	4.51E+00	4.36E+00	4.46E+00	4.06E+00	4.16E+00	3.73E+00	2.34E+00
(V-AV)..2	2.16E+01	2.13E+01	2.25E+01	2.04E+01	1.90E+01	1.99E+01	1.65E+01	1.73E+01	1.39E+01	5.46E+00
DRAG COEFF	1.19E+00	1.21E+00	1.15E+00	1.66E+00	1.79E+00	1.71E+00	2.19E+00	2.09E+00	2.60E+00	7.08E+00
RE	4.31E+04	4.27E+04	4.39E+04	4.18E+04	4.04E+04	4.13E+04	3.76E+04	3.85E+04	3.45E+04	2.16E+04
DPM	9.08E+00	1.03E+01	1.11E+01	1.56E+01	1.53E+01	1.72E+01	2.10E+01	1.99E+01	1.91E+01	2.87E+01
DPM-DPL	4.89E+00	6.24E+00	6.65E+00	1.15E+01	1.14E+01	1.32E+01	1.76E+01	1.63E+01	1.60E+01	2.70E+01
(V-AV)..2/K	1.85E+01	1.82E+01	1.93E+01	1.66E+01	1.55E+01	1.62E+01	1.39E+01	1.46E+01	1.17E+01	4.68E+00
DPM-DPL/K	4.19E+00	5.35E+00	5.70E+00	9.42E+00	9.33E+00	1.08E+01	1.49E+01	1.37E+01	1.35E+01	2.31E+01
MAN. GM	1.59E+00	1.59E+00	1.59E+00	1.59E+00	1.59E+00	1.59E+00	1.35E+01	1.35E+01	1.35E+01	1.35E+01
MAN. THETA	2.84E-01	2.84E-01	2.84E-01	2.84E-01	2.84E-01	2.84E-01	2.84E-01	2.84E-01	2.84E-01	2.84E-01
(ZR1+ZR2)/2	1.22E+00	1.31E+00	1.33E+00	7.40E-01	1.30E+00	8.80E-01	2.00E-02	3.00E-02	2.50E-02	-9.50E-01

K=D.(SIG-RO)/RO

DATA SET 6 POLYMER 25 WPPM

VISCOSITY (FT..2)/SEC 1.744E-05

MANOMETER READING (CM)		ZERO 1	ZERO 2
33.53	36.67	.11	.06
33.50	36.70	.02	.02
33.27	36.93	.09	.06
33.21	36.99	.06	.04
33.23	36.97	.04	.02
33.06	37.14	.10	.06
32.97	37.23	.04	.02
32.35	37.85	.03	.02
I	I	I	I
I	I	I	I

	1	2	3	4	5	6	7	8	9	10
D/D	7.72E-01	7.72E-01	8.38E-01	8.38E-01	8.38E-01	9.02E-01	9.02E-01	9.67E-01	0.	0.
SIGMA-RO/RO	7.23E+00	7.23E+00	7.12E+00	7.12E+00	7.12E+00	7.07E+00	7.07E+00	7.00E+00	0.	0.
(V-AV)	2.93E+00	3.18E+00	1.61E+00	2.01E+00	1.45E+00	5.54E-01	9.58E-01	7.16E-01	0.	0.
(V-AV)..2	8.58E+00	1.01E+01	2.61E+00	4.04E+00	2.09E+00	3.07E-01	9.19E-01	5.12E-01	0.	0.
DRAG COEFF	4.51E+00	3.83E+00	1.59E+01	1.02E+01	1.98E+01	1.44E+02	4.81E+01	9.17E+01	0.	0.
RE	2.71E+04	2.94E+04	1.49E+04	1.86E+04	1.34E+04	5.13E+03	8.88E+03	6.63E+03	0.	0.
DPM	2.23E+01	2.32E+01	2.62E+01	2.72E+01	2.70E+01	2.92E+01	3.09E+01	3.99E+01	0.	0.
DPM-DPL	2.00E+01	2.07E+01	2.50E+01	2.58E+01	2.60E+01	2.89E+01	3.02E+01	3.95E+01	0.	0.
(V-AV)..2/K	7.35E+00	8.66E+00	2.26E+00	3.51E+00	1.82E+00	2.69E-01	8.05E-01	4.53E-01	0.	0.
DPM-DPL/K	1.71E+01	1.77E+01	2.18E+01	2.24E+01	2.26E+01	2.53E+01	2.64E+01	3.49E+01	0.	0.
MAN. GM	1.35E+01	1.35E+01	1.35E+01	1.35E+01	1.35E+01	1.35E+01	1.35E+01	1.35E+01	0.	0.
MAN. THETA	2.84E-01	2.84E-01	2.84E-01	2.84E-01	2.84E-01	2.84E-01	2.84E-01	2.84E-01	0.	0.
(ZR1+ZR2)/2	8.50E-02	2.00E-02	7.50E-02	5.00E-02	3.00E-02	8.00E-02	3.00E-02	2.50E-02	0.	0.

K=D.(SIG-RO)/RO

DATA SET 3 SINGLE STEEL SPHERES IN 50 WPPM POLYMER

VISCOSITY (FT**2)/SEC 1.744E-05

MANOMETER READING (CM)		ZERO 1	ZERO 2
26.55	42.98	-.11	-.18
29.00	40.45	.99	-.40
29.50	40.02	.94	3.28

	1	2	3	4	5	6	7	8	9	10
D/D	3.22E-01	2.58E-01	1.93E-01	0.	0.	0.	0.	0.	0.	0.
SIGMA-RO/RO	6.73E+00	6.76E+00	6.77E+00	0.	0.	0.	0.	0.	0.	0.
(V-AV)	4.50E+00	4.11E+00	4.04E+00	0.	0.	0.	0.	0.	0.	0.
(V-AV)**2	2.03E+01	1.69E+01	1.63E+01	0.	0.	0.	0.	0.	0.	0.
DRAG COEFF	7.41E-01	7.16E-01	5.58E-01	0.	0.	0.	0.	0.	0.	0.
RE	4.17E+04	3.80E+04	3.74E+04	0.	0.	0.	0.	0.	0.	0.
DPM	5.59E+00	3.85E+00	2.90E+00	0.	0.	0.	0.	0.	0.	0.
DPM-DPL	2.06E+00	8.58E-01	-1.62E-01	0.	0.	0.	0.	0.	0.	0.
(V-AV)**2/K	1.87E+01	1.54E+01	1.49E+01	0.	0.	0.	0.	0.	0.	0.
DPM-DPL/K	1.89E+00	7.87E-01	-1.49E-01	0.	0.	0.	0.	0.	0.	0.
MAN. GM	1.59E+00	1.59E+00	1.59E+00	0.	0.	0.	0.	0.	0.	0.
MAN. THETA	2.77E-01	2.84E-01	2.84E-01	0.	0.	0.	0.	0.	0.	0.
(ZR1+ZR2)/2	-1.45E-01	2.95E-01	2.11E+00	0.	0.	0.	0.	0.	0.	0.

K=D.(SIG-RO)/RO

DATA SET 7 50 WPPM POLYMER

VISCOSITY (FT..2)/SEC 1.744E-05

MANOMETER READING (CM)		ZERO 1	ZERO 2
30.84	39.36	.68	.41
30.76	39.44	1.28	.77
31.00	39.20	1.62	.97
29.91	40.29	.23	.14
30.22	39.98	.71	.41
28.84	41.36	1.22	.72
28.59	41.61	.28	.16
28.37	41.83	.38	.22
27.52	42.68	1.54	.92
27.16	43.04	1.20	.72

	1	2	3	4	5	6	7	8	9	10
D/D	1.93E-01	1.93E-01	1.93E-01	2.58E-01	2.58E-01	2.58E-01	3.22E-01	3.22E-01	3.22E-01	3.87E-01
SIGMA-RO/RO	6.77E+00	6.77E+00	6.77E+00	6.76E+00	6.76E+00	6.76E+00	6.73E+00	6.73E+00	6.73E+00	6.72E+00
(V-AV)	3.69E+00	3.44E+00	3.65E+00	4.24E+00	4.04E+00	3.85E+00	4.20E+00	4.28E+00	4.31E+00	4.70E+00
(V-AV)..2	1.36E+01	1.18E+01	1.33E+01	1.80E+01	1.63E+01	1.48E+01	1.77E+01	1.83E+01	1.86E+01	2.21E+01
DRAG COEFF	6.67E-01	7.69E-01	6.81E-01	6.72E-01	7.39E-01	8.15E-01	8.50E-01	8.20E-01	8.10E-01	8.15E-01
RE	3.42E+04	3.18E+04	3.38E+04	3.93E+04	3.74E+04	3.56E+04	3.89E+04	3.97E+04	3.99E+04	4.35E+04
DPM	2.75E+00	2.64E+00	2.38E+00	3.52E+00	3.18E+00	3.99E+00	4.42E+00	4.54E+00	4.81E+00	5.15E+00
DPM-DPL	1.45E-01	1.83E-01	-1.51E-01	2.65E-01	9.44E-02	1.29E+00	1.23E+00	1.45E+00	1.67E+00	1.55E+00
(V-AV)..2/K	1.25E+01	1.08E+01	1.22E+01	1.65E+01	1.50E+01	1.36E+01	1.63E+01	1.69E+01	1.71E+01	2.04E+01
DPM-DPL/K	1.33E-01	1.68E-01	-1.38E-01	2.42E-01	8.65E-02	1.18E+00	1.14E+00	1.34E+00	1.53E+00	1.43E+00
MAN. GM	1.59E+00	1.59E+00	1.59E+00	1.59E+00	1.59E+00	1.59E+00	1.59E+00	1.59E+00	1.59E+00	1.59E+00
MAN. THETA	2.84E-01	2.84E-01	2.84E-01	2.84E-01	2.84E-01	2.84E-01	2.84E-01	2.84E-01	2.84E-01	2.84E-01
(ZR1+ZR2)/2	5.45E-01	1.03E+00	1.29E+00	1.85E-01	5.60E-01	9.70E-01	2.20E-01	3.00E-01	1.23E+00	9.60E-01

K=D.(SIG-RO)/RO

DATA SET 8 50 WPPM POLYMER

VISCOSITY (FT..2)/SEC 1.744E-05

MANOMETER READING (CM)		ZERO 1	ZERO 2
24.79	45.41	1.44	.86
26.52	43.68	.60	.36
21.79	48.41	26.62	18.32
21.49	48.71	1.36	.82
20.58	49.62	.22	.14
12.46	57.74	.14	.08
13.62	56.58	.98	.58
11.26	58.94	1.10	.66
33.94	36.26	.02	.02
33.81	36.39	.10	.06

	1	2	3	4	5	6	7	8	9	10
D/D	3.87E-01	3.87E-01	5.16E-01	5.16E-01	5.16E-01	6.45E-01	6.45E-01	6.45E-01	7.09E-01	7.09E-01
SIGMA-RO/RO	6.72E+00	6.72E+00	7.23E+00	7.23E+00	7.23E+00	7.59E+00	7.59E+00	7.59E+00	7.34E+00	7.34E+00
(V-AV)	4.43E+00	4.51E+00	4.69E+00	4.50E+00	4.68E+00	4.54E+00	4.26E+00	4.23E+00	3.83E+00	4.01E+00
(V-AV)..2	1.96E+01	2.03E+01	2.20E+01	2.03E+01	2.19E+01	2.06E+01	1.81E+01	1.79E+01	1.47E+01	1.61E+01
DRAG COEFF	9.19E-01	8.87E-01	1.17E+00	1.27E+00	1.13E+00	1.65E+00	1.87E+00	1.89E+00	2.46E+00	2.24E+00
RE	4.10E+04	4.18E+04	4.34E+04	4.17E+04	4.33E+04	4.20E+04	3.94E+04	3.92E+04	3.55E+04	3.71E+04
DPM	6.72E+00	5.76E+00	1.43E+00	9.02E+00	9.97E+00	1.56E+01	1.46E+01	1.62E+01	1.68E+01	1.82E+01
DPM-DPL	3.34E+00	2.22E+00	-2.15E+00	5.49E+00	6.41E+00	1.20E+01	1.13E+01	1.29E+01	1.41E+01	1.52E+01
(V-AV)..2/K	1.81E+01	1.87E+01	1.88E+01	1.74E+01	1.88E+01	1.68E+01	1.48E+01	1.46E+01	1.24E+01	1.36E+01
DPM-DPL/K	3.08E+00	2.04E+00	-1.84E+00	4.71E+00	5.49E+00	9.79E+00	9.20E+00	1.05E+01	1.19E+01	1.28E+01
MAN. GM	1.59E+00	1.59E+00	1.59E+00	1.59E+00	1.59E+00	1.59E+00	1.59E+00	1.59E+00	1.35E+01	1.35E+01
MAN. THETA	2.84E-01	2.84E-01	2.84E-01	2.84E-01	2.84E-01	2.84E-01	2.84E-01	2.84E-01	2.84E-01	2.84E-01
(ZR1+ZR2)/2	1.15E+00	4.80E-01	2.25E+01	1.09E+00	1.80E-01	1.10E-01	7.80E-01	8.80E-01	2.00E-02	8.00E-02

K=D.(SIG-RO)/RO

DATA SET 9 50 WPPM POLYMER

VISCOSITY (FT..2)/SEC 1.744E-05

MANOMETER READING (CM)		ZERO 1	ZERO 2
33.64	36.56	0.00	0.00
33.54	36.66	.12	.08
33.37	36.83	.10	.06
33.39	36.81	.04	.02
33.36	36.85	3.48	3.76
32.98	37.22	.02	.01
32.41	37.79	.12	.08

	1	2	3	4	5	6	7	8	9	10
D/D	7.72E-01	7.72E-01	8.38E-01	8.38E-01	8.38E-01	9.02E-01	9.67E-01	0.	0.	0.
SIGMA-RO/RO	7.23E+00	7.23E+00	7.12E+00	7.12E+00	7.12E+00	7.07E+00	7.00E+00	0.	0.	0.
(V-AV)	2.79E+00	3.01E+00	1.79E+00	1.55E+00	1.11E+00	8.15E-01	4.52E-01	0.	0.	0.
(V-AV)..2	7.77E+00	9.08E+00	3.22E+00	2.40E+00	1.22E+00	6.64E-01	2.04E-01	0.	0.	0.
DRAG COEFF	4.98E+00	4.26E+00	1.28E+01	1.72E+01	3.38E+01	6.66E+01	2.30E+02	0.	0.	0.
RE	2.58E+04	2.79E+04	1.66E+04	1.43E+04	1.02E+04	7.55E+03	4.18E+03	0.	0.	0.
DPM	2.13E+01	2.20E+01	2.47E+01	2.47E+01	-9.49E-01	3.08E+01	3.85E+01	0.	0.	0.
DPM-DPL	1.95E+01	2.00E+01	2.35E+01	2.37E+01	-1.77E+00	3.03E+01	3.84E+01	0.	0.	0.
(V-AV)..2/K	6.65E+00	7.78E+00	2.80E+00	2.09E+00	1.06E+00	5.82E-01	1.80E-01	0.	0.	0.
DPM-DPL/K	1.67E+01	1.71E+01	2.05E+01	2.06E+01	-1.54E+00	2.65E+01	3.40E+01	0.	0.	0.
MAN. GM	1.35E+01	1.35E+01	1.35E+01	1.35E+01	1.35E+01	1.35E+01	1.35E+01	0.	0.	0.
MAN. THETA	2.84E-01	2.84E-01	2.84E-01	2.84E-01	2.84E-01	2.84E-01	2.84E-01	0.	0.	0.
(ZR1+ZR2)/2	0.	1.00E-01	8.00E-02	3.00E-02	3.62E+00	1.50E-02	1.00E-01	0.	0.	0.

K=D.(SIG-RO)/RO